Republic of Iraq
Ministry of Higher Education
and Scientific Research
University of Misan
College of Science
Department of Chemistry

Synthesis and Characterization of Electrospun Polymeric Nanofibers for Adsorption of Methylene Blue Dye from Aqueous Solution

Thesis Submitted to
The College of Science / University of Misan as Partial Fulfillment of the Requirements for the Master Degree of Science in Chemistry

By

Mortadha Shehab Ahmed

B.Sc. Chemistry, College of Science / University of Misan (2015)

Supervisor

Assistant Professor

Hind Mahdi Saleh

2025 **1446**

بسم الله الرحمن الرحيم

قُلْ هَلْ يَسْتَوِي الَّذِينَ يَعْلَمُونَ وَالَّذِينَ لَا يَعْلَمُونَ ۗ
إِنَّمَا يَتَذَكَّرُ أُولُو الْأَلْبَابِ

سورة الزمر / أية (9)

صدق الله العلي العظيم

Supervisor Certificate

I am the supervisor of **Mr. Mortadha Shehab Ahmed** and certify that the thesis (**Synthesis and Characterization of Electrospun Polymeric Nanofibers for Adsorption of Methylene Blue Dye from Aqueous Solution**) was done and written under my supervision as a fulfillment of the requirement for master degree of science in chemistry.

Signature……

Assistant Professor
Hind Mahdi Saleh
College of Science
Misan University
Date: 12 2025

Head of Chemistry Department Recommendation

According to the recommendation of the supervisor, this thesis is forwarded to the examination committee for approval.

Signature……

Dr. Mohammed Abdul Raheem Saeed
Head of Chemistry Department
College of Science
Misan University
Date: 12 2025

Dedication

To the Sun and Moon Which Lighting my Life by Pave the Way my Success…

My Father & My Mother

To Those who have Supported me and are Waiting for my Success…

My Wife and My Son

My Brothers and My Sister

To The one who gave me his time and knowledge…

My supervisor

Acknowledgement

Firstly, many blessing to **Allah,** the most merciful, for his blessings, who gave me health, strength, and facilitated the ways to accomplish this work, and the prayer and peace of Allah be upon our master and prophet Muhammad and his divine good family.

To my supervisor, **Asst. Prof. Hind Mahdi Saleh,** there are no words that can match my gratitude. I thank you so much for you interest in my thesis, assistance, and constructive guidance. I totally appreciate it; I can hardly express my gratitude.

I would like to extend my sincere thanks to the Dean of the College of Science, **Dr. Tahseen Saddam Fandi**, for his kind support and encouragement.

My appreciation also goes to **Dr. Mohammed Abdul Raheem**, the head of the chemistry department; **Dr. Salim Nima Saleh**; and **Dr. Zaidon Tareq Hashim** for their support and advice.

Mortadha

Abstract

Industrialization, agriculture, natural disasters, and a lack of water supplies and wastewater facilities are the main causes of water pollution. The industries that are most responsible for this pollution include the nuclear, iron and steel, food, textile, pulp and paper, distilleries, tanneries, and plastics. Various industrial processes can release large quantities of toxic solvents, volatile organic compounds, and both organic and inorganic hazardous chemicals. Such wastes are directly responsible for the escalation of the water pollution problem when they are discharged into bodies of water without being adequately treated. This study primarily examines dyes, the most common of these pollutants. Methylene blue (MB) is a typical cationic dye, with its peculiarities of stability in the environment and toxic, carcinogenic, and mutagenic qualities. The dye is extensively applied in the textile and clothing industries in the dyeing of textiles and in the coloring of paper and leather. Since it has widespread industrial applications, substantial amounts of industrial effluents with methylene blue are released into the surface and groundwater. In humans at high doses of 5 mg/kg, MB inhibition of monoamine oxidase can lead to fatal toxicity linked to high levels of serotonin, as well as cause severe effects to aquatic life within the ecosystem. As such, there is an emergency to remove this pigment in wastewater. The study is devoted to the fabrication and characterization of polyacrylic acid-chitosan (PAA-Chi) nanofibers through the electrospinning method, and the purpose of the study is to develop an effective material that will help remove methylene blue (MB) dye in aqueous solutions. The interaction of chitosan with the PAA framework is a tactical move that will improve the adsorption capability of the nanofibers and make them more effective as adsorbents for various other organic pollutants than methylene blue dye.

There was a significant amount of research done on the structural, compositional, and rheological properties of the fabricated nanofibers. The adsorption of these fibers was studied by kinetic and equilibrium tests, and it was found that initial dye concentration and medium pH affected this adsorption. The results will explain the properties of adsorption of the fibers and their effectiveness in removing dye.

In the first section, Polyacrylic acid-Chitosan (PAA-Chi) nanofibers (70:30) were fabricated via electrospinning, whereas no nanofiber formation was observed for the 50:50 and 85:15 ratios. It is a popular method of producing polymeric fibers with a size between a micrometer and a nanometer. The process provides materials that have a large external area and significant porosity structure. The process entailed certain methodological processes to achieve the production of a homogeneous nanofiber that has valuable qualities that could be used in these applications.

The second section discusses the overall characterization of the prepared nanofibers. Using FESEM showed a homogenous morphology with an average diameter of 276.15 nm. Measurement of zeta potential established that the surface of the fiber is negatively charged. The successful introduction of the discrete functional groups in both PAA and chitosan was confirmed by the Fourier transform infrared (FTIR) spectrum, and these functional groups assist in the dye's improved ability to bind to the sample due to hydrogen bonding and ionic interactions. Moreover, rheological and viscosity analyses provided useful information about the characteristics of the feedstock solution that could be used to create stable and homogenous fibers.

The third section of the work is devoted to the use of PAA-Chi nanofibers as a new adsorbent to treat water, and it is essential to remove the organic pollutant methylene blue (MB). A high removal capacity was given by the adsorption efficiency test of the batch test. The maximum adsorption capacity (q_e) attained

exceeded 60 mg/g with a concentration of MB (200 mg/L), compared to 55 and 31 mg/g initial concentrations of MB dye (100 and 50 mg/L), respectively. The experiments were conducted under ideal conditions, specifically using a mass of 10 mg of PAA-Chi nanofibers (NFs). The temperature was set at 25°C, pH at 6, and a contact time of 720 minutes. These data indicate that PAA-Chi nanofibers remain a viable option for the treatment of industrial wastewater due to their stable morphology, beneficial surface characteristics, and capacity to adsorb cationic contaminants.

Contents

Tables

Figures

List of Abbreviations

Abbreviation	***Key***
CA	Cellulose Acetate
Chi	Chitosan
COPD	Chronic Obstructive Pulmonary Disease
DMSO	Dimethyl Sulfoxide
EDTA	Ethylenediaminetetraacetic Acid
FESEM	Field Emission Scanning Electronic Microscope
FT-IR	Fourier Transform Infrared Spectrophotometry
HA	Hyaluronic Acid
K_1	pseudo-first-order Rate Constant
K_2	pseudo-second-order Rate Constant
K_f	Freundlich Constant
K_L	Langmuir Isothermal Constant
MB	Methylene Blue
MW	Molecular Weight
NC	Nano Composite
NFs	Nano Fibers
NM	Nano Materials
PAA	Polyacrylic acid
PAHs	Polycyclic Aromatic Hydrocarbons

PAN	Polyacrylonitrile-based nanofibers
PBS	Polybutylene Succinate
PCL	Polycaprolactone
PEC	Polyelectrolyte Complex
PG	Polyglycerol
PLA	Polylactic Acid
PLGA	Poly-lactic Glycolic Acid
PLLA	Poly(l-lactide)
PM	Particulate Matter
PNCs	Polymer Nanocomposites
PS	Polystyrene
PSS	Polystyrene Sulfonate
PU	Polyurethane
PVA	Polyvinyl Alcohol
PVDF	Polyvinylidene Fluoride
PVP	Polyvinylpyrrolidone
QA	Quality Assurance
QC	Quality Control
q_e	Adsorption Capacity
Q_m	Maximum Adsorption Capacity
R%	Removal Efficiency
SF	Silk Fibroin
T_m	Melting Point
UV-Vis	Ultraviolet - Visible spectrophotometry
β-CD	β-Cyclodextrin
λ max	Wavelength Maximum

Chapter One

Introduction

1.1 Nanomaterials

Nano means nanos, which means a person of extremely low height or an object of extremely small size. In a system of units, the "nano" is used to indicate parts of units. An example of a nanometer is a billionth of a meter or a billionth of a millimeter; a nanoliter is a billionth of a liter or a millionth of a milliliter; and a nanokelvin is a billionth of a Kelvin [1]. This remarkable category of materials, termed nanomaterials, includes instances with at least one dimension measuring between 1 and 100 nanometers. Through rational design of nanomaterials, exceptionally high surface areas are possible. In contrast to their bulk equivalents, nanomaterials can be synthesized with exceptional magnetic, electrical, optical, mechanical, and catalytic capabilities [2]. As a particle's size decreases, the number of component atoms surrounding its surface increases, resulting in highly reactive particles with distinct chemical, optical, physical, and electronic properties. In addition to its rapid development, nanotechnology has a wide range of applications in the chemical, pharmaceutical, engineering, and food processing industries [3-5]. The words "nanomaterials," "nanoscience," and "nanotechnology" have become common terms in both research and everyday life. In the early meteorites, nanoparticles and nanostructures were formed immediately after the Big Bang. Later, nature created more nanoparticles and nanostructures. Recently, NM's research has been attracting remarkable interest from scientists and engineers all over the world [6].

1.2 Classification of Nanomaterials

In general, nanomaterials can be classified based on several key criteria, including their dimensions, shape, state, and chemical composition [7]. According to Figure 1-1, nanomaterials can be classified according to their size, which ranges from 1 to 100 nanometers in any dimension. These materials are divided into four

categories based on their dimensions and general shape: zero-dimensional materials, one-dimensional materials, two-dimensional materials, and three-dimensional materials. Nanomaterials with zero dimensions (0D) are those whose dimensions are all below 100 nm in size. They include spherical nanomaterials, cubes, nanorods, polygons, hollow spheres, metals, core-shells, and quantum dots (QD). A one-dimensional nanomaterial (1D) is a material whose one dimension does not fall into nanoscale, while the other two dimensions fall into nanoscale. 1D material types include metallic, polymeric, ceramic, nanotube, nanorod, nanowire, and nanofiber filaments. Two-dimensional (2D) nanomaterials have only one dimension within the nanoscale, while the other two dimensions extend beyond this scale. Examples include nanofilms, thin sheets, nanocoatings, and thin films, and these materials may be crystalline or amorphous. Three-dimensional (3D) materials, on the other hand, have all three dimensions exceeding 100 nanometers [8]. Three-dimensional (3D) nanomaterials consist of assemblies of multiple nanocrystals arranged in different orientations. Examples include foams, fibers, carbon nanotubes, nanorods, fullerenes, and columns, as well as polycrystals, honeycomb structures, and layers [9, 10].

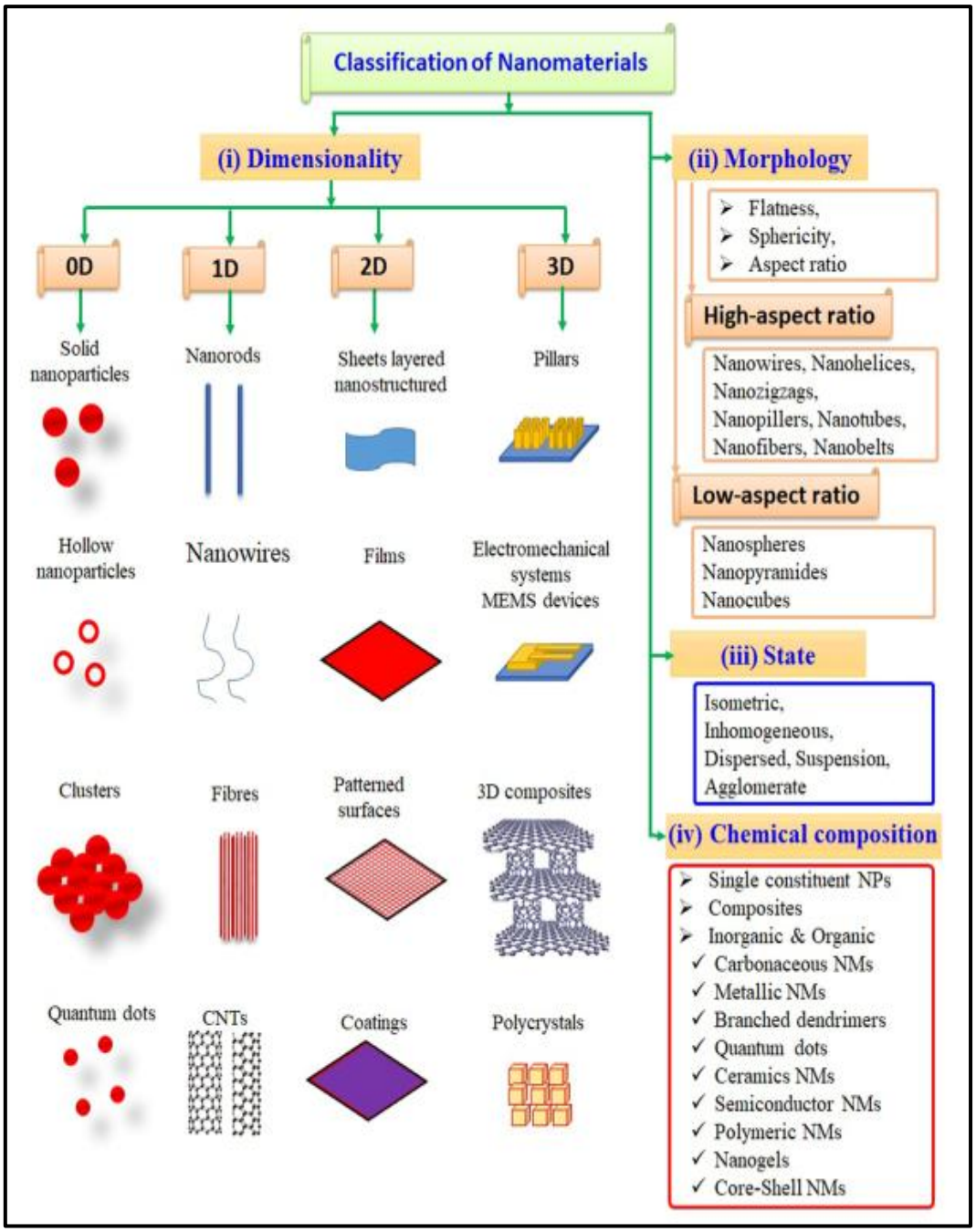

Figure 1-1 *Schematic illustration of the classification of nanomaterials based on different criteria [7].*

1.3 Nanofibers

Research into methods for manufacturing polymer nanofibers remains a major focus of scientific research and has received increasing attention in both academia and industry. A number of methods have been designed to create such fibers, such as electrospinning, drawing, phase separation, self-assembly, and template synthesis.

Among these techniques, electrospinning is the most common and preferred. This is due to its high flexibility, economic efficiency, and ease of use, making it an ideal method for producing polymer nanofibers on a large scale. The technology is based on the use of high electrical voltage as a charge of a jet of polymer solution. This jet is focused onto a metal assembly surface, and when the solvent evaporates, fibers with diameters of submicrons are deposited on the surface. Previous studies have indicated that system properties and operating parameters vary greatly depending on the type of material used [11]. The properties of the polymer solution (such as concentration, viscosity, surface tension, and electrical conductivity) and the processing parameters (such as electrode potential, inter-electrode distance, solution flow rate, and the type of collecting surface) are the key factors that influence the conversion of the solution into ultrafine fibers. Therefore, a thorough study of these parameters is essential for the production of defect-free electrospun nanofibers.

Natural materials have become of interest in recent times because of their availability and structural and functional properties. Chitosan can be obtained as a result of a partial deacetylation of chitin, which is the second biopolymer in nature after cellulose. Its biological properties, such as its biodegradability, low toxicity, antifungal properties, ability to accelerate wound healing, hemostatic effect, and immune-stimulating properties, make it a promising material for medical applications. The improvement of the special properties of chitosan can be conducted through the increase of its specific surface area through the production of nanometer-scale materials or highly porous structures [12]. As a

result, the last ten years have been characterized by the great research potential of the chitosan nanofibers, particularly when produced through electrospinning.

1.4 Electrospun Nanofibers

Differentiation science has enabled the development of specialized nanocomposites specifically designed to encode drugs for specific disease treatments. These carriers come in a variety of forms, including dendrites, liposomes, emulsions, nanoshells, nanotubes, and nanofibers [13]. Electrospinning is a platform nanotechnology used to enable the generation of a wide array of new structured materials in a wide variety of biomedical applications, such as drug delivery, biosensing, tissue engineering, and regenerative medicine. Nanofibers have shown considerable promise as a drug delivery technology compared with synthetic or natural drugs, which have low availability [14]. They are polymeric fibers, which have a diameter of nanometers. The various fibers resemble cell types within the body, improve their attachment and migration, and improve methods of transporting the material. These gains are attributed to their unique structure, which includes small pore sizes, a high surface-to-volume ratio, high knot strength, permeability, light weight, and skin-stretch coupling [15].

1.5 Nanofiber Fabrication

1.5.1 Electrospinning

Electrospinning (as shown in Figure 1-2) is a major research focus because it is a simple, low-cost, and versatile technology. This process relies on the use of electrostatic forces to form long, continuous polymer nanofibers [16]. The electrospun fiber mats produced by these non-mechanical techniques exhibit structural advantages, such as ultrafine structures, high porosity, high surface-to-volume ratio, and tailored morphology. The high encapsulation efficacy of

bioactive compounds can be achieved depending on these advantages. The no-thermal process of electrospinning allows the encapsulation of thermosensitive compounds, which is important for preserving the structure and enhancing the stability and functionality during food processing and storage [17].

Electrospun fibers exhibit unique properties, such as their ultra-small diameters, ranging from 2 nanometers to several micrometers. They also have smaller pore sizes and higher surface areas compared to those produced using conventional spinning techniques [17]. Electrospinning is a method for producing nanofibers from polymer solutions using high-strength electric fields. These fibers have numerous applications in a wide range of fields [18] . The use of electrospinning to incorporate biological products into nanofibers, including microorganisms, cells, proteins, and nucleic acids, has been demonstrated by Martí and Castano [19]. In this field, synthetic polymers are frequently preferred over their natural counterparts. This preference is due to the ease of controlling the properties of synthetic polymers, such as viscosity, which enables the production of relevant and specific properties, which we have not been able to achieve with natural polymers.

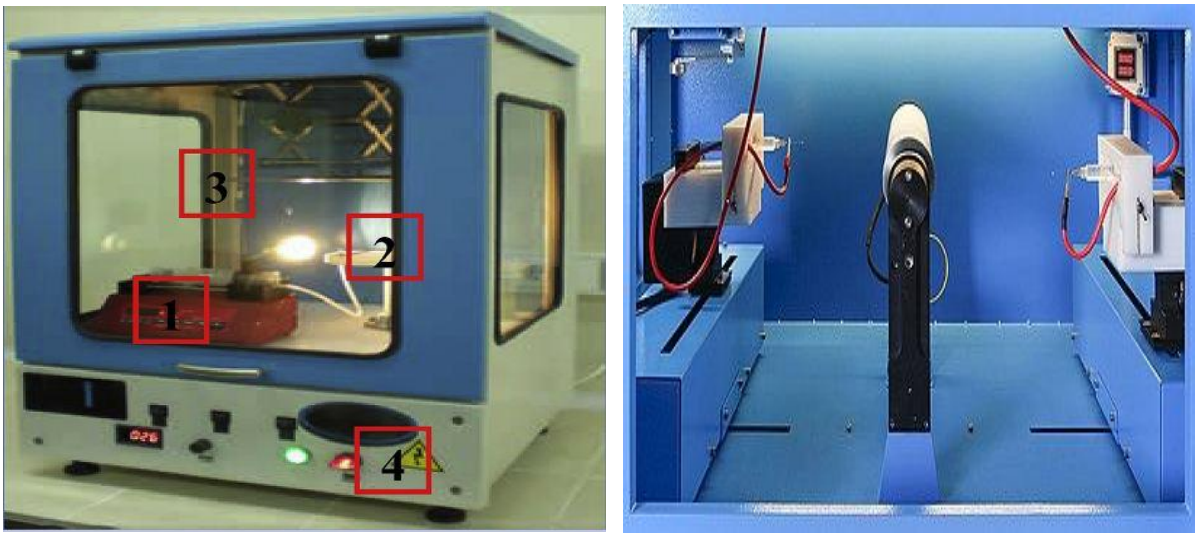

Figure 1-2 *Electrospinning equipment: 1 is the syringe pump, 2 is the tip of the needle and where the voltage is applied, 3 is the collector plate, and 4 is the power supply* [20]

Electrospinning more often uses polymer blends to enhance the physical capabilities of nanofibers. Electrospinning is an efficient technology to generate nanofibers with a realistic morphology of the bone or cartilage tissue and relevant mechanical properties [17, 21].

1.5.1.1 Classification of Electrospinning Methods

Literature has revealed four types of electrospinning [20]. Co-electrospinning is a process through which a drug is mixed with a polymer, and then embossing of the polymer is commenced. It is incorporated into the polymer matrix in the appropriate operating condition under which the drug is dissolved or dispersed. The technology is used to create polymer fibers that are graded with drugs. These polymer matrices automatically experience adsorption and diffusion or dissolution and erosion [22].

Cengiz et al. (2019) Another form of electrospinning that was reported is called coaxial electrospinning, where two polymer solutions are both spun. The method is used when the polymer blend solutions cannot chemically be replaced by differing solvent systems.

The other useful technique in getting drug-releasing nanofibers is coaxial electrospinning, which has been used successfully in the delivery of various drugs [20].

In the experiment conducted by Keirouz *et al.* (2019), The researcher used the method of emulsion electrospinning, which involves emulsifying a drug substance into an aqueous solution of protein using a polymer solution. This technique is applied in encapsulating polar and hydrophilic molecules, including proteins. Surfactants that have a low level of water-to-lipid are used to achieve stability of the emulsion [23]. A continuous polymer electrospinning process has to be used

to form the emulsion. The solutions must have sufficient electrical conductivity and a high concentration of polymers. They also need to include a polymer weight, and a surface tension, and consequently a polymer density.

Gugulothu *et al*. (2019) said that the fourth method of electrospinning technique is referred to as nozzleless electrospinning. The electrode is drilled on the tube and spread to some extent across the cross-section. The fibers are then put under an electrostatic field without the need of needles [24].

1.5.1.2 The Electrospinning Setup

Electrospinning, also referred to as electrospinning, is a production process of scaffolds in the form of nanofibers. These scaffolds consist of fibers with nanometer diameters. These fibers have random orientations, and various shapes. These nonwoven-based fabricated scaffolds have found application in the regenerative tissue engineering processes, as well as in the effective delivery of drugs to the wounds [25].

The electrospinning system is comprised of three primary parts: namely, a high-voltage power supply, a spinneret, and a plateau-grounded collector. The feeding apparatus typically consists of a sharp metal end that is attached to a syringe. This syringe will contain either a polymer solution to be used in wet electrospinning or molten polymers to be used in melt electrospinning [26].

SalehHudin *et al*. (2017) documented that an intense electric potential, typically between 5 and 60 kV, is applied between the metal needle and the metal assembly surface [27]. Electric charges are generated on the surface of the molten polymer solution droplet at the tip of the needle, causing it to assume a conical shape known as a Taylor cone. When the electric force exceeds the surface tension of the solution, a jet of polymer is ejected from the tip of the cone toward the collector.

Meanwhile, the solvent evaporates from the liquid jet and is replaced by a new jet, and this process continues. As the jet expands, a network of non-woven nanofibers eventually forms on the collector surface, as shown in Figure 1-3 [28].

In conventional single-needle electrospinning, a syringe with a blunt needle acts as a spinneret. The polymer solution is fed to this syringe at a controlled flow rate. When a high voltage, typically up to 30 kV, is applied between the needle and the collector, a charged droplet forms at the tip of the needle and deforms into a conical shape known as a Taylor cone [29].

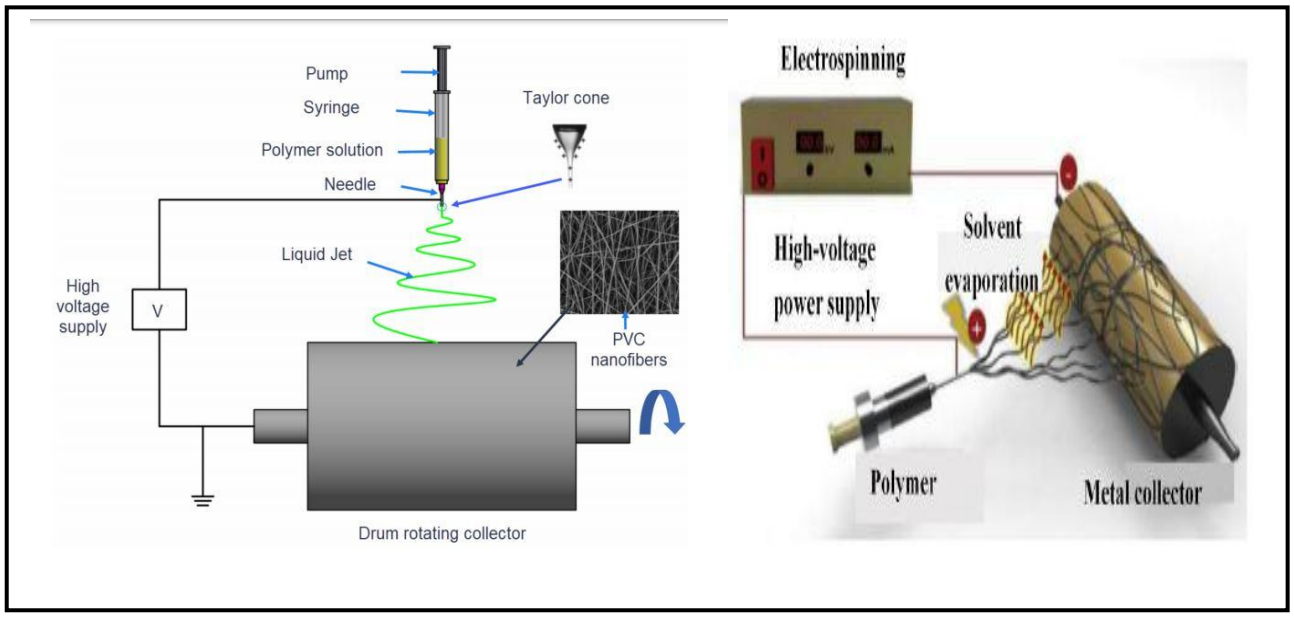

Figure 1-3 *Schematic setup illustrations for the electrospinning process* [29].

1.5.1.3 Influence of Parameters in the Electrospinning Process

Chavan and Kanu (2015) confirmed that most soluble or fusible polymers could be electrospun if several parameters governing the electrospinning process are suitably tuned. These variables are divided into solution and molecule parameters, process parameters, and environmental parameters.

Aman et al. (2020) reported in their study that the solution parameters and molecular properties that affect the spinning process include a wide range of factors. These factors include:

1- Solution-related properties include solubility, viscosity, pH, solvent vapor pressure, conductivity, and surface tension. 2- Polymer molecular properties: such as crosslinking, molecular weight, glass transition temperature, melting point, crystallization rate, density, and distribution [30]. In contrast, process parameters include factors such as the electrode geometry, the tip-to-collector distance, the applied electric field, and the feed or flow rate. Ambient environmental parameters include humidity and medium temperature [31].

A study by Li et al. (2014) confirmed that changing these parameters directly affects the shape and diameter of the resulting fibers. The study demonstrated that optimal selection of these parameters ensures the production of uniform nanofibers through the electrospinning process, while minimizing the formation of knots or "beads" along the length of the yarn, resulting in the desired shape and diameter [32]. Figure 1-4 and Table 1-1 describe some of these parameters and, in some cases, their effect on the properties of nanofibers produced using electrospinning [33].

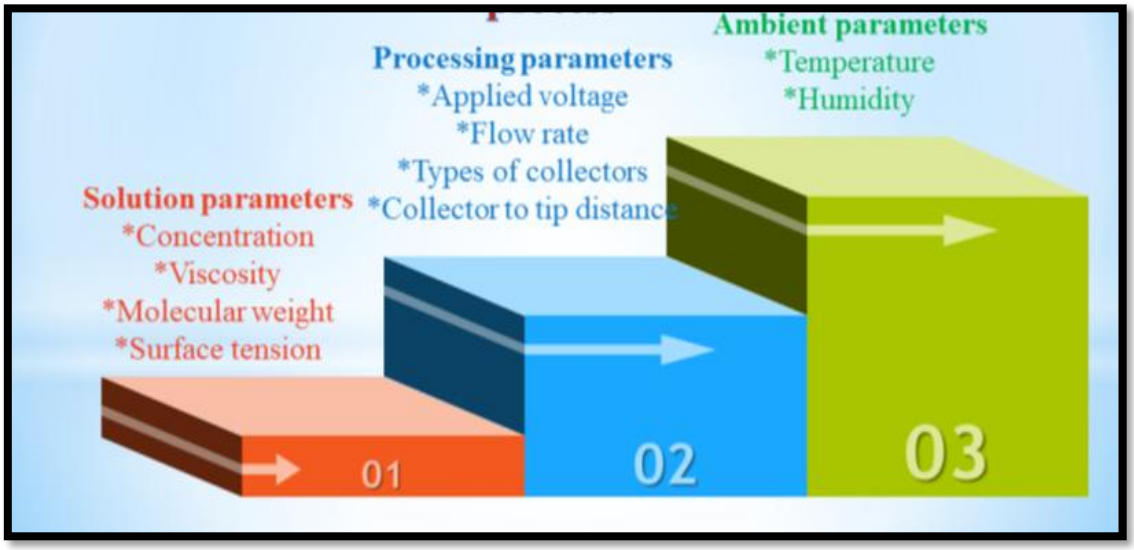

Figure 1-4 *The different parameters affecting the electrospinning process* [34].

Table 1-1 *Electrospinning parameters (solution, processing, and ambient) and their effects on fiber morphology.*

Solution parameters	Effects on fiber morphology
Viscosity	Highly viscous solutions tend to form droplets as they move from the needle to the collection surface, resulting in granules rather than continuous fibers [35].
Polymer concentration	An increase in concentration increases viscosity and increases fiber diameter, forming droplets that become dried as they reach the collector.
The molecular weight (MW) of the polymer	Decreased in the number of beads and droplets with increased molecular weight.
Conductivity	The fiber diameter decreases as the conductivity increases.
Surface tension	There is no conclusive link with fiber morphology; high surface tension results in instability of jets.
Processing parameters	
Applied voltage	Decrease in fiber diameter with an increase in voltage [17].
Distance between tip and collector	Generation of beads with too small and too large distances, the minimum distance required for uniform fibers.
Feed rate (Flow rate)	As the flow rate increases, the volume of the polymer solution in the Tylor cone increases, thus decreasing the diameter initially. Further increase in flow rate forms beads [15].
Ambient parameters	
Humidity	High humidity results in circular pores on the fibers and increases the pearl effect [36].
Temperature	An increase in temperature increases the concentration of the solution, thus increasing viscosity. This increased viscosity reduces the beaded morphology. Increase in temperature results in a decrease in fiber diameter [37].

1.5.1.3.1 Viscosity

Huan *et al*. (2015) noted that solution viscosity is one of the most important factors affecting the diameter and shape of nanofibers in the electrospinning process. When a solid polymer is dissolved in a solvent, the solution viscosity is directly related to the polymer concentration, and these factors are also related to the polymer's molecular weight [31].

There are numerous studies that consider viscosity an important factor in the formation of various fibers. When viscosity is very low, surface work becomes the primary factor leading to the formation of beaded or granular fibers. This, in turn, increases the efficiency of the polymer jets flowing, resulting in more structure [38, 39].

In addition, studies have shown that a controlled increase in solution viscosity or concentration results in the production of fibers with larger and more uniform diameters. This relationship between polymer viscosity or concentration and electrospun fibers has been investigated in several research systems [40].

1.5.1.3.2 Surface Tension

Zhao *et al*. (2021) affirmed that the characteristics of the solvent used in the solution are a critical aspect during the electrospinning procedure [25]. When all other factors are held constant, surface tension can define the top and lower boundaries of the electrospinning process, while SalehHudin et al. (2017) indicated that the creation of fibers, beads, and droplets is contingent upon the solution's surface tension:

(a) Reduced surface tension: enables electrospinning and permits its occurrence with a diminished electric field. (b) Elevated surface tension: obstructs electrospinning by inducing jet instability, resulting in the generation of spray droplets rather than nanofibers.

Generally, nanofibers can be obtained without beads with a fixed concentration by lowering the surface tension of the NFs solution [41]. The surface tensions of the solution are substantially influenced by the solvents used in the electrospinning process [42].

1.5.1.3.3 Molecular Weight

The molecular weight of a polymer affects both the shape of the electrospun fibers and their electrical properties, including conductivity, viscosity, surface tension, and dielectric strength. The solution viscosity is also largely determined by the number of entanglements that the polymer chains have in the solution, which is also dependent on the molecular weight of the polymer. The solubility parameter of a solvent is essential in the formation of a homogenous polymer solution, but a solvent with a high solubility parameter is not necessarily one that will form a solution to be used in electrospinning [41].

Mercante et al. (2017) stated that the concentration and molecular weight of the polymer are two elements that influence the shape of the fibers, as the viscosity of the solution depends on these criteria. High molecular weight polymers have significantly greater viscosity than low molecular weight polymers due to an increased number of polymer chain entanglements [43].

Krumreich et al. (2019) demonstrated that surface defects in the form of granules on the fibers were formed when there is low polymer molecular weight or low solution concentration. On the contrary, more concentration or molecular weights cause the solution viscosity to rise, leading to homogeneous fibers having few granules. On the other hand, these conditions result in the production of helical, curly, and wavy fibers in enormous amounts.

1.5.1.3.4 Conductivity/Surface Charge Density

Thenmozhi et al. (2017) explained that another factor, that influences fiber morphology is the electrical conductivity of the solution. It helps in the elongation of droplets and the production of single or multiple jets [44]. Conductivity of a solution is determined by several factors, which encompass the nature of the polymer, the type of solvent employed, and the availability of salts [45]. The addition of salts, ions, or conductive polymers to the polymer solution can also lead to conductivity, thus producing nanofibers of higher quality with fewer defects and at smaller diameters.

The natural polymers, unlike the synthetic ones, are difficult to form into fibers due to their electrolytic nature. The ions present in them increase the charge-carrying capacity of the polymer jet, resulting in increased tension under the influence of the fiber's electric field. Typically, the electrical conductivity of the solution can be controlled by adding ionic salts, such as sodium chloride (NaCl), potassium phosphate (KH_2PO_4), sodium phosphate (NaH_2PO_4), and others [17].

1.6 Polymers

Since life began, polymers like DNA, RNA, proteins, and polysaccharides have played crucial roles in plant and animal life. In ancient times, man utilized naturally occurring polymers for clothing, decorations, shelter, tools, weapons, writing materials, and other purposes. Today's polymer industry has its origins in the nineteenth century, when important discoveries were made regarding the modification of certain natural polymers [46]**.**

The processability, surface area, stability, adjustable features, and cost efficiency of polymer nanocomposites (PNCs) have garnered the interest of researchers and technicians in water purification recently. This review presents current insights into the function of PNCs in the elimination of metal ions, dyes, and microbes

from contaminated water, demonstrating rapid decontamination efficacy with great selectivity [47].

Polymer nanofibers have a superior surface area per unit mass, and the incorporation of surface functions is easier compared to polymer microfibers. This has seen polymer nanofiber mats being considered for use as filters and scaffolds in tissue engineering, protective clothing, strengthening of composite materials, and security devices. Several of these applications have been marketed, albeit still in the development phase. A significant volume of research has been undertaken on polymer nanofibers and nanofiber mats in recent years. Nevertheless, a thorough review of the issues pertaining to these nanofibers has not been published. This article examines contemporary trends in the processing and characterization techniques of polymer nanofibers [48].

1.6.1 Polymers Used in Electrospinning

A polymer is a chemical compound with molecules bonded together in long, repeating chains. Polymers usually have high melting point. Because of their structure, polymers have unique properties tailored for different uses [49]. Throughout the years, over 200 more polymers have been electrospun for diverse uses, and this number continues to rise [50].

Table (1-2) presents various polymers utilized in the electrospinning procedure. Three categories of polymers are utilized in the fabrication of electrospun nanofibers.

1.6.1.1 Synthetic Polymers

Synthetic polymers are designed macromolecules that can be generated through a well-known chemical polymerization of monomers through either addition or

condensation reactions to gain materials with physical, chemical, and mechanical properties that can be fine-tuned. Their molecular structure (including its length, chain branching, and functional group composition), unlike that of natural polymers, can be precisely designed to fulfill a desired performance need. Polyacrylic acid, polyvinyl alcohol, and polyacrylamide are also commonly used as synthetic polymers in water treatment because of their stability, modification flexibility, and functional group addition to increase adsorption or separation properties. The polymers can be prepared as membranes, resins, or nanofibers, and through these methods, dyes, heavy metals, and other pollutants can be removed efficiently by using the following: electrostatic interaction, chelation, and size exclusion. Synthetic polymers, due to their versatility and scalability, are becoming a key factor in the creation of high-performance and advanced systems of water purification. Some of these synthetic polymers include polylactic acid (PLA), polyvinyl alcohol (PVA), polyethylene oxide (PEO), polylactic glycolic acid (PLGA), polyurethane (PU), polystyrene (PS), and polyglycerol (PG). Synthetic polymers exhibit strength and cost-effectiveness and facilitate straightforward electrospinning [51, 52].

1.6.1.2 Natural Polymers

Natural polymers are macromolecules derived from biological sources (such as plants, animals, or microorganisms) composed of repeated structural units interconnected by covalent connections. Examples of polymers include chitosan, cellulose, starch, polynucleotides, gelatin, and silk fibroin. Due to biodegradation, renewability, and biocompatibility inherent to natural polymers, there has been immense interest in the use of natural polymers in the environment, especially in water treatment. The high levels of functional groups (hydroxyl, amine, and carboxyl groups) allow them to interact with different pollutants in a strong manner by way of electrostatic attraction, hydrogen bonding, and complexation.

Natural polymers can be used as adsorbents, flocculants, and membrane material in aqueous remediation and constitute an environmentally friendly substitute for synthetic polymers, yet with equal efficacy in the removal of dyes, heavy metals, and organic impurities. The combination of natural polymers with other systems also enhances their structural stability and adsorption capacity [51].

Natural polymers are also coming as a promising substitute for synthetic bodies that are extremely useful in adsorption and wound healing. Nonetheless, the degree of biodegradability and the mechanical characteristics of these natural materials are restrictive. Natural polymers utilized in electrospinning comprise collagen, laminin, fibroin, elastin, chitosan, gelatin, pectin, and agarose [53].

These polymers have biocompatibility and nontoxicity, but the poor mechanical properties, and the difficulty in electrospinning have made them mostly reinforced with synthetic polymers [15, 51].

1.6.1.3 Hybrid Polymers

Hybrid polymers are advanced materials: hybrid polymers are the new materials that are developed by combining two or more different classes of polymers, such as a synthetic polymer with a natural polymer or a polymer and an inorganic filler, to merge and enhance the strength of each other. When these elements are mixed together, the material will tend to have a high level of mechanical toughness, chemical resistance, and specialized capability that neither of the elements alone could have. The hybrid polymers have a number of benefits in water remediation. Their biodegradability and functional groups of natural polymers, as well as the durability and tunability of synthetic polymers, have led to their high adsorption capacity, contaminant selectiveness, and enhanced recyclability. Thanks to this, researchers are also resorting increasingly to such composites to create effective, environmentally friendly, and multifunctional systems of water contamination

cleaning. A combination of synthetic and natural polymers overcomes the weaknesses of each: synthetic polymers bring about toughness and hardiness, whereas natural polymers bring biocompatibility and bioactivity. As an example, chitosan is a natural polymer that cannot be electrospun in its form. Its blending with other polymers like polyethylene oxide (PEO), polycaprolactone (PCL), or polyacrylic acid (PAA) has a significant effect on enhancing its electrospinning. This hybrid method takes advantage of the strengths of the two types of polymer to create high-performance tunable hybrid materials for a wide variety of uses [54-56].

Table 1-2 *Certain polymers have been utilized in the electrospinning process.*

No.	Polymer	Application	References
1	Poly acrylic acid (PAA)/chitosan	water purification	[57]
2	Chitosan	Wound dressing, Water Treatment	[58, 59]
3	Chitosan/PVA blend loaded with Metal–Organic Framework (UiO-66) and nanodiamond	Removal of both Methylene Blue and Congo Red dyes in water	[60]
4	Polycaprolactone (PCL)	Bone tissue engineering	[61]
5	Polyvinyl alcohol (PVA)	Antimicrobial agent	[62]
6	Polyvinyl Alcohol/Chitosan (PVA/CS) reinforced with $CeAlO_3$ nanoparticles	Efficient removal of Methylene Blue from aqueous solutions	[63]

7	polyamide-6,6/chitosan	Tissue engineering	[64]
8	Collagen	Tissue engineering	[65]
9	Polyamide-6 nanofibers loaded with SiO_2 and TiO_2 nanoparticles	Removal of Methylene Blue from aqueous solutions	[66]
10	Collagen-PEO	Wound treatment, biomaterial development, coagulation agents	[67]
11	Collagen/chitosan	Biological materials	[68]
12	Cellulose	Affinity membranes	[69]
13	Cellulose acetate	Adsorbent membrane	[70]
14	Poly (vinyl alcohol)/cellulose acetate (PVA/CA)	Biological materials	[71]
15	Polyvinyl carbazole	Sensor and filter	[71]
16	Cellulose Acetate (CA) converted to cellulose with activated carbon and EDTA-modification	Removal of Methylene Blue from water	[72]
17	PAN/β-Cyclodextrin (PAN/β-CD) composite nanofiber membrane	Removal of Methylene Blue from water	[73]
18	Poly vinylpyrrolidone PVP	Wound healing	[74]
19	Silk fibroin SF	Nanofibrous scaffolds for wound healing	[75]
20	Polystyrene PS	Air filtration and Electrical application	[76]
21	Hyaluronic acid HA	Wound healing	[77]
22	Polyurethanes (PU)	Biomedical uses	[78]
23	Polyacrylonitrile (PAN)	Carbon nanofiber	[79]
24	Polyacrylonitrile (PAN) coated with	Removal of Methylene Blue and Congo Red	[80]

	chitosan/graphene oxide nanolayer	dyes from aqueous solution	
25	Poly(l-lactide) (PLLA)	3D cell substrate	[81]
26	Polyurethane (PU)	Biomedical applications	[78]
27	poly(vinyl pyrrolidone) (PVP)	Drug release	[82]
28	poly(ethylene oxide) (PEO)	Biomedical applications	[83]
29	poly(acrylonitrile-co-glycidyl methacrylate)	Affinity separation	[84]
30	Polystyrene sulfonate (PSS) + Polybutylene succinate (PBS) composite nanofibers	Removal of Methylene Blue from aqueous solution	[85]
31	Polyvinylidene fluoride (PVDF)	Filtration	[86]

1.7 Chitosan (Chi)

In the ongoing search for sustainable and high-performance water purification methods, adsorption is being increasingly considered as a low-cost and simple method of eliminating a broad spectrum of contaminants [87, 88]. Here, chitosan, a natural biopolymer of chitin, has turned out to be a highly promising adsorbent [89, 90]. Chitosan (Chi), chemically, is a positively charged polymer that is composed of repeating units of N-acetyl-D-glucosamine as well as D-glucosamine, and the units are interconnected with 1,4-glycosidic bonds. Chitosan is a linear polysaccharide derived from chitin via demineralization and deproteinization, possessing a wide range of medical and agricultural applications [91]. Prior research has investigated the antibacterial properties of chitosan, and more recently, several derivatives of chitosan have been produced to further its inherent antibacterial efficacy. Chi demonstrates additional remarkable biological

properties, including biocompatibility, biodegradability, and nontoxicity. These have rendered it beneficial across various sectors, including medical, food, agricultural, textile, cosmetics, and others (Figure 1-5).

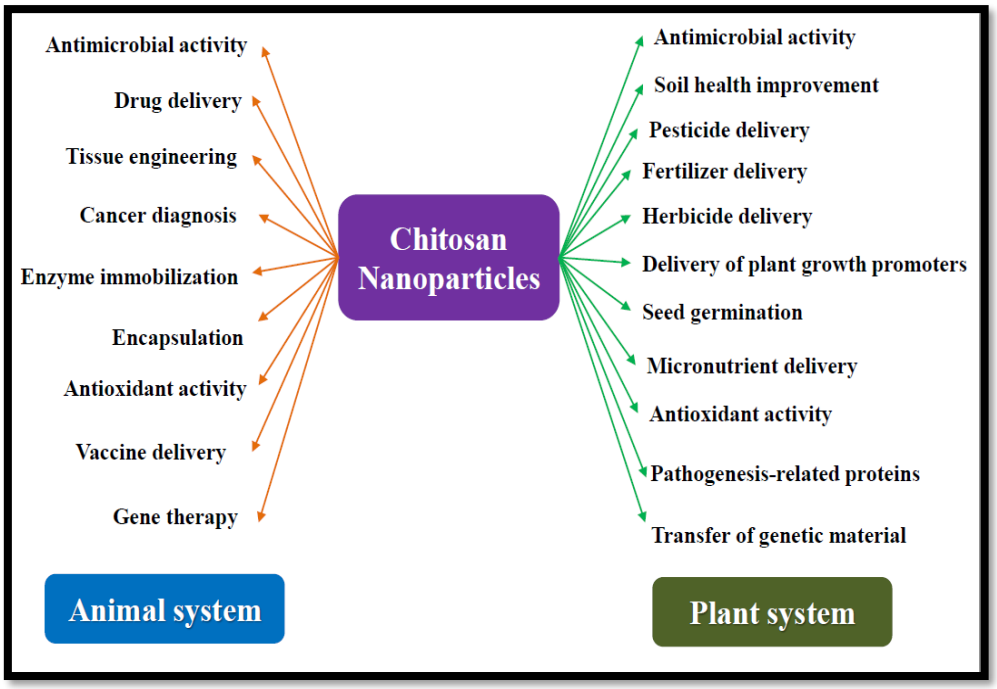

Figure 1-5 *Applications of chitosan nanoparticles* [92]

Deacetylation of chitin, the main component of insect exoskeletons, crustaceans (like shrimps), and fungal cell walls, produces it. Chitin is a polymer of -(1,4)-N-acetyl-D-glucosamine that deacetylates in an alkaline environment to form chitosan, a polymer of N-acetyl glucosamine and D-glucosamine units [93]. The chemical structure of chitosan is presented in Figure (1-6).

An amino group enhances chitosan's functional and structural features at the C-2 position of the glucosamine unit. This amino group symbolizes its cationic nature and confers wound healing and antibacterial action. Chitosan has functional groups strategically placed to provide these unique polysaccharide qualities [94].

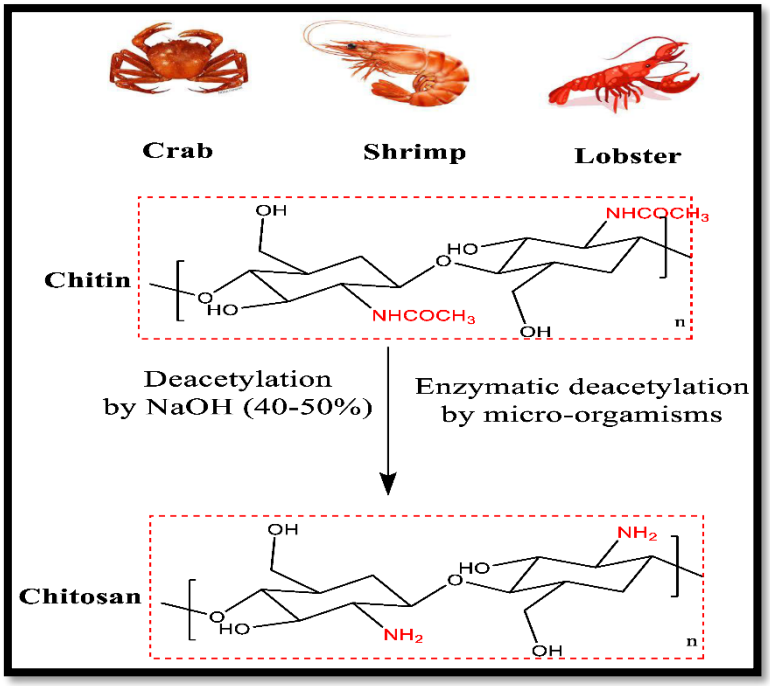

Figure 1-6 *Sources and chemical structure of chitosan* [95]

Its appeal stems from its unique combination of properties, including biodegradability, biocompatibility, non-toxicity, and the existence of many amino ($–NH_2$) and hydroxyl (–OH) functional groups that function as active sites for pollutant binding [87, 96, 97]. The chitosan-based materials have demonstrated a high level of adaptability because they are able to remove a wide variety of dangerous pollutants, such as heavy metal ions (arsenic, chromium, lead, and copper), synthetic dyes, and even the recently emerging contaminants, like pharmaceutical residues in water samples [89, 97, 98]. In reality, though, chitosan, when pure, does not perform as well due to its low surface area, weak mechanical properties, and dissolution in acidic solution [87, 99]. It has hence been the direction of recent studies to develop new chitosan composites and functionalizations to overcome these disadvantages [89, 100]. The physicochemical properties of chitosan can be enhanced dramatically by adding an additive like graphene oxide, activated carbon, or metal-organic frameworks, or using chemical modification techniques, including cross-linking and grafting [88, 101, 102]. These advancements lead to adsorbents with improved surface

area, greater stability, and higher adsorption capacities, paving the way for their use in high-performance, sustainable water treatment systems.

1.8 Poly Acrylic Acid (PAA)

Polyacrylic acid (Figure 1-7) It is a synthetic polymer made from acrylic acid monomers. Polyacrylic acid is a high molecular weight polymer characterized by excellent water solubility. Polyacrylic acid also appears in cross-linked forms. Polyacrylic acid is a significant polymer utilized in the production of polymeric blends and nanocomposites [103]. Polyacrylic acid (PAA) is an economically viable commercial polymer. It is a water-soluble, non-toxic, biodegradable, and biocompatible polymer [104, 105]. PAA can undergo cross-linking to create a stable structure. The cross-linking of PAA improves its mechanical characteristics. Polymeric modifiers in PAA may enhance their strength characteristics [103]. Furthermore, the cross-linked PAA has a significant water absorption capability. PAA possesses exceptional optical characteristics and resistance to weathering. The cross-linked PAA may create a gel-like configuration. An illustration of chemical cross-linking is provided by PAA-graft-chitosan (Figure 1-8).

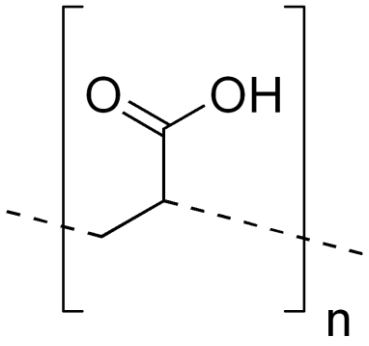

Figure 1-7 *Chemical structure of Polyacrylic acid*

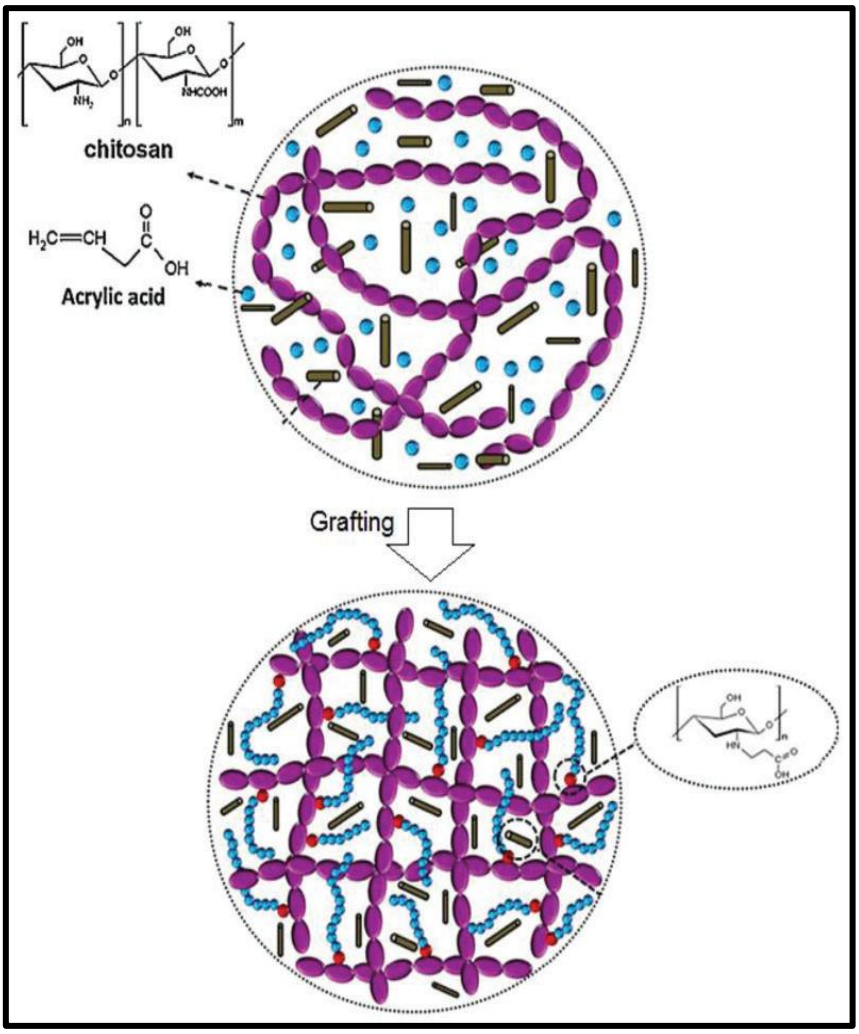

Figure 1-8 *Synthesis of poly(acrylic acid)-grafted chitosan incorporating cellulose nanofibers* [106]

Due to its hydrophilic properties, PAA provides enhanced adhesion to objects, such as a stabilizing agent. The cross-linked polyacrylate can absorb and retain one hundred times its weight in moisture [107].

Polyacrylic acid (PAA) is a polyelectrolyte rich in carboxylic acid (–COOH) groups. In aqueous solutions, especially at neutral to high pH, these groups deprotonate to $–COO^-$, creating a negatively charged network. This enables strong electrostatic attraction of positively charged (cationic) dye molecules (e.g., methylene blue, rhodamine B) [108].

Polyacrylic acid, with its abundant carboxylate functionality, is an effective polymeric adsorbent for cationic dyes in wastewater. Its performance can be greatly enhanced via composites (e.g., with cellulose, graphene, and metals) [108], often outperforming unmodified natural adsorbents. However, practical use must contend with regeneration, kinetics, and environmental concerns.

Nanofibers (NFs) have garnered significant interest due to their distinctive physical and structural characteristics, including a large surface area, enhanced porosity, reduced pore size and fiber diameter, and greater flexibility after surface functionalization [109].

1.9 Nanofibers (NFs)

Among the most promising applications of electrospun materials in biomedics, nanofibers can be mentioned. In case these therapeutic fibers are designed with a multilayer structure, they provide a broad range of options, which can be used to control the kinetics of drug release. The manipulation of the structure of the network of fibers, in turn, allows regulating the release of an active substance, which involves minimizing the occurrence of an abrupt, high-dose burst and provides a more gradual and slower therapeutic effect.

Sylvester et al. (2020) studied the characteristics of nanofibers and identified solid-state linear nanomaterials that are found to be below 100 nm in diameter. Nevertheless, in the industrial and technical worlds, the name "nanofiber" is commonly used to refer to any fiber that has a submicron diameter [110]. Nanofibers may be made of a wide range of polymeric materials, which may either be naturally obtained or artificial.

The outstanding feature of natural polymers is their superior biocompatibility compared to synthetic polymers, where compositions and properties are more flexible and customizable by the designer in synthetic polymers [111].

Preparation of nanofibers utilizes a rich assortment of chemical, mechanical, and optical methods. Since they were first fabricated, researchers have built an extensive arsenal of tools to fabricate fibrous materials in the nanoscale. Nowadays nanofibers can be produced by means of electrospinning, self-assembly, template-based methods, polymerization, sonochemical methods, and dozens of other innovative systems [112].

The different paths through which nanofibers can be generated are illustrated in figure 1-9. In addition to the traditional processes described, there is also freeze-drying (lyophilization) of cellulose to nanofibers. A number of the state-of-the-art and emerging methods are influencing the field today, such as electro-hydrodynamic writing, plasma-induced fabrication, solution-blow writing, centrifugal jet writing, and CO_2 laser supersonic writing.

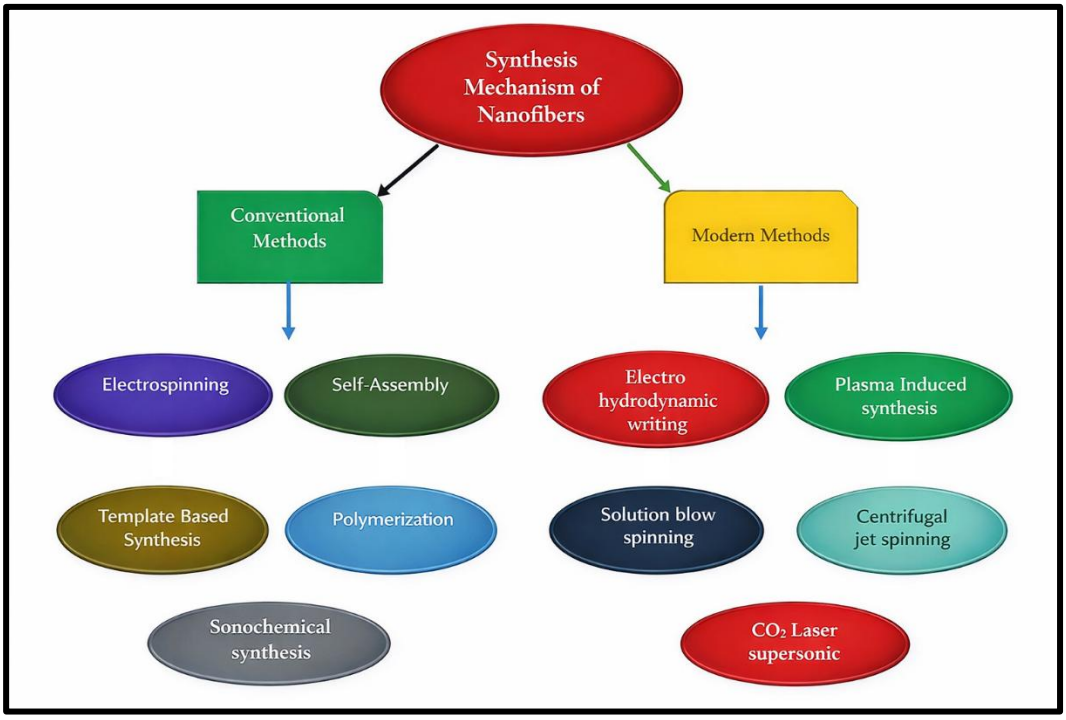

Figure 1-9 *Depiction of Traditional and Contemporary Techniques for Nanofiber Synthesis [113]*

It is the ability to provide a tremendous surface area in relation to volume that makes nanofibers valuable in most fields. They have a structure full of small holes, or holes in any case, which are distributed on the micro- and nanoscale and, in combination with their light weight and flexibility, causes them to be very versatile. These distinctive properties make nanofibers excellent candidates for different applications in pharmaceuticals and biomedical fields [114].

The problem of nanofiber characterization is examined in relation to three aspects: (I) physicochemical properties, (II) mechanical properties, and (III) bioactivity and interactions [115].

1.9.1 Applications of NFs

Electrospun fibers and mats have been sought after due to a host of advantages, including excellent porosity, a very high surface-to-volume ratio, and improved physicomechanical characteristics [61]. Furthermore, electrospinning is very versatile, as fibers can be engineered to take very diverse forms using numerous different polymers. Electrospun nanofibers are extensively utilized in water treatment and employed across numerous domains, as illustrated in Figure (1-10).

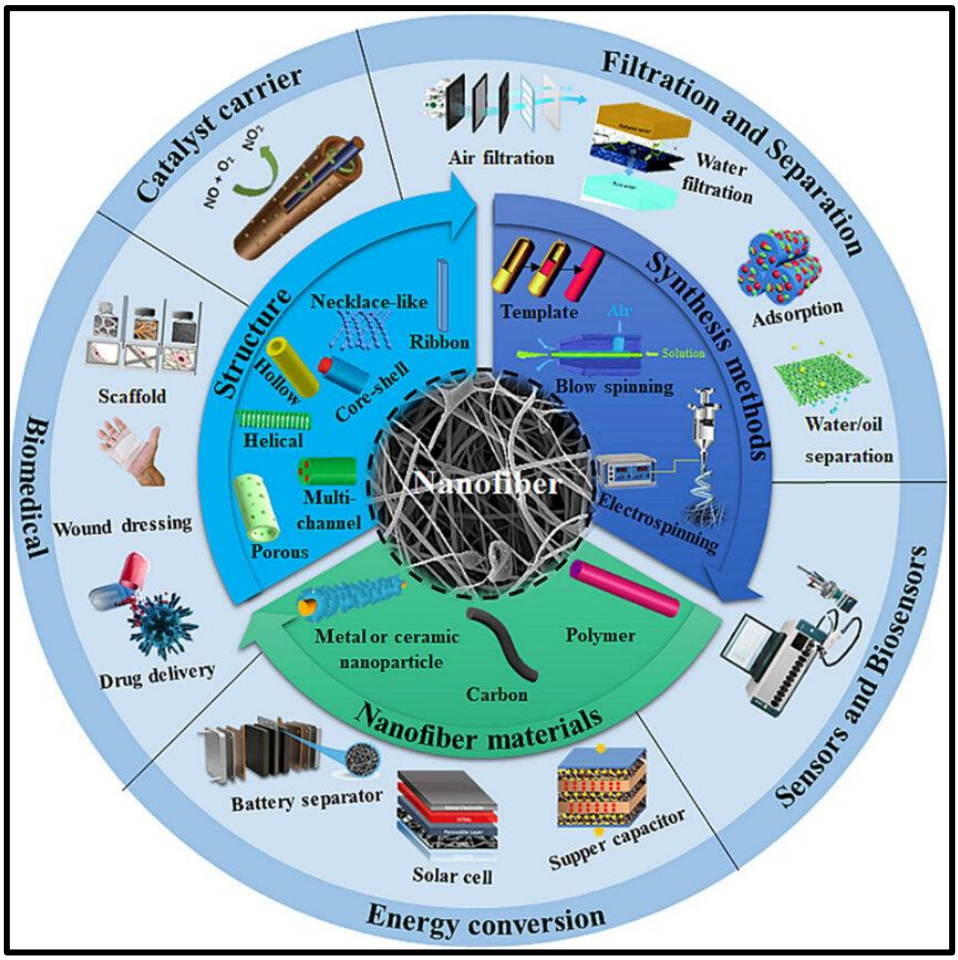

Figure 1-10 *Some applications of electrospun fibers in different fields* [34].

1.9.1.1 Adsorption

Nanofiber adsorption has emerged as a powerful water-treatment application because electrospun mats offer extremely high surface-area-to-volume ratios, tunable pore structures, and abundant functional sites that can be tailored for selective uptake of organic dyes. Functionalization (e.g., with chitosan and graphene oxide) imparts complementary electrostatic and π–π interactions that boost capture of both cationic methylene blue and anionic Congo red on PAN-based nanofiber membranes, while maintaining good reusability after regeneration cycles [80]. In cellulose-acetate systems, embedding adsorptive/coordination sites via MOFs has achieved very high methylene-blue capacities and typically follows Langmuir isotherms with pseudo-second-order

kinetics, highlighting monolayer chemisorption on well-defined sites [116]. In addition to single-polymer systems, composite polystyrene-sulfonate/PBS nanofibers exhibit significant dye absorption and regeneration, with adsorption accurately characterized by the Freundlich model and pseudo-second-order kinetics, demonstrating the heterogeneous surface energetics typical of fibrous adsorbents [85]. Hybrid designs increasingly couple adsorption with photocatalysis (e.g., Nb_2O_5-integrated PAN/PVDF fibers), enabling rapid preconcentration of dyes on the fiber surface, followed by in-situ photodegradation, which mitigates fouling and improves long-term performance [117]. The recent surveys indicate that in comparison with pressure-based membranes, electrospun nanofiber adsorbents reduce energy consumption, can be easily functionalized by incorporating amines, carboxyls, and sulfonates, and can be made into durable mats or modules that can be scaled up to achieve effective dye removal for wastewater treatment [118].

1.10 Pollution

One of the most significant, intricate, and challenging environmental issues is the contamination of soil, saltwater, rivers, lakes, and groundwater. This pollution arises from discernible industrial waste and byproducts, in addition to the application of chemicals, including synthetic fertilizers in agriculture and insecticides. It also originates from refuse generated by residences, structures, and various establishments [119]. The issue of pollution escalates with the rise in chemical production and utilization in companies, as the disposal of these substances contaminates the soil, water, and the environment overall. The magnitude of the pollution issue stemming from industry escalates when there is negligence or disinterest in the proper disposal of chemical factory waste, hence, safeguarding soil and water from contamination.

The soil and water often contain various dangerous substances, i.e., microbiological pathogens, organic (herbicides, insecticides, phenols, and hydrocarbons), and heavy-metallic (lead, cadmium, arsenic, and mercury) ones. These environmental pollutants possess a considerable capacity to negatively impact human health [120].

The pollution of air, water, and soil is a worldwide concern with significant consequences for the ecosystem and human society. The elimination of various contaminants, including inorganic and organic chemicals, from the environment presents a significant problem. Adsorption techniques are commonly utilized because of their inherent simplicity and outstanding efficiency [121].

The adsorbing capacity of the material depends mostly on its inherent properties, most importantly, its porous structure and its surface chemistry. Consequently, the adsorption procedure is acknowledged as a straightforward, simply executed, and efficient technique for the elimination of diverse contaminants [122, 123]. Furthermore, the adsorption process can prevent the secondary pollution because it does not produce any harmful byproducts.

The efficiency of an adsorption system is dependent on the selection of an appropriate adsorbent. Optimal adsorbents are characterized by a high specific surface area, high pore volume, and surface groups with good interaction with contaminants. This has fuelled the massive work carried out on porous materials to clean the environment. Developers have manufactured a various of options, including activated carbon, pillared clays, zeolites, mesoporous oxides, polymers, and metal-organic frameworks, all of which exhibit a different degree of proficiency in extracting toxic waste in air, water, and soil [123-126].

1.10.1 Air Pollution

Air pollution is one of the most acute problems of our time that affects climate change and predetermines increased morbidity and mortality. The complex combination of pollutants in the form of particulates in the air and ozone in the atmosphere has proven to be a major cause of environmental health hazards in all regions of the world [127]. These contaminants have been associated with a vast range of diseases, with the respiratory and cardiovascular systems being the most predominant. Chronic obstructive pulmonary disease (COPD), asthma, lung cancer, and several cardiovascular events are often associated with air pollution [127]. Recent multi-city studies indicated that fine particulate matter (PM2.5) and ozone interact in a so-called synergistic manner; each pollutant increases the harmful effects of the other one, resulting in increased risks of total, cardiovascular, and respiratory deaths [128].

1.10.2 Soil Pollution

Soil pollution is caused by a combination of perpetrators, industrial activities and military conflicts, mining operations, and the aggravation of modern farming, which results in soil pollution as an ever-growing environmental threat. This contamination adversely impacts human life, vital flora and fauna, industrial progress, living standards, and cultural heritage [129]. Diffuse pollution is a kind of danger, especially sneaky in nature; it spreads over large distances and often goes unnoticed. Natural and man-made agents can contaminate the soil. The natural culprits are geogenic contaminants, like the background radioactivity, volcanic ash, and naturally occurring polycyclic aromatic hydrocarbons (PAHs). The anthropogenic ones, however, take the first aspect of the list: industrial activities, by-products of household and city waste, mining, extraction of fossil fuels, infrastructure development, transport, and poor disposal of domestic chemicals and plastics all contribute to the silent contamination of soil [130].

1.10.3 Water Pollution

There are four major sources of water contamination: industrial activity, agriculture, natural events, and ineffective systems of water and sewage. Industry is the worst offender among them. The industries of distilleries and tanneries to pulp and paper, textiles, food processing, iron-steel production, and even nuclear facilities produce a cocktail of pollutants—everything, including heavy metals and organic acids, inorganic salts, and volatile organic compounds. When these wastes go unresolved through proper treatment, they cause havoc to rivers, lakes, and groundwater and convert what was once a clean water body into a dead trap [131, 132]. The pollutants are broadly classified into two categories, namely organic and inorganic. These contaminants are manifested in a wide variety of forms in wastewater: physical, chemical, biological, and even radiological, and each of them requires a specific approach to removal. Figure 1-11 illustrates the process of transforming dirty water into clean and usable water in a sequence of specific treatments that remove every form of contamination [133]. A typical ion-exchange unit, which removes dissolved anions and cations, usually initiates the treatment process. This is then followed by electrochemical cells targeting stubborn pollutants and then bioremediation, which feeds microbes to degrade organic substances. The flocculation and precipitation then agglomerate loose particles, and it becomes easy to skim them away. Adsorption rescues the difficult-to-get traces. Activated carbon, biochar, or advanced nanoparticles introduce enormous surface areas and specific functional groups, which bind to heavy metals, dyes, pesticides, and pharmaceuticals and drag them out of the water column at even small concentrations. The pH is then adjusted by neutralization, dissolved gases are removed by aeration, and the solids that remain are brought to the surface by settling. A polish is provided by filtration and a disinfectant of choice (ozone, chlorine, or UV) to wipe the remains of the pathogen and any other fine particulates. It is through these processes woven together that the wastewater is converted into clean, safe water to be either reused or discharged [134].

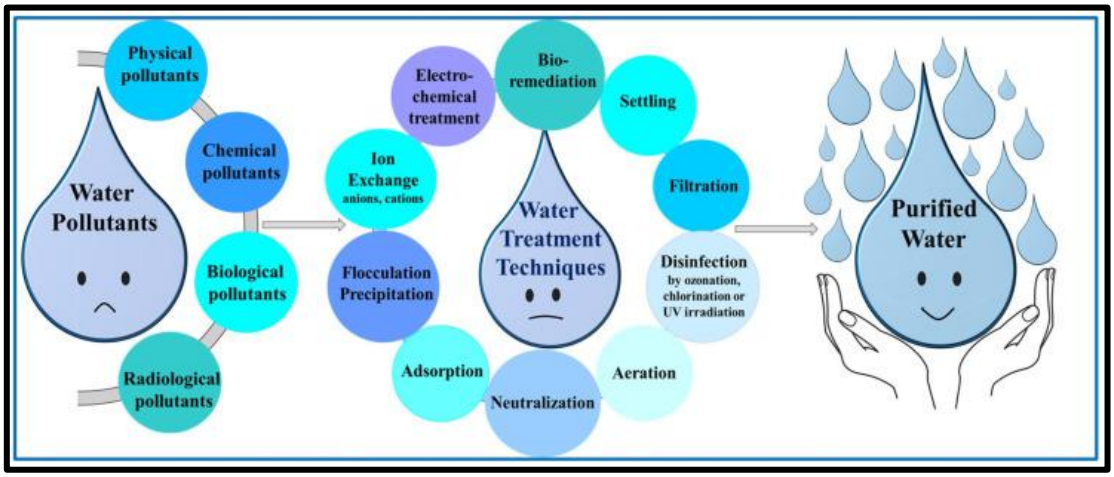

Figure 1-11 *Water treatment technologies used to obtain purified water* [108]

1.11 Types of Pollutants

1.11.1 Inorganic Pollutants

Chemical pollution is the primary source of most contaminants in aqueous solutions, a category that encompasses heavy metals such as Cu, Cr, Pb, and Ni, as well as metalloids like Se and As [135].

Common inorganic substances in water include heavy metals, halides, oxyanions, cations, and radioactive materials. Due to their non-biodegradable nature, these inorganic pollutants can persist in aqueous systems for extended periods, leading to the progressive deterioration of water quality [136].

1.11.2 Organic Pollutants

Organic pollution occurs when excessive amounts of organic compounds are introduced into a water body. These pollutants include a wide range of substances such as pesticides, fertilizers, hydrocarbons, phenols, plasticizers, detergents, oils, pharmaceuticals, proteins, and carbohydrates. The primary sources are domestic sewage, urban runoff, agricultural wastewater, and industrial effluents, particularly from sewage treatment plants and industries like food processing,

pulp and paper manufacturing, and aquaculture. The decomposition of these organic pollutants by microorganisms consumes dissolved oxygen, often at a rate faster than it can be replenished. This leads to oxygen depletion, which has severe consequences for aquatic biota. Furthermore, wastewater containing organic pollutants often carries high quantities of suspended solids. These solids reduce light penetration, inhibiting photosynthesis, and alter the riverbed upon settling, rendering the habitat unsuitable for many invertebrate species [137, 138]. Among the most prevalent organic pollutants are dyes, which have been selected as the major pollutant of focus for this thesis due to their widespread use and environmental impact.

1.12 *Dyes*

The dye industry produces about 700,000 tonnes of dye annually, comprising more than 10,000 types of dyes, of which the majority are required by the textile industries. Using such dyes in the environment is highly dangerous due to their long-lasting effect, taking months or years; they may be toxic to a wide variety of organisms, and they accumulate in the living tissues. The most popular and hazardous azo dyes with a benzidine core are the most common of them and of particular concern because of their carcinogenic nature and thus require immediate examination and measures to be taken [139]. This paper analyzes the present condition of cationic and anionic dyes.

Dyes represent a significant environmental hazard to water ecosystems. Their inherent toxicity and propensity to absorb sunlight disrupt aquatic photosynthesis, compromising the well-being of these environments. Consequently, the removal of dyes from wastewater is a subject of major importance worldwide [140-143].

Techniques to eliminate organic dyes in water are broadly classified into three categories, namely physical, chemical, and biological. Physical methods typically consist of adsorption, coagulation/flocculation, or filtration. Electro-Fenton reactions, photocatalysis, or ozonation are frequent chemical processes on which

chemical treatment is based. Biological methods involve the use of enzymes and microbes for processes such as biosorption and biodegradation. The identification of an excellent method is dependent on a particular kind of dye and the manufacturing environment where it is used [144].

The coloration of natural dyes is caused by chromophores, which are responsible for the absorption of light. Chromophores tend to be conjugated π electron systems, i.e., think of the double bonds or the aromatic rings, which absorb specific colors of visible light. On the other hand, auxochromes are functional groups that improve the color of the dye and stabilize its color. They achieve these effects by extending the conjugation of the chromophore or by facilitating a stronger bond with the substrate [145]. They cause the molecule containing them to turn chromogenic [146]. The only way to dye a chromogenic molecule is to add additional atom groups known as "auxochrome" [146]. Auxochromic groups are used both to adjust the color of the dye and to fix it onto the surface. These groups are divided into two basic groups (e.g., $-NH_2$, -NHR, $-NR_2$) and acidic groups (e.g. -COOH, $-SO_3H$, -OH). The remaining atoms of the molecular structure constitute the third component of the dye, which is known as the matrix [147]. Functional compounds included in textile dyes, such as carboxylic, amine, and azo groups, are difficult to handle using traditional techniques [148].

1.12.1 Methylene Blue Dye (MB)

Methylene blue (MB) is a widely used cationic dye known for being environmentally persistent, toxic, carcinogenic, and mutagenic. It is commonly applied in the textile, paper, and leather industries to dye various materials. Consequently, large volumes of wastewater containing MB are discharged into ground and surface water. MB poses a significant risk to human health; at doses exceeding 5 mg/kg, its monoamine oxidase inhibitory properties can induce fatal serotonin toxicity. It also presents a threat to the fauna of aquatic ecosystems. Therefore, the removal of MB from wastewater is imperative, and various

removal strategies have been reported in the literature to address this contamination [149].

Methylene blue (3,7-bis(dimethylamino)phenothiazin-5-ium chloride) (Figure 1-12) is one of the synthetic dyes that are widely used as a colorant for materials such as paper, wool, silk, and cotton [149, 150]. In addition, the food, cosmetics, and pharmaceuticals industries are not left behind in consuming a large quantity of MB dye for their productions [151]. It is used in various fields such as medicine, biology, and chemistry [152, 153] However, MB is mostly used in textile industries for coloring fabrics.

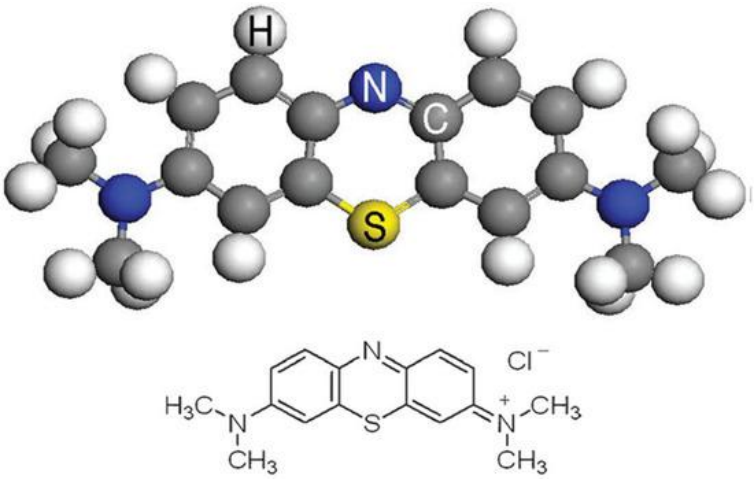

Figure 1-12 *Methylene blue molecular structure and model* [149]

1.12.1.1 Properties of Methylene Blue

MB is a solid, odorless, dark green powder at room temperature and yields a blue solution when dissolved in water [154, 155]. MB dye has a pK_a of 3.8 [156, 157]. It is soluble in methanol, 2-propanol, water, ethanol, acetone, and ethyl acetate [158]. The point of melting (Tm) of MB ranges from 100 to 110 °C [159].

1.12.1.2 Applications of Methylene Blue Dye

Methylene blue, a phenothiazine dye with a rich history dating back to the 19th century, it has transcended its initial use as a textile colorant to become a molecule of significant and expanding interest across various scientific disciplines [160]. While traditionally recognized for its role as a biological stain and in the treatment, of methemoglobinemia, recent research has illuminated its vast therapeutic potential and diverse applications [160, 161]. Extensive modern studies are exploring its efficacy in neurodegenerative diseases, such as Alzheimer's, by targeting mitochondrial dysfunction and protein aggregation [162]. Furthermore, its role as a photosensitizer in antimicrobial and anticancer photodynamic therapy is a rapidly growing field of investigation, with systematic reviews confirming its effectiveness against various cancer types in preclinical studies [163]. Beyond its medical uses, methylene blue is also being investigated for its utility in environmental remediation to remove pollutants from wastewater, highlighting the compound's remarkable versatility [161, 164]. This multifaceted nature, from neurology to oncology and environmental science, underscores the continued relevance and promising future of methylene blue in scientific research and clinical practice.

1.12.1.3 The Toxicity of Methylene Blue Dye

The paradoxical nature of methylene blue, which has been long used both in medicine and industry, is that it is a therapy drug and a highly toxic environmental pollutant. It has clinical applications in the treatment of methemoglobinemia and vasoplegic syndrome when used in the treatment of encephalopathy induced by ifosfamide, and there is an active body of research on its neuroprotective role. But its increasingly toxic history is of concern [162, 165]. In humans, the dose-response relationship of toxicity is increasing: toxicity causes severe effects at high levels, such as hemolysis, chest pain, and hypertension, and in combination with serotonergic compounds, it has the potential to cause a potentially lethal serotonin syndrome [165]. In addition to the clinic, methylene blue is considered a hazardous, carcinogenic, and non-biodegradable pollutant as it leaks out during the industrial processes, particularly in the production of textiles, into the water bodies. The resultant effluent is harmful to the aquatic life and may have devastating health effects on men, leading to respiratory discomfort, digestive diseases, and even tissue necrosis due to polluted water [160]. Due to the two vastly different functions of methylene blue, it is important to examine its toxicology carefully; hence, to ensure that its clinical benefits will not be at the cost of environmental protection and human health.

1.12.1.4 Adsorption of Methylene Blue Dye

To address difficult pollutants in the water, particularly the biodegradable pollutants, adsorption is widely applied. Therefore, a significant amount of research has been dedicated to eliminating such contaminants like methylene blue (MB) in industrial wastewater sources, especially that produced by the textile, paper, and printing industries [166]. Various treatment methods, such as physical, chemical, and biological methods, have evolved to eliminate the dyes in

wastewater [167]. Even though these approaches perform well, they are stuck with the disadvantages, which include the formation of toxic by-products, intensive energy use, and costly nature [168].

Table (1-3) provides a qualitative evaluation of the primary chemical techniques utilized for the elimination of methylene blue (MB) from aqueous solutions. The analysis compares the two treatments based on their efficiency, selectivity, the speed of a reaction, amount of waste, and energy consumption, relying on peer-reviewed studies published within the preceding seven years. In general, adsorption is characterized by high efficiency of removal, a minimum of energy requirement, and a low generation of waste. Conversely, the advanced oxidation processes (AOPs) and photocatalysis have rapid comprehensive degradation but at a higher energy cost. Fenton oxidation proffers rapid reaction and high efficiency but amounts to a lot of sludge. A good amalgamation of high removal and rapid response is offered by electrocoagulation, which has the drawbacks of moderate waste production and higher energy usage. Lastly, the conventional chemical precipitation and coagulation/flocculation are still effective in the removal of methylene blue and are associated with increased sludge volumes. This comparative study enables one to make informed decisions on which technique to use depending on the task at hand and also the environmental effect. The adsorption process has been widely used effectively for the removal of colorants from wastewater due to the low cost, regeneration, and reusability of the adsorbents [169, 170].

The experiments look into the adsorption of methylene blue (MB) onto nanofibers and the effect of the pH of the solution and initial dye load. The result show a significant enhancement in adsorption capacity, particularly in the case of the addition of chitosan (Chi), because the PAA-Chi nanofibers demonstrate excellent functionality. The pH-dependent trend highlights how the environmental conditions contribute to the adsorption process, and greater concentrations of the dye give a greater force to the nanofibers to adsorb the pollutant [171].

Table 1-3 *Comparison of Methylene Blue Removal Methods*

Method	Efficiency	Selectivity	Kinetics	Waste Generation	Energy Consumption	Reference
Adsorption	High	Moderate	Moderate	Low	Low	[172]
Photocatalysis	High	Low	Moderate	Low	Low	[173]
Fenton Oxidation	High	Low	High	High	Moderate	[174]
Advanced Oxidation	High	Low	Moderate	Low	High	[160]
Electrocoagulation	High	Low	High	Moderate	High	[175]
Chemical Precipitation	Moderate	Low	Moderate	High	Low	[175]
Coagulation /Flocculation	High	Moderate	High	Moderate	Low	[176]

1.13 The Aims of This Study

1- **To synthesize optimal PAA-Chi (70:30 ratio) using electrospinning techniques:** Develop electrospun nanofiber materials by incorporating functional nanomaterials into polymer matrices to enhance surface properties and adsorption efficiency.

2- **To characterize the synthesized PAA-Chi nanofibers using various analytical techniques:** Employ techniques such as Field Emission Scanning Electron Microscopy (FESEM), Fourier Transform Infrared Spectroscopy (FTIR) and zeta potential.

3- **To examine the adsorption efficacy of the composites in eliminating Methylene Blue dye from aqueous solutions:** Analyze parameters like initial dye concentration, contact time, and pH for determining the ideal adsorption conditions.

4- **To Apply adsorption isotherm and kinetic models to understand the adsorption mechanism**: Analyze experimental data using models such as Langmuir and Freundlich isotherms and pseudo-first-order and pseudo-second-order kinetic models to elucidate the adsorption process.

Chapter Two

Experimental

2.1 Equipment and Materials

This investigation presents the instruments used in the study including their models, manufacturers, and origins in Table 2-1, and the chemical compounds in Table 2-2.

Table 2-1 *Equipment utilized in the investigation, models, corporations, and sources*

Ser.	Device	Company	Source	Laboratory
1	Field Emission Scanning Electronic Microscope (FESEM)	Zeiss	Germany	Tehran University/ Advanced Materials Characterization Institute
2	UV-Vis. Spectrophotometer, UV-1800	Shimadzu	Japan	University of Misan /College of Science/ Chemistry Dept.
3	pH meter, pH 7110	Inolab	Germany	University of Misan / College of Science/ Chemistry Dept.
4	Stirring water bath, KBLEE 2010	Daiki	Japan	University of Misan / College of Science/ Chemistry Dept.
5	FT-IR Spectrophotometer, FT-IR-1800	Shimadzu	Japan	Tehran University/ Advanced Materials Characterization Institute
6	Electrospinning Machine, 2ESII-II	Nanoazma	Iran	Ahvaz Jundishapur University/ Nano Technology Research Center

Table 2-2 *Utilized chemicals, chemical formula, manufacturer, and source*

Ser.	Chemicals	Chemical Formula	MW g/mol	Company	Source	Purity
1	Chitosan	$[C_6H_{11}NO_4]_n$	300000	SDFCL	India	75%
2	Poly Acrylic Acid	$[C_3H_4O_2]_n$	250000	Sigma Aldrich	USA	-
3	Methylene blue	$C_{16}H_{18}ClN_3S.$ xH2O(x=2,3)	355.88	Thomas Baker	India	99%
4	Hydrochloric acid	HCl	36.46	Applichem	USA	97%
5	Sodium hydroxide	NaOH	39.997	Chem Lab	UK	98%
6	Acetic Acid	$C_2H_4O_2$	60.052	SDFCL	India	99%
7	Formic Acid	CH_2O_2	46.03	Alpha Chemika	India	98%

2.2 Preparation of PAA–Chi Electrospinning Nanofibers

Polyacrylic acid-chitosan nanofiber synthesis using the electrospinning technique in a 50:50, 70:30, and 85:15 ratios required a sequence of perfectly organized processes aimed at producing homogeneous and functional fibers suitable for the development of various applications. Electrospinning is an adaptable system to use in the creation of polymeric fibers of nanometer to micrometer diameter and provides a high surface area and porosity, which are important characteristics in biomedical and environmental use.

It was initiated by making individual solutions of polyacrylic acid (PAA) and chitosan (Chi). Chitosan, which is soluble only under acidic conditions, was solubilized in a 2% (v/v) acetic acid solution to a concentrations of 1.5%, 2.5%, and 0.75% (w/v). At the same time, polyacrylic acid was also dissolved in deionized water to 3.5%, 2.5%, and 4.25% (w/v) concentrations. The resulting solutions were stirred by vigorous stirring until fully dissolved.

The two polymer solutions were then mixed in their 70:30, 50:50, and 85:15 proportion weight of PAA to Chitosan following the dissolution process. Then the mixture was stirred for several hours to ensure uniformity and prevent the separation of phases. The final blend was then measured and adjusted in terms of viscosity and conductivity as well as pH. The pH was governed to be 4-5 so that the chitosan remains soluble and is made compatible with PAA, and the viscosity was adjusted to allow the relationship of continuous formation of fibers during electrospinning [171].

The metallic needle was used to insert the homogeneous polymer blend into a syringe. A grounded collector, a syringe pump, and a high-voltage power supply comprised the electrospinning apparatus. A voltage of 25 kV was applied between the collector and the needle, which was positioned 15 cm from the needle point. The flow rate of the polymer solution was maintained at 1.5 ml/hr. The PAA-Chi solution under the effect of the electric field was pulled off the tip of the needle to form a jet, which extended and solidified into nanofibers with the evaporating solvent [60].

Conversely, the electrospinning procedures reported in Table 2-3 did not yield any products when using nanofibers with PAA/Chi proportions of 50:50 and 85:15. The mixture of polymers at a 50:50 ratio had an overly high viscosity due to the large share of chitosan with high molecular weight; thus, the solution solidified in the syringe, and a small amount appeared as discrete strands punctuated by beads and nodes, which is evidence that the polymer jet was not

stable, and it was not able to form continuous fibers. On the other hand, the 85:15 ratio resulted in a mixture that was not viscous enough to allow the entanglement of the chain, hence suppressing any fiber development. The process instead got deviated to spraying drops and a fine mist from the syringe tip, and no fiber structure could develop. These facts reveal the importance of solution rheology and viscosity, in particular, and molecular-weight-induced entanglement, in particular, when it comes to the viability of the electrospinning method. Low-viscosity solutions result in droplet formation instead of fibers, but excessive viscosity prevents the formation of jets and clogs the spinneret; hence, the need to balance these parameters to guarantee nonstop and flawless nanofiber growth [177].

Table 2-3 *Electrospinning performance and outcomes of different PAA–Chi blending ratios.*

PAA:Chi Ratio	Observation/Outcome	Reason for Success or Failure
70:30	bead-free, Uniform, continuous nanofibers	Balanced viscosity and chain entanglement enabled stable jet formation and solvent evaporation.
50:50	Solidification inside syringe, discontinuous fibers with beads and nodes	Excessive viscosity caused by high molecular weight chitosan prevented smooth flow and a stable jet.
85:15	No fibers, only droplets/mist formation	Very low viscosity, insufficient polymer chain entanglement, leading to electrospraying instead of electrospinning.

2.3 Rheological Behavior Method

Using a rheometer, we measured the nanofiber solutions' rheological properties. At different temperatures and shear rates, the viscoelastic and viscosity characteristics of PAA-Chi solutions (30% Chi) were tested [178]. Rheological test results offer insight on the solutions' viscoelastic properties and flow behavior, revealing whether or not they were suitable for the electrospinning process.

2.4 Zeta Potential

To determine the zeta potential of the PAA-Chi nanofibers and observe the variation in the surface charge, we measured the zeta potential of the nanofibers at Malvern Zetasizer (Malvern Instruments, UK). To test the suspension, we used ultrasonic dispersion of nanofibers in DMSO (0.01 g/100 mL) to make a suspension. The process is done at room temperature.

2.5 Sample Preparation

2.5.1 Stock Solution of MB Dye (1000 mg/L)

A methylene blue (MB) solution (molecular weight = 319.86 $g.mol^{-1}$) was made by dissolving 100 mg of the dye in deionized water in a beaker. Subsequently, it was directly transferred to a volumetric flask with a volume of 100 ml and diluted to the calibration mark with deionized water. Standard solutions (50, 100, and 200 mg/L) were prepared via serial dilution of the stock solution.

2.6 Determination of Calibration Curve

To determine the standard calibration curve for MB dye, a series of standard solutions (0-100 mg/L) of methylene blue dye were prepared. Absorbance measurements were carried out at a wavelength of 664 nm employing a UV–Visible spectrophotometer. The absorbance values of the prepared solutions were recorded as shown in the table (2-4), and the absorbance values were plotted against the concentration to obtain the standard calibration curve as shown in the figure (2-1).

Table 2-4 *Concentrations of methylene blue standard solutions and their corresponding absorbance values at λmax = 664 nm.*

Concentration $mg.L^{-1}$	Absorbance
0	0
10	0.067
20	0.125
30	0.185
40	0.259
50	0.341
80	0.587
100	0.812

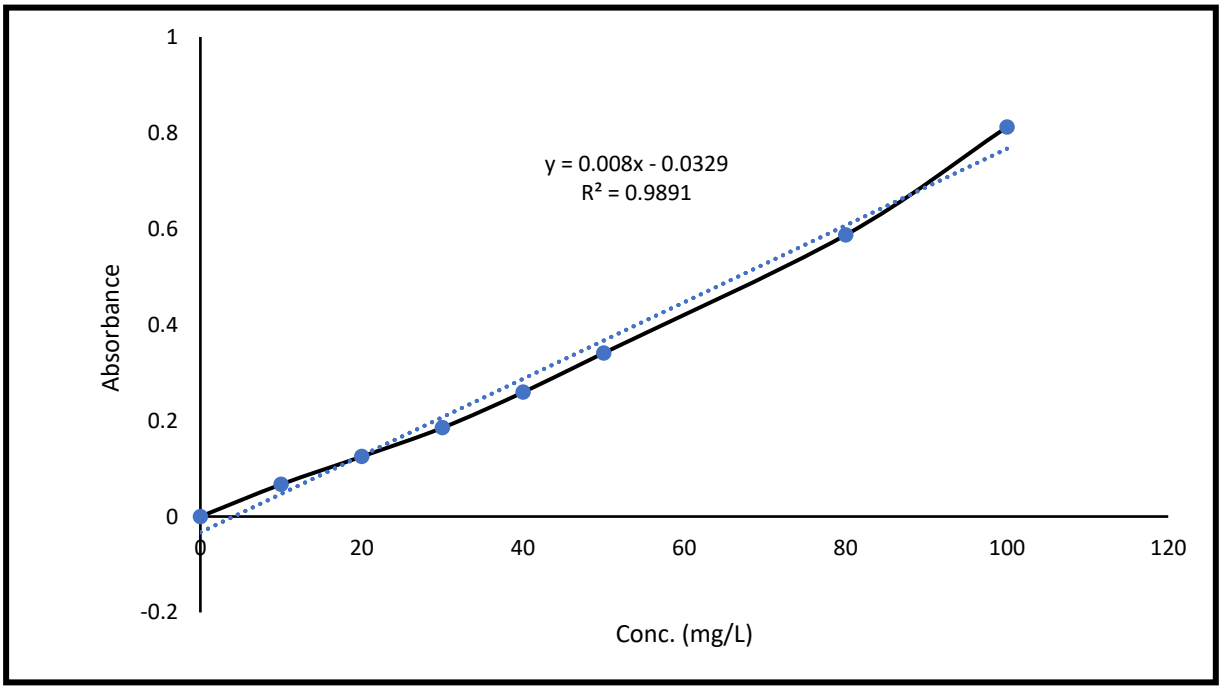

Figure 2-1 *Standard calibration curve for MB dye at 664 nm.*

2.7 Dye Adsorption Measurement of PAA-Chi NFs

Systematic adsorption of dye on the PAA-Chi NFs was conducted in a batch-type of equilibrium under controlled conditions of the environment as represented in Figure 2-2. Experiments of all adsorption were carried out at room temperature (25°C) by constant agitation at 100 rpm to achieve uniform distribution and to limit the effect of mass transfer. In both of the tests, the dry weight of the composite (10 + 0.0001 mg) was introduced into a 50 mL methylene blue solution, which had an initial concentration of 100 $mg.L^{-1}$ and a pH of 6. After the adsorption, the composite underwent centrifugation at 5000 rpm for a duration of 5 minutes. The remaining dye in the supernatant was measured using UV-Vis 1800 (Shimadzu, Japan) at 664 nm. To achieve accurate quantification, an MB dye calibration curve against its 664 nm maximum was drawn. The adsorption capacity of the PAA-Chi nanocomposite (q_e) and the dye removal efficiency (R) were obtained by using the following equations:

$$q_e = \frac{(C_0 - C_e) \times V}{W} \qquad Eq.(1)$$

$$R\% = \frac{(C_0 - C_e)}{C_0} \times 100 \qquad Eq.(2)$$

q_e is the capacity of PAA-Chi NFs (mg/g) to adsorb. C_o and C_e are the concentrations of initial and equilibrium dyes (mg/L), respectively. V and W are the dry weight of PAA-Chi adsorbent (g) and the solution volume (L).

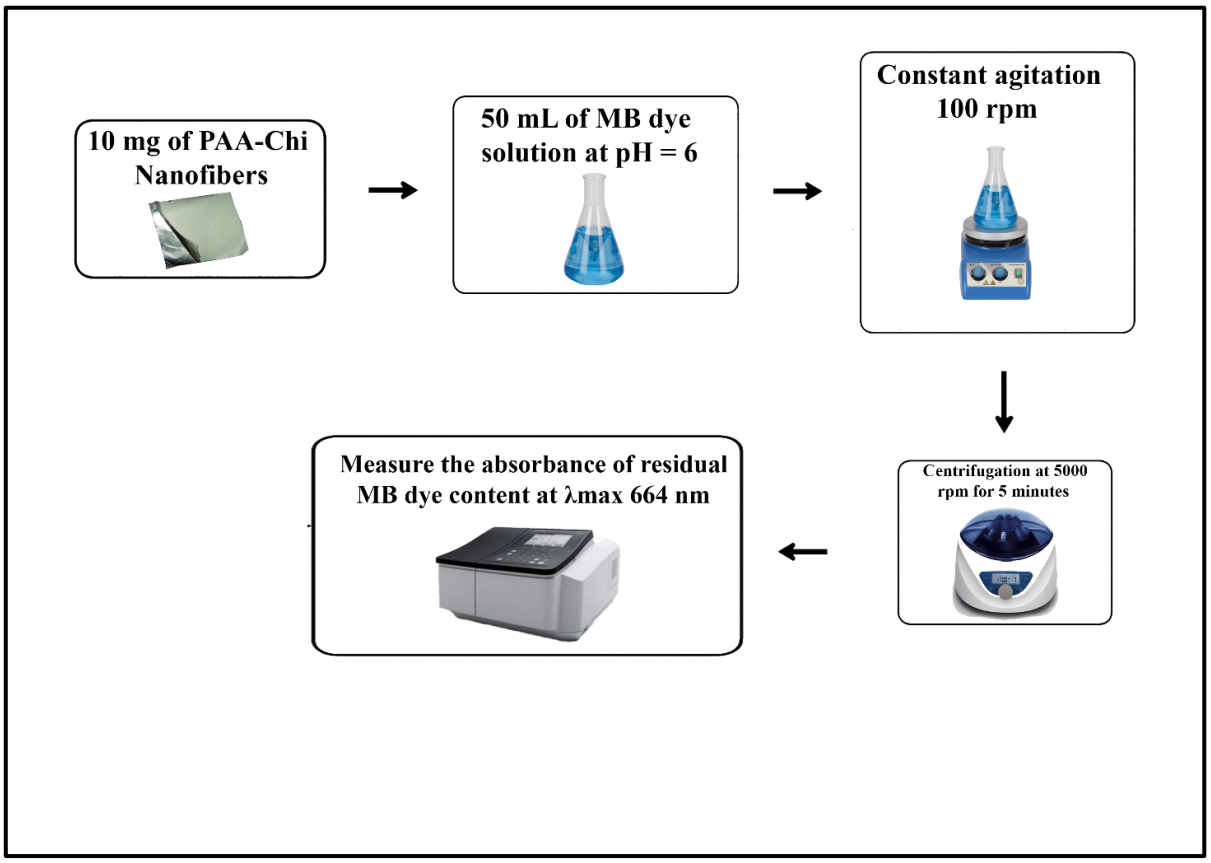

Figure 2-2 *Flow diagram of methylene blue adsorption experiment*

2.8 Quality Control and Quality Assurance (QC/QA)

To ensure the reliability and reproducibility of the results, all adsorption experiments were conducted in triplicate, and the result values are reported in the mean ± standard deviation. Blank samples where the Methylene Blue (MB) was placed in distilled water with no adsorbent were also done as control experiments to verify that there were no interferences. Calibration of the spectrophotometer was done periodically using standard solutions, and before every measuring series, the spectrophotometer was set on a baseline to ensure analytical accuracy.

2.9 Study of the Effects of MB Dye Concentration

The concentration of methylene blue (MB) dye on its adsorption character was examined by making a range of MB solutions prepared with initial concentrations of 50, 100, and 200 $mg.L^{-1}$ in 50 mL volumetric flasks. Then, PAA-Chi nanofibers (10 mg) were added to the solution, and the adsorption process was followed at various contact periods (1, 2, 4, 6, 8, 10, 12 h). 5 mL of aliquots were sampled with a syringe, and nanofibers were centrifuged at a speed of 5000 rpm in 5 minutes. The residual dye concentration was then determined by measuring the absorbance at the peak wavelength of 664 nm.

2.10 Study of the MB Dye's pH Effect

Methylene blue (MB) dye was first prepared at 100 mg/L before the adjustment of its pH value to various desired values (2, 4, 5, 6, 7, 8, and 10) was maintained by adjusting with 0.1 M HCl and 0.1 M NaOH to the solution in a 50 mL solution flask, which was monitored with a calibrated pH meter. The initial absorbance measured 664 nm. The adsorption process was monitored (12 hours) following the addition of 10 mg of PAA-Chi nanofibers to the solution. A 5 mL sample was extracted using a syringe, and the nanofibers were centrifuged at 5000 rpm. The

residual dye concentration was then determined by measuring the absorbance at the peak wavelength of 664 nm.

2.11 Kinetic and Isotherm Method

2.11.1 Kinetic Model Fitting of MB Adsorption

To conduct a more thorough examination of the adsorption dynamics of MB on the PAA-Chi composites, two kinetic models, namely pseudofirst-order and pseudosecond-order, were employed. These two models are described by equations (3) and (4), respectively [179, 180]:

$$Log(q_e - q_t) = Log\ q_e - K_1 t \qquad Eq.(3)$$

$$\frac{t}{q_t} = \frac{1}{K_2 q_2^2} + \frac{t}{q_e} \qquad Eq.(4)$$

The equilibrium quantity of methylene blue (MB) adsorbed is denoted by q_e (mg/g), where q_t expresses the amount of dye adsorbed at time t. The pseudofirst-order and pseudosecond-order models were utilized to assess the kinetics of adsorption. (K_1 min^{-1}) and (K_2 $g.mg^{-1}$ min) were utilized to ascertain the relevant rate constants. According to the pseudofirst-order model, at any time t is directly proportional to the difference between (q_e), the equilibrium capacity, and the amount adsorbed at time (q_t). This model is presumed to be relevant during the initial phases of physical adsorption or interactions occurring on surfaces with minimal adsorbate presence.

2.11.2 Isotherm Model Fitting of MB

To investigate the equilibrium adsorption of PAA-Chi NFs, the Langmuir and Freundlich isotherm models were used. This is indicated in equations 5-6 [179]:

$$\frac{C_e}{q_e} = \frac{1}{q_0\ K_L} + \frac{1}{q_0 C_e} \qquad Eq.(5)$$

$$Log\ q_e = \log K_f\ + \frac{1}{n}\ Log\ C_e \qquad Eq.(6)$$

The Langmuir isothermal constant, denoted by K_L ($L.mg^{-1}$) and q_0 ($mg.g^{-1}$), denotes the adsorption rate and adsorption capacity, respectively. The Freundlich constants for adsorption capacity and strength are denoted as (K_f L/g) and 1/n, respectively.

Chapter Three

Results and Discussion

3.1 Fabrication and Characterization of PAA–Chi NFs

Recent research has focused on nanofibrous materials because of their high specific porosity surface area and adjustable structural properties. Electrospinning produces nanofibers from various polymer mixtures precisely and efficiently. Due to various basic factors, electrospinning polyacrylic acid-chitosan (PAA-Chi) composite nanofibers has become important. The goal was to employ PAA and Chi to create a material with better MB adsorption. Electrospinning is ideal for making practical materials due to its adaptability and customization.

3.2 Fourier Transform Infrared (FT-IR) Spectroscopy

The FTIR spectra are presented in Figure 3-3, and Table 3-3 of PAA, Chi, and the synthesized PAA–Chi nanofibers (NFs) confirm the successful interaction between the two polymers.

In the spectrum of pure PAA (Figure 3-1) and Table 3-1, a wide band at 3441.55 cm^{-1} correlates to O–H stretching vibrations, whereas the presence of a peak at 1730.20 cm^{-1} indicates the C=O stretching vibration characteristic of carboxylic groups. The band at 2947.77 cm^{-1} reflects the stretching vibrations of $–CH_2$ and –CH groups inside the polymer backbone [181].

Table 3-1 *FTIR spectral analysis of pure PAA showing characteristic absorption bands, bond types, and functional group assignments.*

Wavenumber (cm^{-1})	Vibration Type	Bond Type	Functional Group / Source
3441.55	O–H stretching	O–H	Hydroxyl group in PAA
1730.20	C=O stretching	Carboxylic (C=O)	Carboxylic groups in PAA
2855.68	$–CH_2$ / –CH Symmetric	C–H	Aliphatic backbone of PAA
2947.77	$–CH_2$ / –CH Asymmetric		

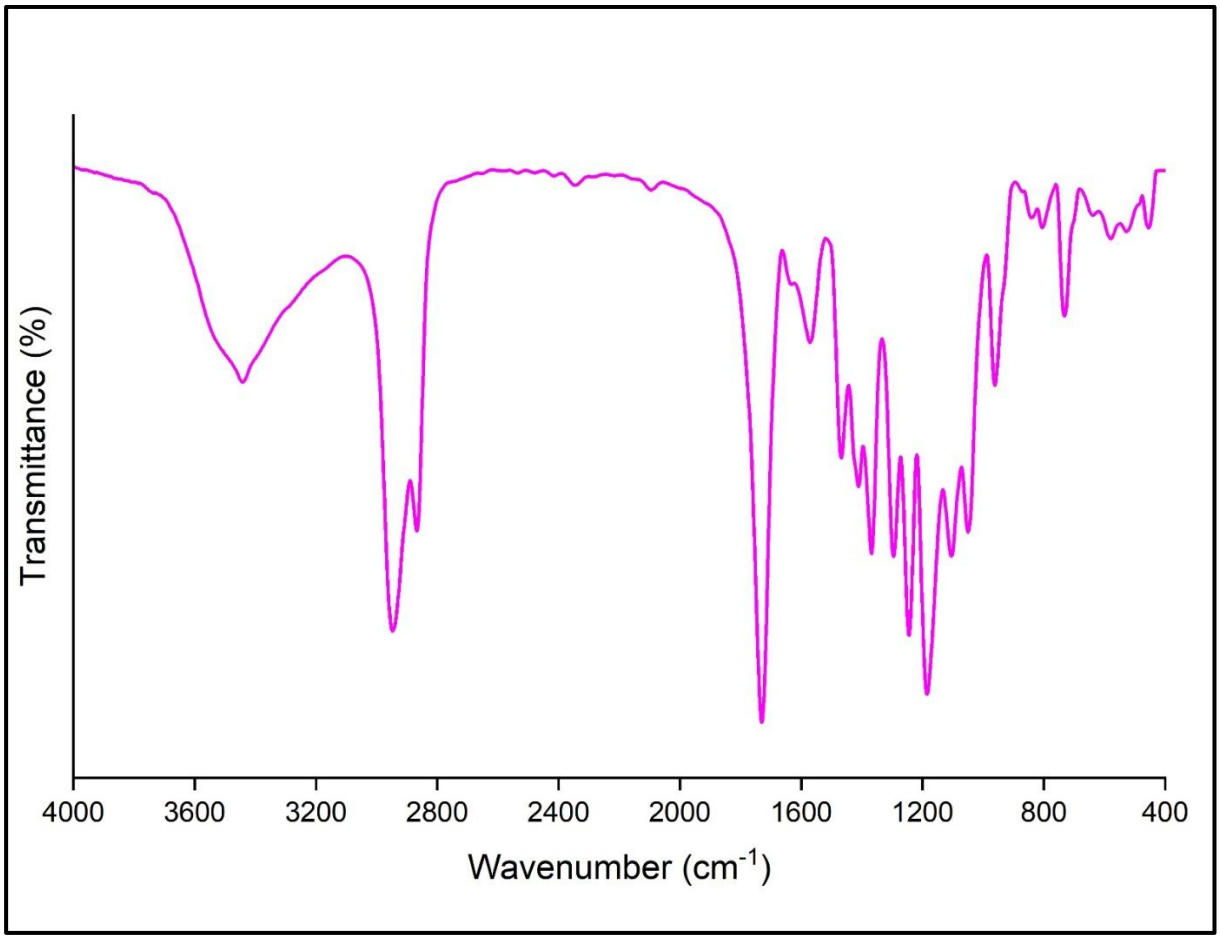

Figure 3-1 *FT–IR spectra of pure Polyacrylic Acid (PAA)*

The chitosan spectrum (Figure 3-2) and Table 3-2 exhibit a broad band at 3452.72 cm^{-1} due to overlapping O–H and N–H stretching vibrations, indicative of extensive hydrogen bonding. Peaks appearing at 1654.41 cm^{-1} and 1590.41 cm^{-1} can be attributed to the amide I (C=O stretching) and amide II (N–H bending) vibrations of residual acetyl groups, respectively. The C–H stretching vibration appears at 2857.43 cm^{-1}, while the band at 1403.3 cm^{-1} corresponds to C–N and C–O stretching vibrations.

Table 3-2 *FTIR spectral analysis of pure Chi showing characteristic absorption bands, bond types, and functional group assignments.*

Wavenumber (cm^{-1})	Vibration Type	Bond Type	Functional Group / Source
3452.72	O–H / N–H stretching (overlapping)	O–H and N–H	Hydroxyl and amine groups in chitosan
1654.41	C=O stretching (Amide I)	Amide C=O	Residual acetyl groups in chitosan
1590.41	N–H bending (Amide II)	Amide N–H	Residual acetyl groups in chitosan
2857.43	C–H stretching	C–H	Aliphatic groups in chitosan
1403.30	C–N / C–O stretching	C–N and C–O	Present in chitosan structure

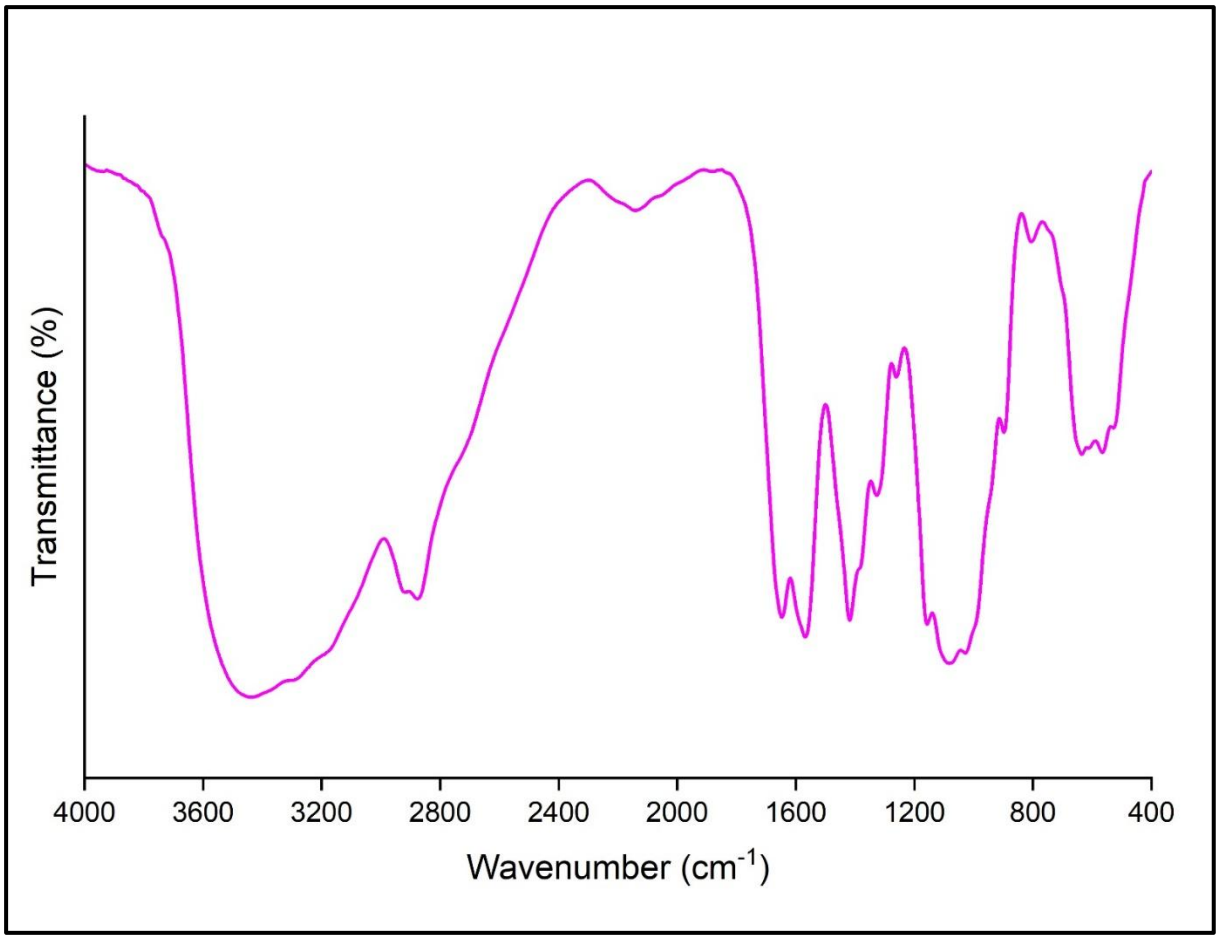

Figure 3-2 *FT–IR spectra of Pure Chitosan (Chi)*

In the FTIR spectrum of the PAA–Chi nanocomposite (Figure 3-3) and Table 3-3, noticeable shifts and reductions in peak intensity were observed in the characteristic absorption bands of both polymers. Any shift in the O–H and N–H stretching region indicates the formation of H-bond between the carboxylic group of polyacrylic acid and the NH_2 or OH groups of chitosan. Additionally, the C=O stretching peak of PAA and the amide I/II bands of chitosan exhibit shifts and noticeable intensity changes, further confirming the interaction. These spectral modifications support the formation of a new intermolecular network between PAA and Chi through hydrogen bonding and possible electrostatic interactions, contributing to the structural integrity and enhanced functionality of the nanofibers.

Table 3-3 *FTIR spectral analysis PAA–Chi nanofibers showing characteristic absorption bands, bond types, and functional group assignments.*

Wavenumber (cm^{-1})	Vibration Type	Bond Type	Functional Group / Source
(Shifted region)	O–H / N–H stretching (shifted)	Hydrogen bonding	Indicating H-bonding between PAA and Chi in nanocomposite
(Shifted region)	C=O and Amide I/II shifts	C=O and N–H	Interaction between PAA and Chi functional groups

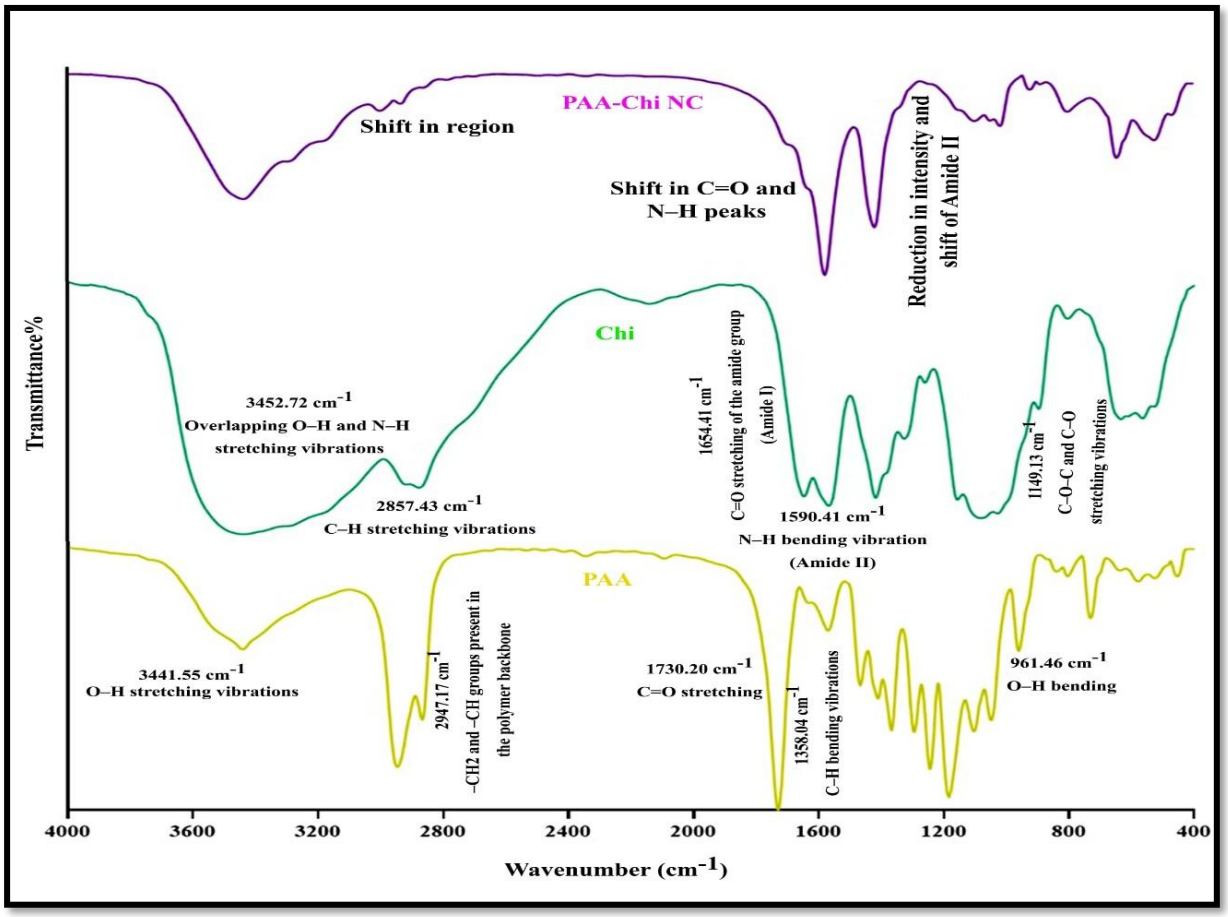

Figure 3-3 *FT–IR spectra of free PAA, free Chi, and PAA–Chi NFs*

The FTIR spectra of the manufactured PAA-Chi nanofibers showed observable changes in the typical absorption patterns of polyacrylic acid and chitosan, which signified a strong interpolymer interaction. It is important to note that the broad OH/NH stretch at 3440–3450 cm^{-1} was shifted, and the PAA C=O at 1730 cm^{-1} and chitosan amide I/II at 1654 and 1590 cm^{-1} were shifted and weakened. These spectral changes prove the existence of hydrogen bonds and electrostatic interactions between the carboxyl functionalities of PAA and the amino/hydroxyl functionalities of chitosan, which finally leads to the development of a stable intermolecular network, which forms the basis of the stability and adsorption capability of the nanocomposite.

These results align with previously documented polymeric mixes. For instance, in PCL–CH nanofibers, comparable shifts and peak modifications were observed, which were attributed to interpolymer bonding interactions, highlighting the molecular compatibility between PCL and chitosan [171]. Similarly, studies on PAA–CS-based hydrogels also revealed analogous spectral changes, where a broad absorption band in the 3000–3600 cm^{-1} region (O–H , N–H stretching) and characteristic peaks at 1637 cm^{-1} (C=O stretching) and 2921–2854 cm^{-1} (C–H stretching) confirmed strong hydrogen bonding and polymeric network formation [182]. Furthermore, the FTIR spectra of CS–PAA NPs obtained through polymerizing acrylic acid in a chitosan medium showed a marked decrease in the intensity of the amide I (1662 cm^{-1}) and amide II (1586 cm^{-1}) peaks, together with the formation of novel absorption peaks at 1731 cm^{-1} (C=O of PAA) and 1628 cm^{-1} (NH_3^+ of CS). FTIR spectra showing additional peaks at 1532 and 1414 cm^{-1}, assigned to asymmetric and symmetric COO^- stretching modes, verify the formation of a polyelectrolyte complex due to electrostatic attraction between deprotonated carboxylate groups of PAA and protonated amino sites of CS [183].

Overall, the FTIR analysis provides clear evidence of successful interaction of PAA and Chitosan leading to a stable and highly functional nano composite structure.

3.3 Field Emission Scanning Electron Microscopy (FESEM)

The FESEM images of the PAA-Chi NFs are shown in figure 3-4 (A, B), accompanied by the respective particle diameter distribution images. They all have a homogenous bead-free morphology emphasizing a controlled and reproducible fabrication process. The PAA-Chi nanofibers are smooth, and their average diameter is 276.15 ± 108.20 nm. Notably, the PAA-Chi nanofibers have an uninterrupted uniform surface, which is beneficial in numerous ways, such as adsorption.

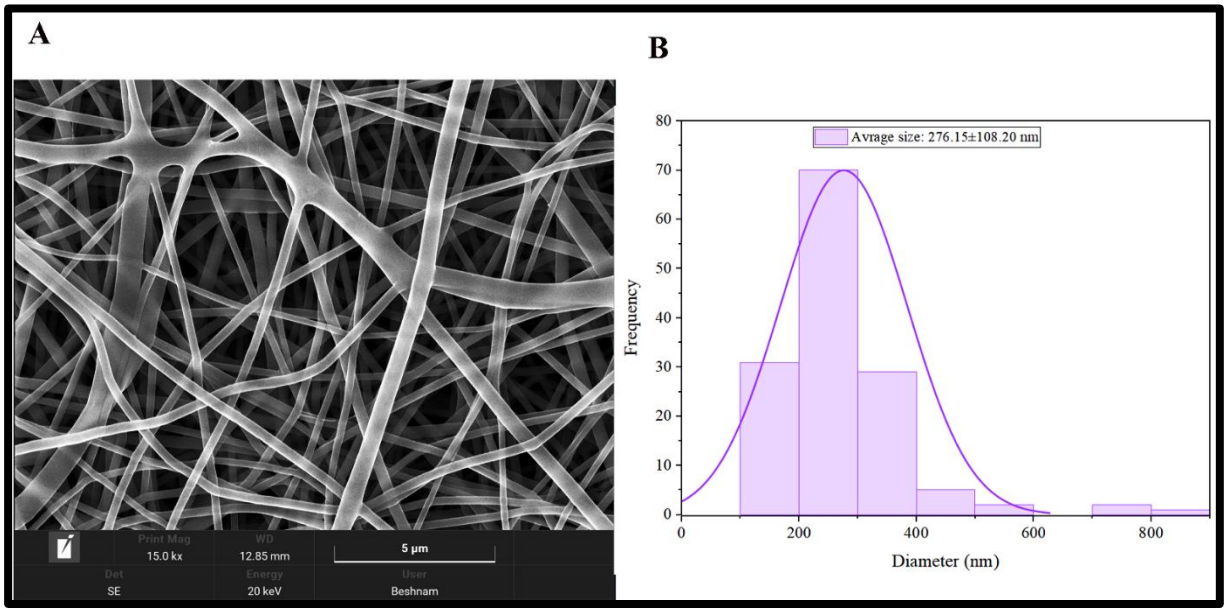

Figure 3-4 *FESEM images of the PAA–Chi nanofibers along with histograms of their diameter distributions (A,B).*

Table 3-4 *Fiber Morphology Analysis*

Parameter	Result
Fiber diameter range (nm)	100 – 800 nm
Average fiber diameter (nm)	276.15 ± 108.20 nm
Morphology description	Continuous, bead-free, randomly oriented, smooth surface nanofibers

The obtained mean diameter of about 276 nm fits the nanoscale requirement, which increases the surface area to volume ratio, which can be advantageous in adsorption and other surface-intensive applications. The structural features of the nanofibers and details of the homogenous surface of the polyacrylic acid-chitosan (PAA-Chi) nanofibers were proven to be even and advantageous by field-emission scanning electron microscopy (FE-SEM). Combined, these results highlight the application of these NFs to numerous adsorption reactions such as the elimination of methylene blue (MB) in water. The comparatively large range of diameter can be explained by the variability of processing conditions, including solution viscosity, concentration, flow rate, and ambient conditions all of which are known to affect fiber morphology. Notably, the fiber diameter is a very crucial factor in the functional performance of nanofiber membranes: smaller fiber diameter tends to enhance the filtration and adsorption performance because of the increased surface-to-volume ratio and the diminished pore size [184].

More recent reviews have highlighted the exceptional potential of electrospun nanofibrous membranes to water-remediation applications due to their large surface area, interwoven porosity, and easily modifiable morphology that allow contaminants to be removed by adsorption, filtration, and even catalytic degradation [185, 186]. These nanoscale fibers are smooth fibers, thus likely to

display favorable adsorption and separation properties, particularly in those situations where high surface contact and small pore-size networks are desirable.

3.4 Zeta Potential Analysis

Figure 3-5 illustrates the distribution of zeta potential of the produced PAA–Chi NFs. The estimated zeta potential value was –21.5 mV, with a standard deviation of ±4.78 mV and a conductivity of 0.0136 mS/cm. The distribution curve has a narrow peak at -21.5 mV, indicating that there is a steady and homogenous surface charge in the dispersion of nanoparticles.

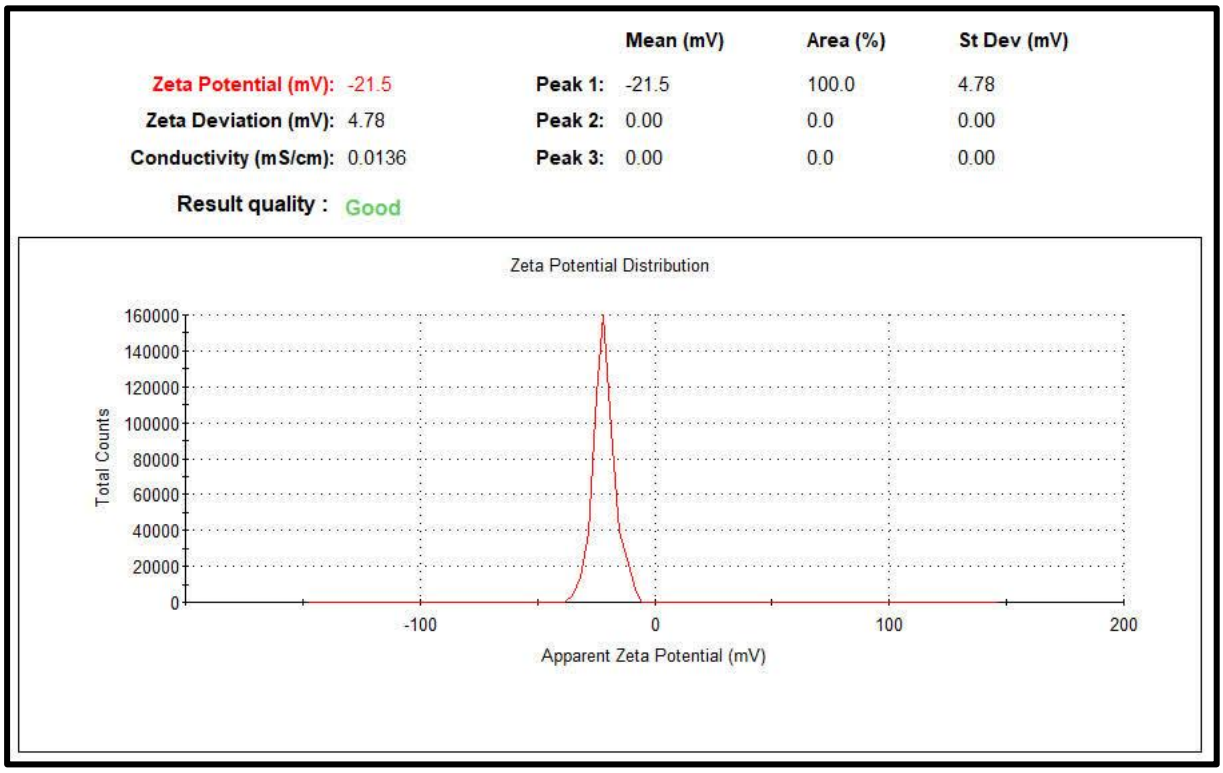

Figure 3-5 *Zeta potentials of PAA–Chi nanofibers.*

The negative surface charge that is observed may be attributed primarily to the ionized carboxyl groups ($–COO^-$) of polyacrylic acid, which control the surface of the particle even, though the protonated amino groups ($–NH_3^+$) of chitosan are

present. This means that surface modification has been achieved and that the two polymers react to each other.

According to the principles of colloidal stability, the values of zeta potential between approximately ±20 and ±30 mV show that the suspension has a moderate stability [187]. Therefore, the zeta potential of -21.5 mV shows that the PAA-Chi nanocomposite is sufficiently stable in colloidal suspensions, and the aggregation of particles in the ambient environment is sufficiently inhibited.

The relative negative surface charge enhances the interaction properties of the nanocomposite with positively charged matter such as cationic dyes or metal ions, which makes it a promising choice in wastewater treatment as well as adsorption. The quantified zeta potentials show that the PAA–Chi nanofibers synthesized disperse with a reasonable stability and provide a net negative surface charge, which is beneficial in further application in aqueous conditions, specifically in dye removal or controlled drug delivery.

3.5 Rheology Test

The rheological behavior of the PAA–Chi nanofibers formulation was systematically evaluated to understand its flow characteristics. Figures (3-6) and (3-7) present the variation in shear stress (Pa) and apparent viscosity (Pas) in terms of shear rate (S^{-1}), respectively. As shown in Figure 3-6, the shear stress exhibits a gradual and nearly linear increase across the full range of shear rates tested, indicating a stable rheological response without sudden fluctuations. This steady increase in shear stress suggests a homogeneous internal structure and strong intermolecular interactions between PAA and chitosan chains, contributing to consistent deformation under applied forces.

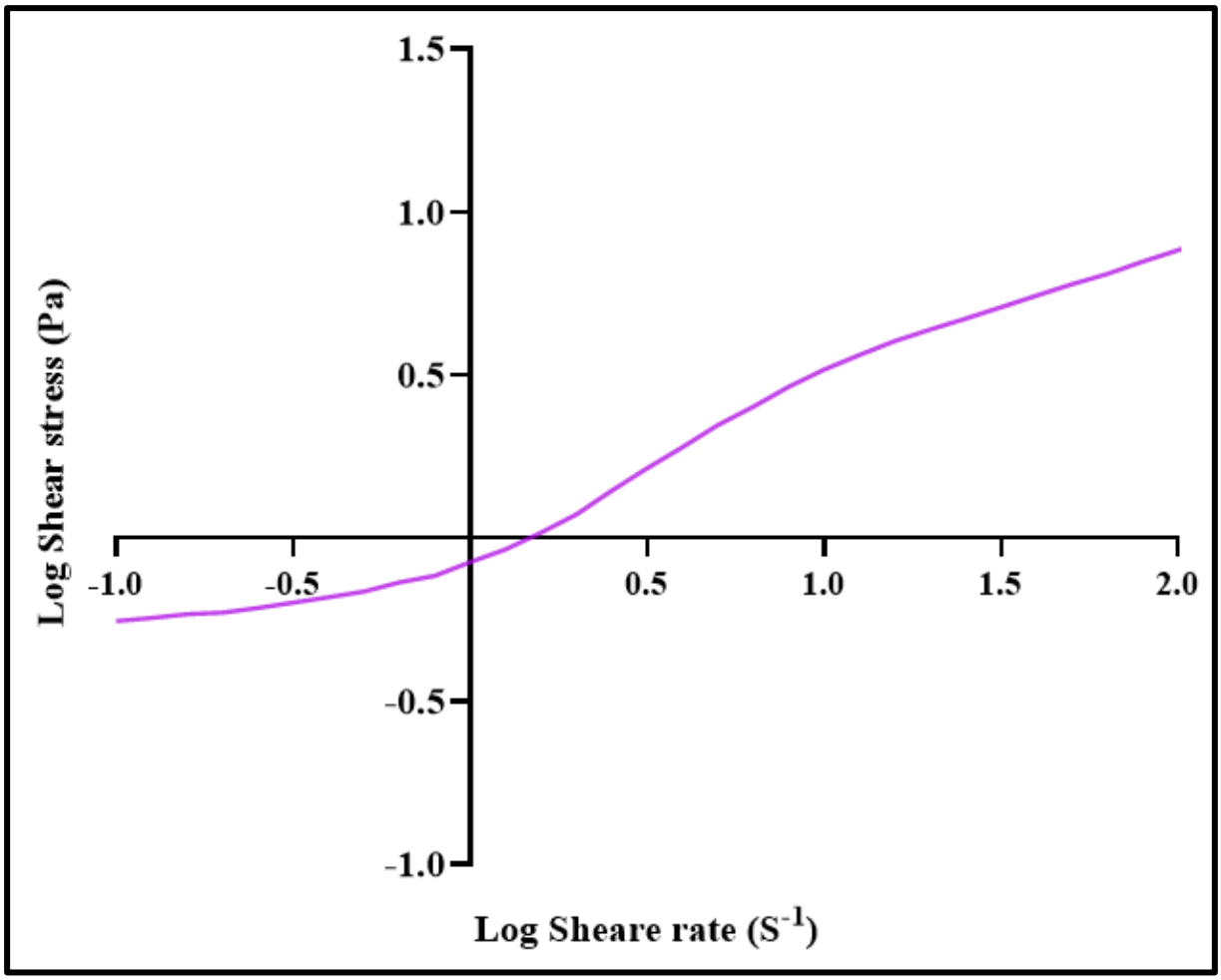

Figure 3-6 *Rheological Behavior of the nanofibers PAA-Chi*

In parallel, Figure 3-7 demonstrates a typical shear-thinning behavior, as the apparent viscosity decreases noticeably with increasing shear rate. This inverse relationship confirms the pseudoplastic nature of the PAA–Chi formulation, which becomes less viscous under higher shear conditions. Such rheological behavior is advantageous in dynamic processes like electrospinning, where reduced viscosity facilitates polymer jet elongation and fiber formation.

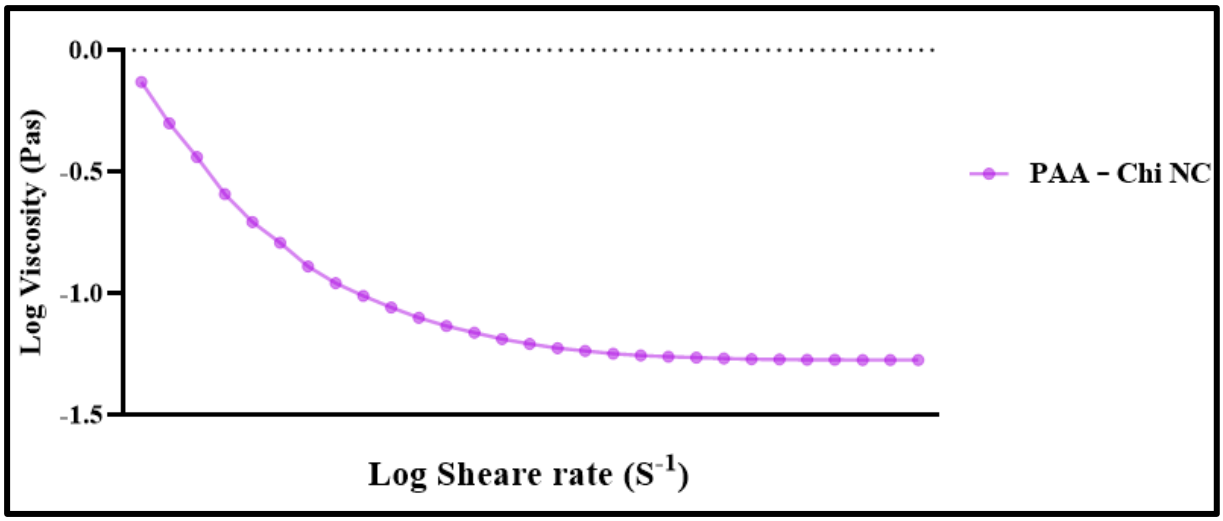

Figure 3-7 *Apparent viscosity (Pa) in terms of shear rate (S^{-1}) for the PAA–Chi NFs*

The flow behavior that was found reveals that the PAA-chi nanofiber solution is fluid-like at high shear rates, which is subsequently advantageous to its spinnability and uniformity. This is the most important behavior to keep the fiber in continuous production and to regulate the morphology produced. As supported by previous findings, the viscosity–shear rate profile plays a key role in determining the electrospinning ability and final fiber properties of polymer blends [50]. Finally, the rheological stability, including the predictable shear stress and viscosity reactions, highlights why the PAA-Chi system is a good choice to create nanofibers. Adjusting viscosity to changes in shear rate provides less control over the process that is necessary for the creation of homogenous, functional electrospun nanofibers.

These findings are highly consistent with previous studies about chitosan-derived systems. Chitosan solutions perform significant shear-thinning at a variety of concentrations and temperature ranges, which is believed to be due to disentangling of polymer chains due to the shear [188]. Similarly, cellulose-chitosan mixtures as solutions in ionic liquids were reported to exhibit the properties of pseudoplastic fluids, and the viscosity decreased with the proportion

of chitosan-contributing polymer-polymer interactions, confirming the perception that high-affinity polymer-polymer interactions determine rheology [189].

Further, combinations of chitosan and PEO demonstrated a significant positive change of zero-shear viscosity, which indicated the formation of hydrogen-bonded chain entanglements to facilitate the non-Newtonian ideal of flow in electrospinning [190]. Combined with the results of the rheology, the combination of a consistent increase in shear stress and the strong shear-thinning nature of the PAA–Chi formulation confirms that there are powerful interchain interactions and pseudoplasticity. The characteristics play an important role in the production of mechanically strong, flawless nanofibers and highlight the suitability of the formulation in the dye adsorption of the study.

3.6 Adsorption Uptake of Methylene Blue

Adsorption activity of (PAA-Chi) was tested against MB dye. The MB dye solutions were formulated at 50, 100, and 200 $mg.L^{-1}$. The absorption spectrum was obtained as shown in Figure 3-9 (λmax=664 nm). At a wavelength of 664 nm, this value corresponds to the peak absorbance of MB. In order to ensure precise concentration measurements during adsorption analyses, a standard calibration curve for methylene blue was constructed at its maximum absorbance wavelength of 664 nm.

3.7 Standard Calibration Curve

The calibration curve of methylene blue at λmax = 664 nm is presented in Figure (3-8). The results indicate that the absorbance increases progressively with increasing concentration, indicating conformity with the Beer–Lambert law within the studied range. The regression equation obtained was:

$$\mathbf{A=0.008C-0.0329}$$

with a correlation coefficient of R^2=0.9891. This high R^2 value demonstrates a strong linear relationship between concentration and absorbance, confirming the reliability of the calibration curve for the determination of unknown methylene blue concentrations in subsequent adsorption experiments.

At higher concentrations, a slight deviation from perfect linearity can be observed, which is commonly attributed to molecular aggregation effects or instrumental limitations at elevated absorbance values. Nevertheless, the curve remains valid and suitable for quantitative analysis within the examined concentration range.

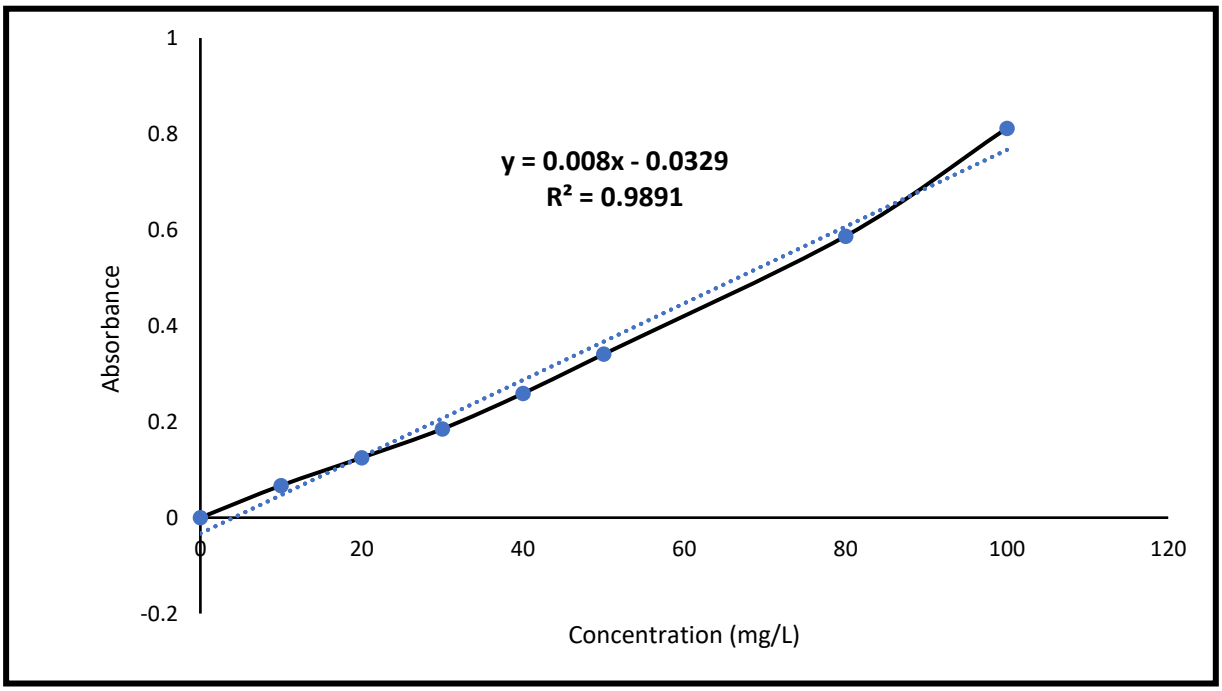

Figure 3-8 *The Standard Calibration Curve for Methylene Blue Dye*

The subsequent formulae were employed to calculate the PAA-Chi NFs adsorption capacity (q_e) and dye removal effectiveness (R%):

$$q_e = \frac{(C_0 - C_e) \times V}{W} \qquad \text{Eq. (1)}$$

$$R\% = \frac{(C_0 - C_e)}{C_0} \times 100 \qquad \text{Eq. (2)}$$

q_e denotes the adsorption capacity (mg/g) of PAA-Chi NFs. C_o and C_e denote the concentrations ($mg.L^{-1}$) of the initial and equilibrium dyes, respectively. V and W denote the solution volume (L) and the dry weight of the PAA-Chi NFs (g), respectively. C_e represents the concentration of the dye solution determined at various time intervals throughout the adsorption process, as shown in tables (3-5), (3-6), and (3-7), respectively.

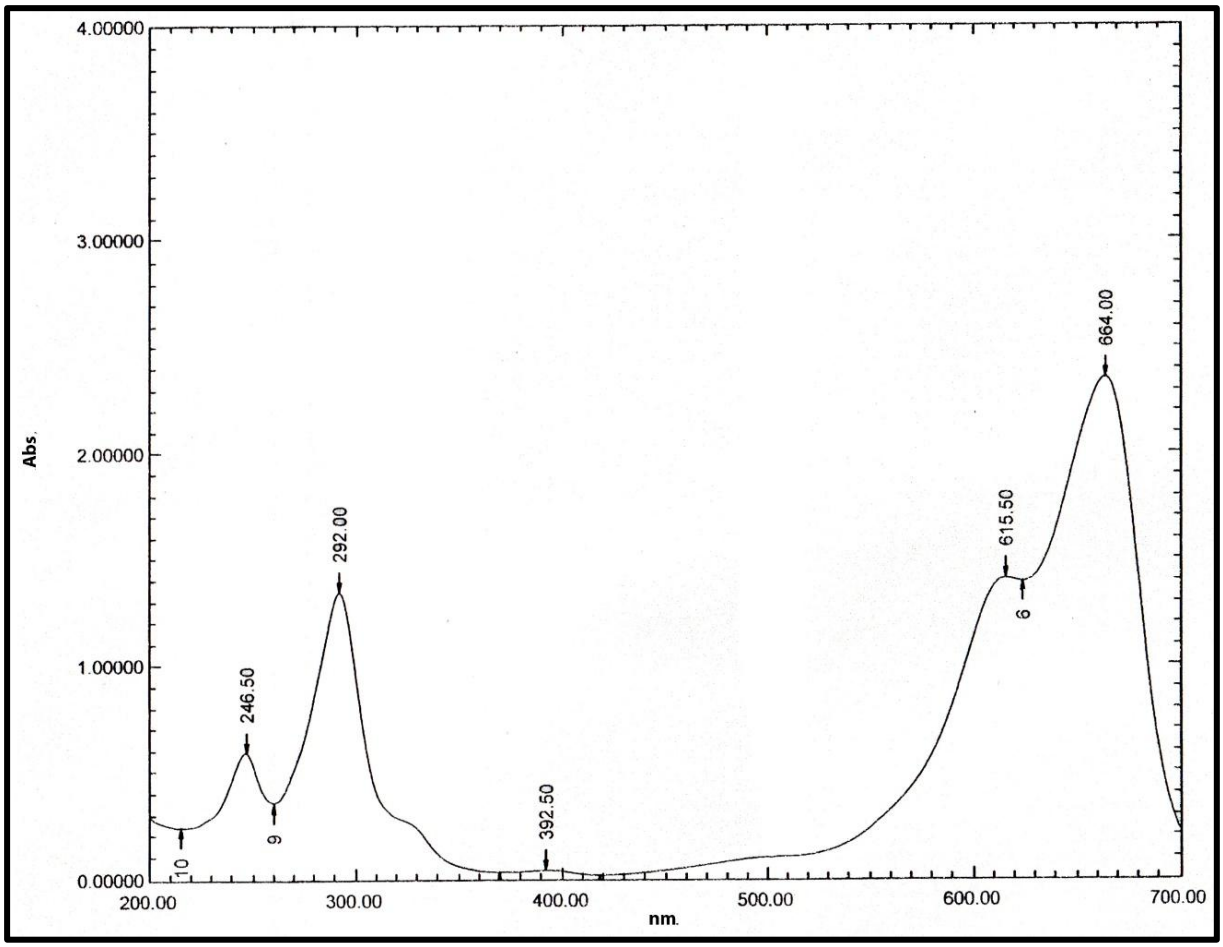

Figure 3-9 *Absorption spectrum of MB dye*

The adsorption performance of the PAA–chitosan nanofibers toward methylene blue (MB) at different initial concentrations (50, 100, and 200 mg.L^{-1}) is presented in Figures (3-10), (3-11), and (3-12), respectively. In all cases, the relative concentration (C_e/C_0) decreased progressively with contact time, confirming the effective uptake of MB molecules by the nanofiber surface. At a lower initial concentration (50 mg·L^{-1}), the adsorption proceeded rapidly and reached a significantly lower equilibrium C_e/C_0 value (0.86), indicating higher removal efficiency. This phenomenon is ascribed to the presence of several active adsorption sites (–NH_2, –OH, and –COOH groups) relative to the number of dye molecules, which allows more effective interaction through electrostatic attraction and hydrogen bonding.

Table 3-5 *Adsorption of MB (50 mg.L-1), V=50 ml by PAA-Chi NFs W=10 mg*

Time (min)	Absorption n=3	SD	RSD	C_t (mg/L)	q_t	R%	C_t/C_o
0	0.3671	0	0	50	0	0	0
60	0.3534	±0.00334	0.945173	48.2820	8.590	3.44	0.9656
120	0.3376	±0.006498	1.924621	46.3187	18.407	7.36	0.9264
240	0.3295	±0.005407	1.641117	45.2980	23.510	9.40	0.9060
360	0.3160	±0.002616	0.827744	43.6180	31.910	12.76	0.8724
480	0.3145	±0.003979	1.26491	43.4287	32.857	13.14	0.8686
600	0.3142	±0.00363	1.155227	43.3900	33.050	13.22	0.8678
720	0.3131	±0.005639	1.800925	43.2487	33.757	13.50	0.8650

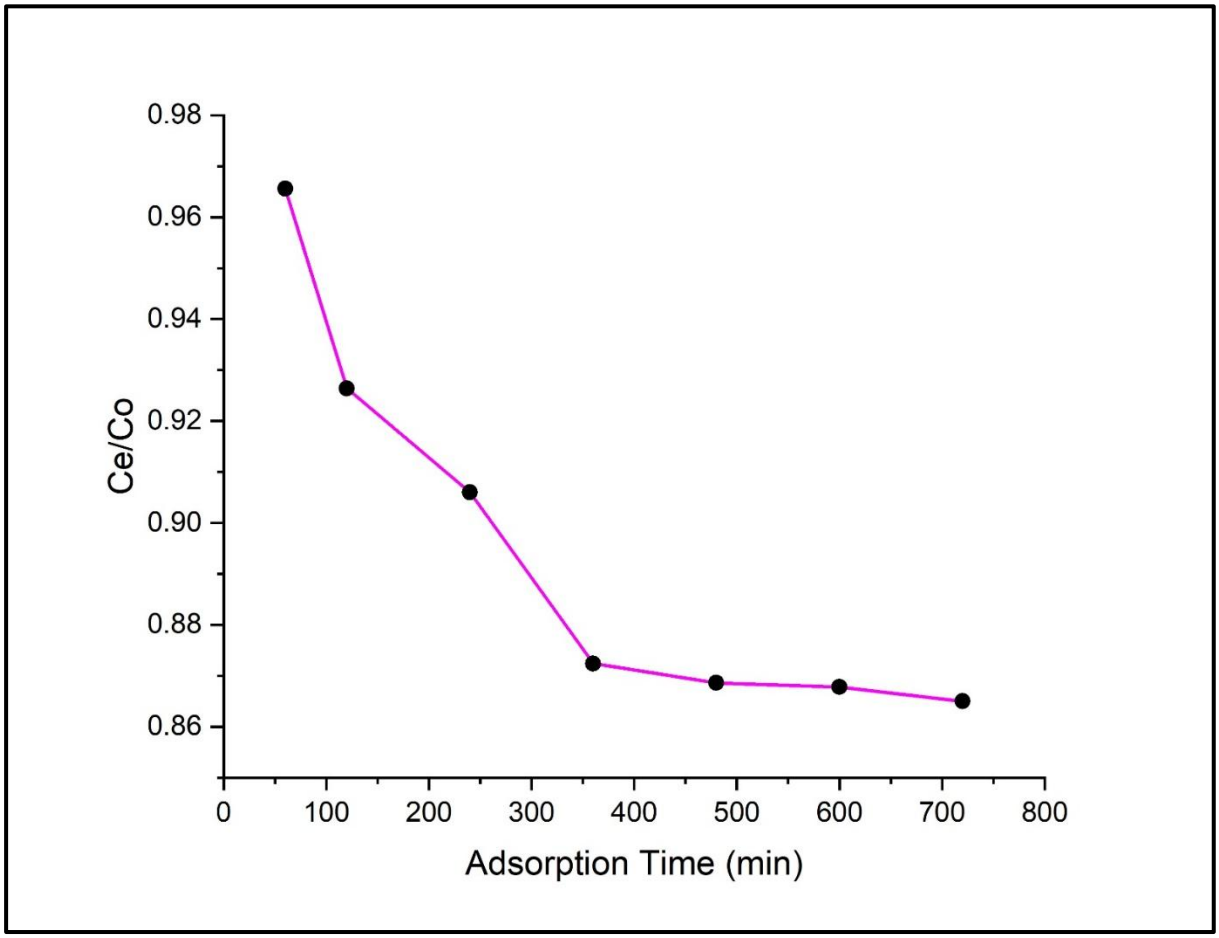

Figure 3-10 *Adsorption efficiency of MB dye (50 mg.L-1) by PAA-Chi Nanofibers*

Table 3-6 *Adsorption of MB (100 mg.L-1), V=50 ml by PAA-Chi NFs W=10 mg*

Time (min)	Absorption n=3	SD	RSD	C_t (mg/L)	q_t	R%	C_t/C_o
0	0.7671	0	0	100	0	0	0
60	0.7514	±0.00358	0.476366	98.0427	9.787	1.96	0.9804
120	0.7357	±0.003443	0.46795	96.0793	19.603	3.92	0.9608
240	0.7168	±0.005797	0.808791	93.7133	31.433	6.29	0.9371
360	0.6984	±0.003753	0.537365	91.4127	42.937	8.59	0.9141
480	0.6803	±0.008756	1.286981	89.1607	54.197	10.84	0.8916
600	0.6788	±0.005046	0.743352	88.9647	55.177	11.04	0.8896
720	0.6783	±0.008571	1.263669	88.8973	55.513	11.10	0.8890

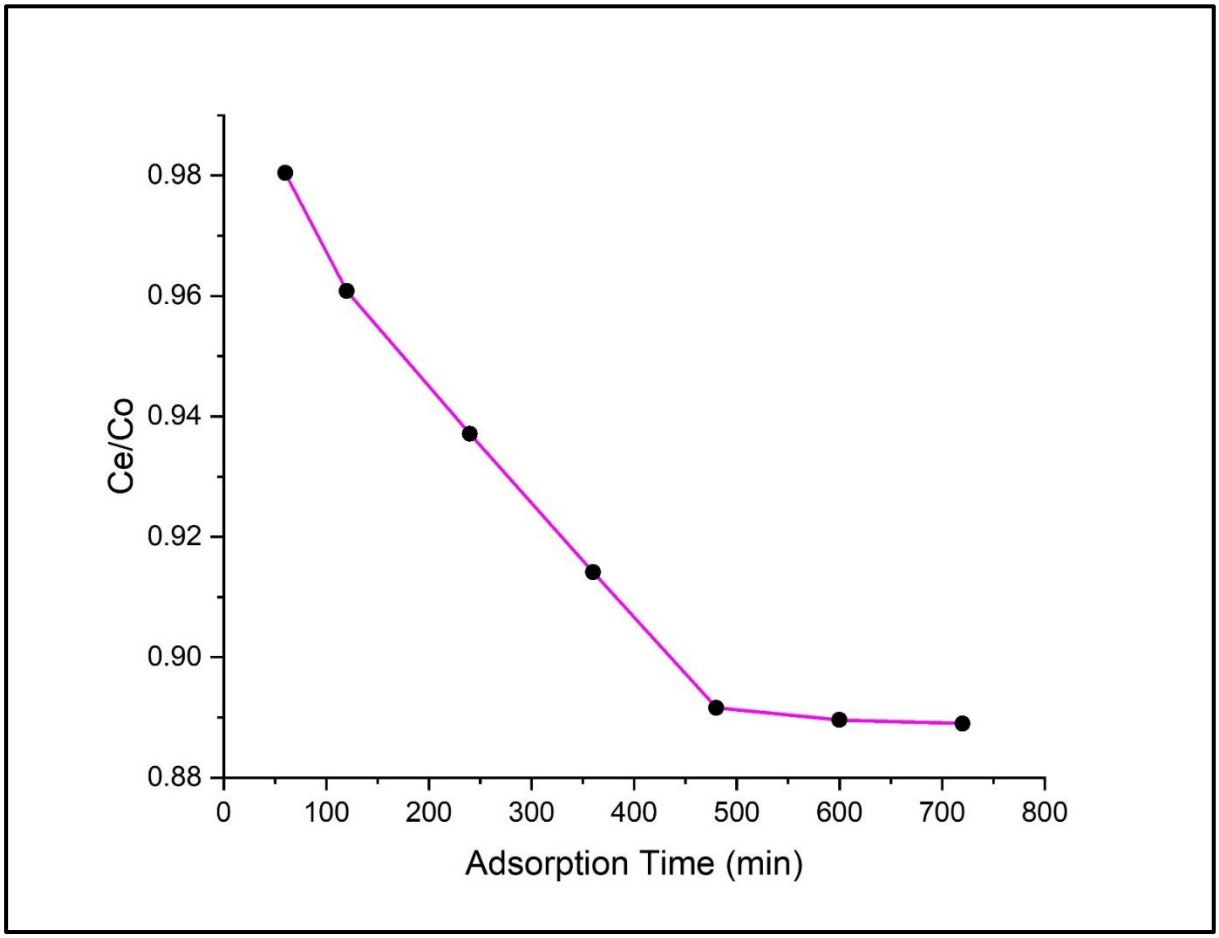

Figure 3-11 *Adsorption efficiency of MB dye (100 mg.L-1) by PAA-Chi Nanofibers*

Table 3-7 *Adsorption of MB (200 mg.L-1), V=50 ml by PAA-Chi NFs W=10 mg*

Time (min)	Absorption n=3	SD	RSD	C_t (mg/L)	q_t	R%	C_t/C_o
0	0.7671	0	0	200	0	0	0
60	0.7499	±0.001196	0.159518	195.6893	21.553	2.16	0.9784
120	0.7345	±0.001358	0.184838	191.8573	40.713	4.07	0.9593
240	0.7245	±0.002208	0.304781	189.3560	53.220	5.32	0.9468
360	0.7198	±0.004043	0.56165	188.1720	59.140	5.91	0.9409
480	0.7192	±0.005566	0.773924	188.0253	59.873	5.99	0.9401
600	0.7186	±0.003704	0.515413	187.8747	60.627	6.06	0.9394
720	0.7182	±0.00395	0.549966	187.7833	61.083	6.11	0.9389

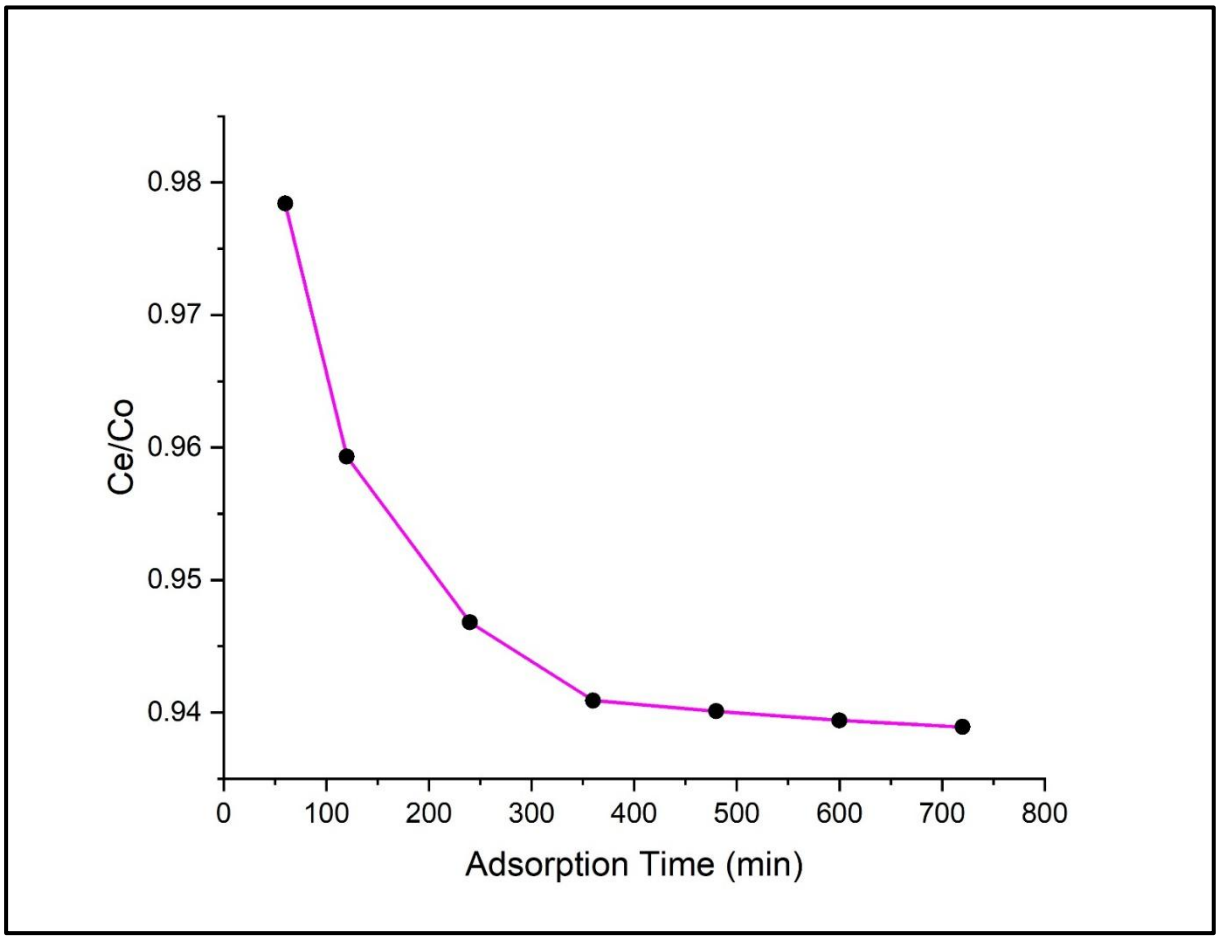

Figure 3-12 *Adsorption efficiency of MB dye (200 mg.L-1) by PAA-Chi Nanofibers*

At higher concentrations (100 and 200 mg·L^{-1}), the removal efficiency decreased, as evidenced by higher equilibrium C_e/C_0 values. This reduction is mainly due to the saturation of available adsorption sites on the PAA–chitosan nanofibers, where the excess MB molecules remain unadsorbed in solution. Moreover, competition among dye molecules for the limited active sites leads to lower overall uptake. A similar trend has been reported for other chitosan-based and PAA-modified adsorbents, where adsorption efficiency decreases with increasing pollutant concentration due to site saturation and intraparticle diffusion limitations.

The time-dependent behavior further shows that most adsorption occurred during the initial 200–300 minutes, followed by a gradual approach to equilibrium. This rapid initial stage can be explained by the high concentration gradient and abundant vacant sites on the fiber surface, while the slower second stage corresponds to progressive site occupation, electrostatic repulsion among adsorbed cations, and diffusion of MB into the interior regions of the fiber network. Such kinetic profiles are characteristic of chemisorption–physisorption coupled processes commonly observed in electrospun biopolymer-based nanofibers.

The fibers had a rapid initial absorption and a slower equilibrium, which is typical of an adsorption process in which a large population of surface interactions (cationic MB/anionic carboxylate electrostatic interaction and hydrogen bonding with chitosan amine groups and complexation with chitosan amine groups) together with diffusion into the porous fiber network. The superior performance at lower initial MB levels arises from the abundance of accessible adsorption sites compared to the number of dye molecules, leading to minimal site occupancy, whereas the diminished efficiency at elevated concentrations results from competing occupancy and a scarcity of available sites on the nanofibers. The PAA residue provides carboxyl (–COOH/COO^-) functionality to increase the electrostatic binding and swelling/tunable pore properties, whereas chitosan

provides primary amine ($–NH_2$ /NH_3^+) sites, which are known to have high affinity to cationic dyes, jointly forming a polyelectrolyte complex (PEC) to stabilize the fibrous network and facilitate adsorption. Kinetically, the profile is compatible with a rapid surface adsorption stage followed by slower intraparticle/intramatrix diffusion, commonly modelled by pseudo-second-order kinetics coupled with intraparticle diffusion controls in similar chitosan-based electrospun adsorbents. These observations align with recent reports on chitosan-containing electrospun membranes and PAA-modified adsorbents demonstrating effective MB removal and confirm the suitability of the fabricated PAA–CS nanofibers for dye remediation applications [171, 191, 192].

The adsorption results indicate that the hybrid network composed of polyacrylic acid (PAA) and chitosan (Chi) exhibits high efficiency in removing methylene blue dye from aqueous media. This performance is attributed to the three-dimensional polymeric network formed through physical interpenetration of the two polymer chains [59]. Functional groups such as amine ($–NH_2$) and hydroxyl (–OH) in chitosan, along with carboxyl (–COOH) groups in PAA, play a central role in the adsorption process [59, 193].

These groups contribute to the formation of effective hydrogen bonds with methylene blue molecules, while electrostatic attraction occurs between the negatively charged carboxyl groups and the positively charged dye. Additionally, hydrophobic interactions between the aromatic nuclei of methylene blue and the non-polar regions of the network further stabilize the adsorption process [194, 195]. The main interactions between the dye and the adsorbent, which include hydrogen bonding and hydrophobic interactions, indicate a multimodal adsorption mechanism [194].

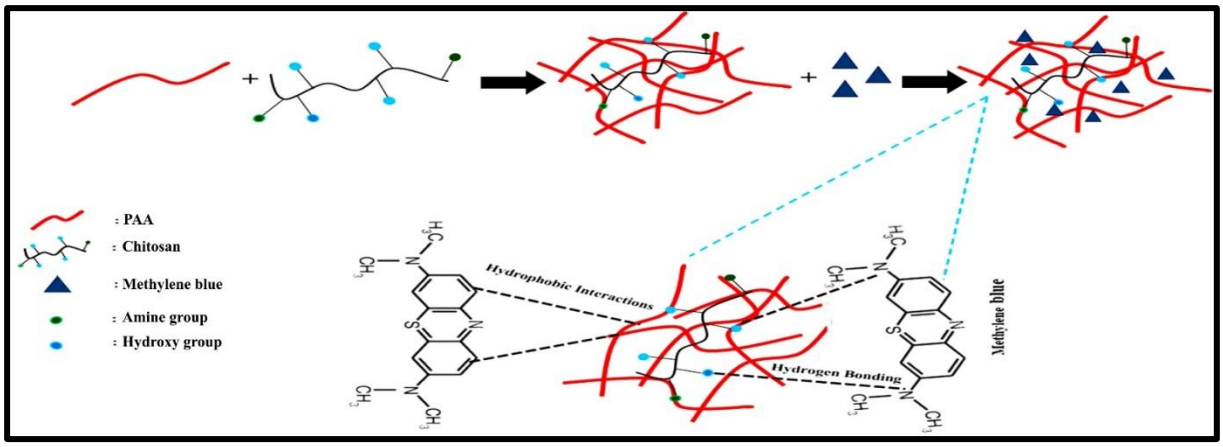

Figure 3-13 *The adsorption mechanism of nanofibers (PAA–Chi)*[171].

Methylene blue adsorption onto PAA-Chi nanofibers is a complicated process, which is guided by the physicochemical properties of the dye and the nanofibrous surface. Chitosan/polyacrylic acid creates a nanofiber matrix that has increased structural stability, uniformity, and porosity, which allows efficient uptake of dye.

[171, 196, 197]. These structural characteristics are crucial in ensuring that a stable and readily accessible surface is available for the adsorption of methylene blue, thereby enhancing the total efficacy of the process. The synergistic Chi and polyacrylic acid combination not only improves the adsorption capabilities of the combination but also increases the stability of the structural integrity of the nanofibers during the process of adsorption [171, 198]. This structural stability is needed in the guarantee of uniform and repeatable performance in adsorption applications. The adsorption of methylene blue on PAA Chi nanofibers is controlled by a complex of hydrogen bonds as well as the unique surface properties of the nanofibrous matrix [171, 199].

It is important to understand these aspects in order to maximize nanofiber design as a good adsorbent to cationic dyes like methylene blue. This is because the hydrophobic characteristics allow it to interact with the hydrophobic parts of the nanofibers and thus improve the process of adsorption, as shown in Figure 3-13. Chitosan is important in increasing adsorption of methylene blue (MB) on

nanofibers. Its amino ($–NH_2$) and hydroxyl (–OH) functional groups have many active sites that can form hydrogen bonds and participate in electrostatic interactions with cationic MB molecules, thus enhancing dye binding. According to recent research, the introduction of chitosan into the PCL matrix enhances the porosity and surface area of the nanofibers, providing additional sites for adsorption and triggering the overall process faster. Additionally, the amino groups in chitosan are pH-responsive: they are protonated under acidic conditions, leading to positive surface charges and potential electrostatic repulsion with MB, while in alkaline environments, deprotonation reduces this repulsion and promotes stronger adsorption. The structural compatibility of chitosan with PCL is also improved by the hydrogen bonding between its amino groups and the carbonyl (C=O) groups of PCL, resulting in a mechanically stable and cohesive nanofiber network. This synergy not only maintains structural integrity during adsorption but also significantly boosts performance, with higher chitosan contents (30% w/w) achieving more than a fourfold increase in MB adsorption capacity compared to pure PCL, due to the greater number of active sites and improved surface properties [171].

Another study confirmed chitosan in the PAA–Chi nanofibers system enhances methylene blue adsorption by providing amino and hydroxyl groups for hydrogen bonding and electrostatic interactions, increasing hydrophilicity and surface reactivity, and forming a stable network with PAA via $–NH_3^+$/$–COO^-$ attraction. These features boost the number of active sites, improve stability, and significantly increase adsorption capacity [200].

Accordingly, the findings confirm that the PAA–Chi material possesses favorable physicochemical properties that qualify it as a promising candidate for the treatment of industrial wastewater contaminated with organic dyes. Its bio-based nature and reusability add significant economic and environmental advantages to its use in sustainable remediation applications.

3.8 Influence of Contact Duration and pH on the Adsorption of Methylene Blue.

The results presented in Figure 3-14 and Figure 3-16 show that the adsorption performance of MB dye by the PAA–Chi nanocomposite fibers gradually increases with increasing contact time and concentration until reaching equilibrium after approximately 8 hours, with the equilibrium adsorption rate (q_e) reaching approximately 60 mg/g. This trend suggests that the adsorption process proceeds rapidly at the initial stage because numerous active sites are available on the nanofiber surface. Over time, the adsorption rate gradually decreases until saturation, indicating that the process depends on the dispersion of molecules throughout the fiber matrix and their attachment to the active sites.

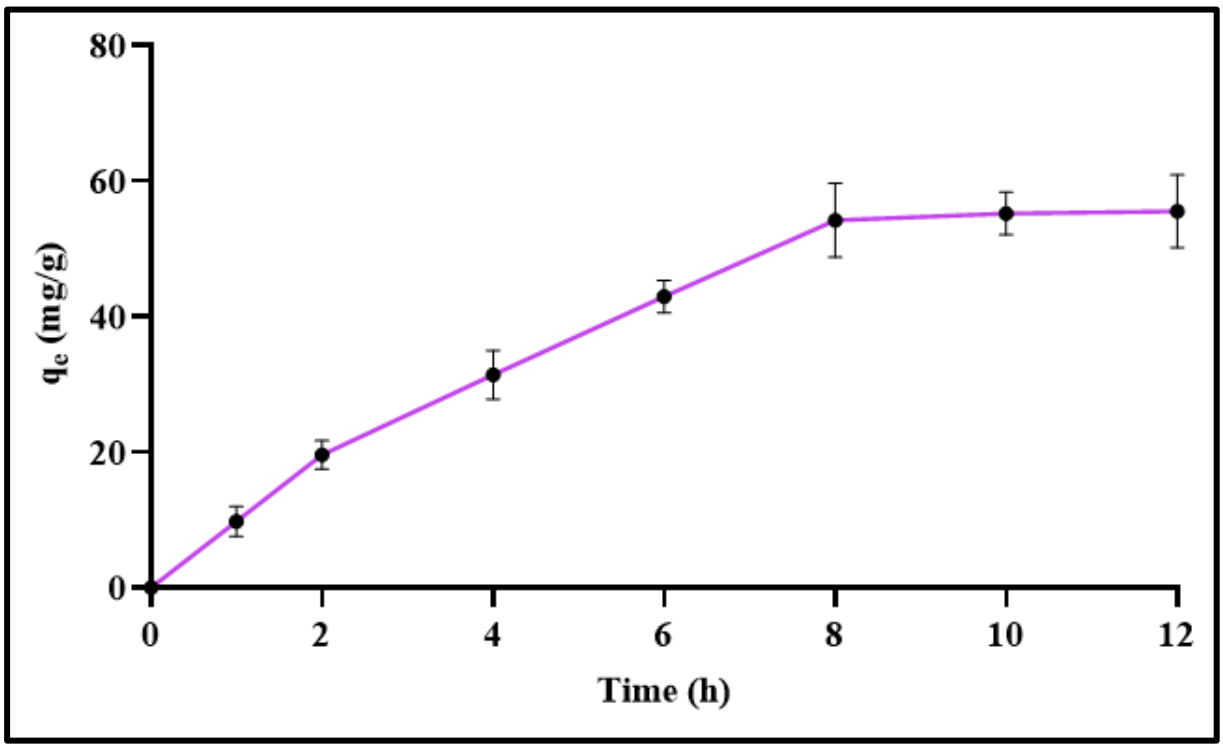

Figure 3-14 *Effects of starting MB adsorption time*

Figure 3-15 and Table 3-8 illustrate the influence of solution pH on adsorption performance. Efficiency was observed to increase with increasing pH, reaching a peak at pH = 6, with an adsorption rate exceeding 40%. This can be explained by the fact that the highly acidic medium leads to the protonation of the binding sites in chitosan, weakening the electrostatic attraction between the cationic surface and the methylene blue molecules, which are also positively charged. In contrast, at a neutral pH, the carboxyl groups in PAA are negatively ionized, enhancing interaction with MB via electrostatic attraction. After pH = 6, the efficiency begins to decrease again due to reduced surface activity and competition of hydroxide ions with MB molecules for active sites.

Table 3-8 *Effects of MB Solution pH*

PH	Absorbent Efficiency	C_e	R%
2	7.17	48.57	2.87
4	18.29	46.34	7.31
5	32.45	43.51	12.98
6	42.94	41.41	17.17
7	38.63	42.27	15.45
8	31.79	43.64	12.72
10	27.43	44.51	10.97

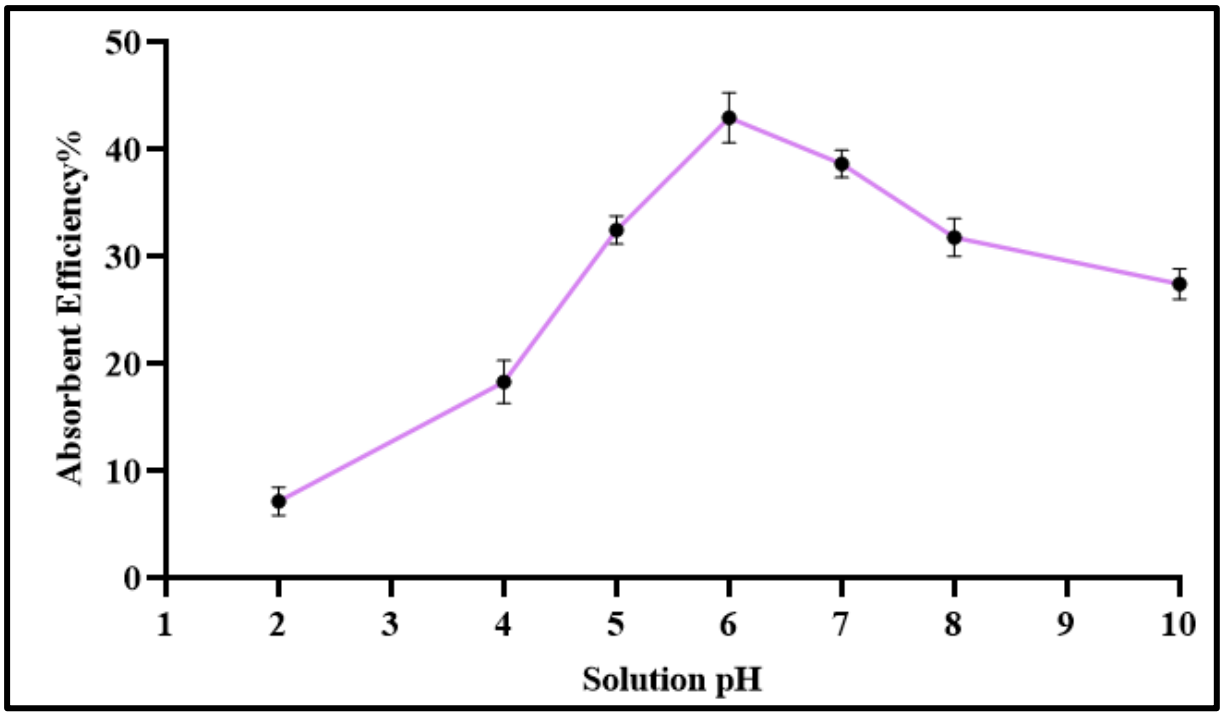

Figure 3-15 *Effects of MB Solution pH*

A direct relationship emerges between surface charge and dye removal performance. The negative zeta potential of –21.5 mV implies that, under near-neutral pH conditions, the nanofibers bear negatively charged carboxyl groups derived from PAA. These negatively charged sites strongly attract the cationic MB molecules through electrostatic interactions, which explains the observed maximum adsorption efficiency at pH = 6. Conversely, in acidic environments, protonation of chitosan's amino groups reduces or reverses the negative surface charge, leading to electrostatic repulsion with MB molecules and lower adsorption efficiency. At higher alkaline pH, despite the retention of negative charge, adsorption efficiency decreases due to competitive interactions between hydroxide ions and MB molecules for active binding sites. Therefore, the zeta potential results do not only confirm the stable and uniformly charged surface of the PAA–Chi nanofibers but also provide mechanistic insight into the pH-dependent adsorption behavior. The combined analysis clearly demonstrates that modulation of surface charge via protonation–deprotonation processes is the

dominant factor governing the interaction between the nanocomposite and MB dye molecules.

3.9 Effects of Initial MB Dye Concentrations

In Figure 3-16, the impact of the dye's initial concentration values of 50, 100, and 200 mg·L^{-1} on adsorption capacity over time was studied. The highest adsorption capacity (q_e) was achieved at 200 mg/L, reaching over 60 mg/g, compared to 45 and 30 mg/g at 100 and 50 mg/L, respectively. This is explained by the fact that a higher dye concentration provides a higher number of MB molecules available for adsorption on the surface, increasing the concentration difference and enhancing the migration of molecules to the binding sites. However, it should be noted that increasing the concentration may eventually lead to saturation of the adsorbent surface, limiting relative efficiency over time. These findings are in agreement with recent studies on CS/PAA systems, which also reported optimal MB removal under near-neutral conditions due to favorable surface charge characteristics [171, 182].

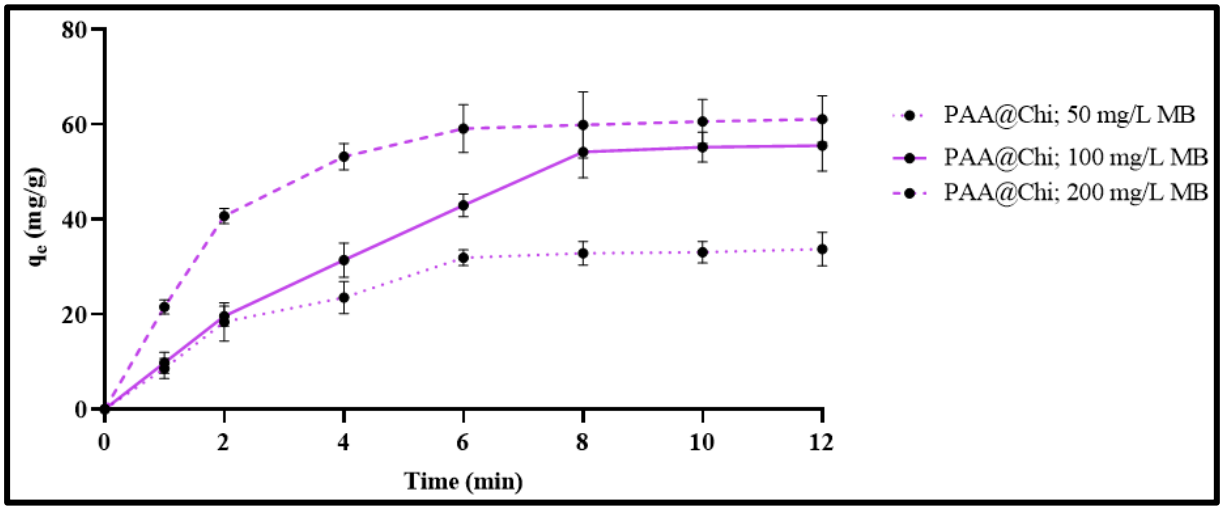

Figure 3-16 *Effects of MB Solution Concentrations*

The adsorption performance of methylene blue (MB) on PAA–Chi nanofibers was found to be exceptional, as demonstrated by a study evaluating the effects of pH and initial dye concentration. This high performance is explained by the use of chitosan (Chi) that contributes greatly to the uptake of the dye in the material. It was observed that the process was extremely pH-dependent, which places emphasis on the environmental conditions, and also when initial dye concentrations were high, they formed a stronger driving force, which facilitated the process of adsorption [171].

On the whole, these findings support the efficiency of PAA Chi nanofibers in eliminating the methylene blue dye of aqueous solutions. This is because of the synergistic chemical composition of the hydrophobic functional group and electrostatic functional group on the two polymers, which confers to them appropriate surface properties that allow them to be adsorbed successfully.

3.10 Kinetic Analysis

The kinetics of adsorption of PAA-Chi nanocomposite were studied by the pseudofirst-order and pseudosecond-order models, and the results were illustrated in Figures (3-17) and (3-18), respectively, and Table (3-9). The pseudofirst-order model provided the rate constant (K_1) of 0. 0.0041 min^{-1} and (q_e) of 64.06 $mg.g^{-1}$. The coefficient of determination (R^2) of this model was, 0.9833, which showed that there was a poor fit against the experimental data. Comparatively, the pseudosecond-order model fitted far better (R^2 = 0.9859). The given model gave a rate constant (K_2) of 0.0005 $g.mg^{-1}.min^{-1}$ and an equilibrium adsorption capacity (q_0) of 43.10 mg/g. The greater value of R^2 of the pseudosecond-order model indicates that it is closer to the adsorption kinetics of the PAA-Chi nanofibers. The better fit of the pseudosecond-order model suggests that the rate-limiting step in the adsorption process is presumably chemisorption. The valency force arises

from the transfer or the transfer of electrons occurring between the adsorbent and the adsorbate.

This interpretation aligns with the chemical structure of PAA-Chi NFs, which may form strong interactions with the adsorbate molecules.

***Table 3-9**. Adsorption kinetics of MB Dye on PAA–Chi NFs.*

Kinetic Analysis				
Model	**Curve Equation**	**Parameters**		
pseudofirst-order	y = -0.0018x + 1.8066	R^2 = 0.9833	K_1= 0.0041 (min^{-1})	q_e= 64.06
pseudosecond-order	y = 0.0232x - 1.064	R^2 = 0.9859	K_2= 0.0005 ($gr.mg^{-1}.min^{-1}$)	q_e= 43.10

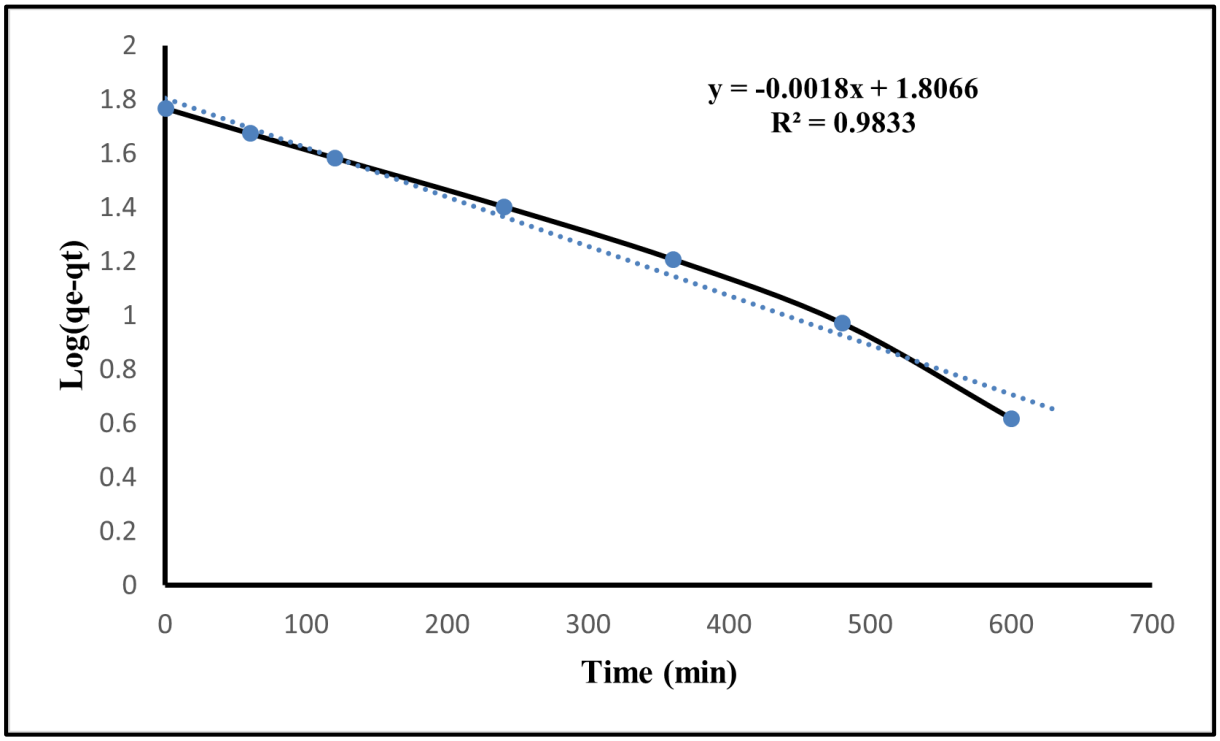

***Figure 3-17** The pseudofirst order was employed to analyze the adsorption kinetics of MB dye onto PAA-Chi NFs. The black line denotes the primary findings, whereas the blue line signifies the anticipated outcomes.*

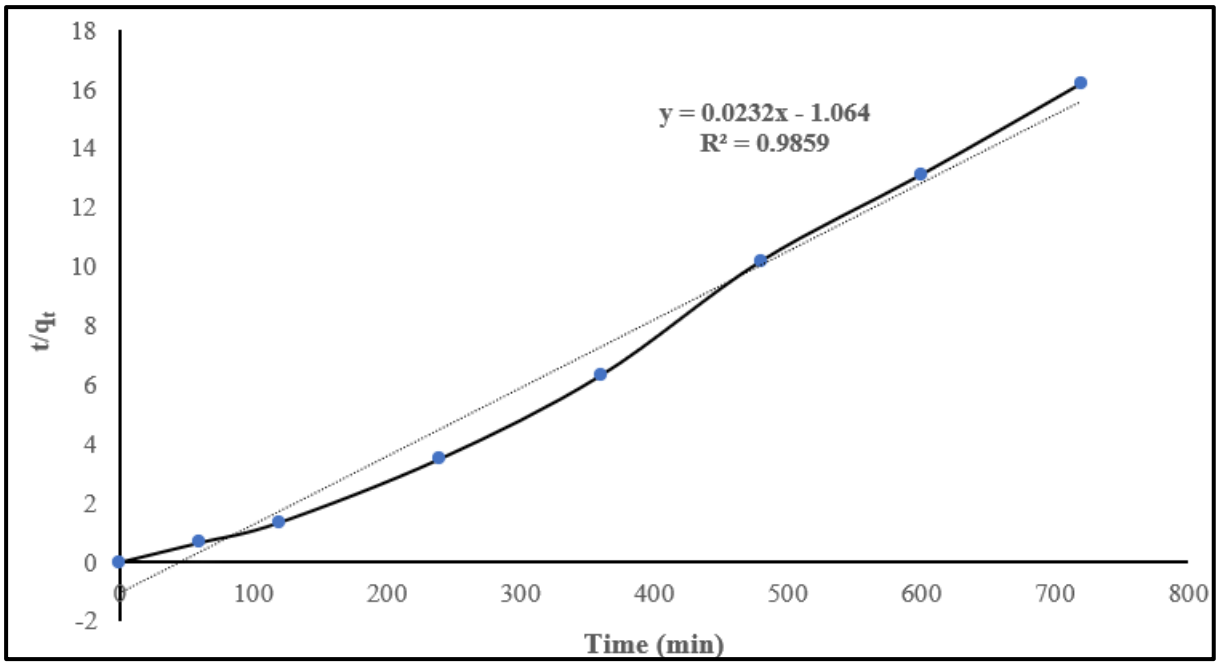

Figure 3-18 *The pseudosecond order was employed to analyze the adsorption kinetics of MB dye onto PAA-Chi NFs. The black line denotes the primary findings, whereas the blue line signifies the anticipated outcomes.*

3.11 Adsorption Isotherms

The adsorption isotherms modeled using the Langmuir and Freundlich equations are presented in Figures (3-19) and (3-20), respectively, as well as in Table (3-10). The Langmuir isotherm model showed an excellent fit with an R^2 value of 0.9789. The Langmuir constant (K_L) was determined to be 0.021 L/mg, and the maximum adsorption capacity (Q_m) was calculated as 78.125 mg/g. This high R^2 value suggests that the adsorption process closely follows the Langmuir model assumptions, suggesting the formation of a monolayer on a uniform surface containing a limited number of equivalent sites.

***Table 3-10**. Adsorption Isotherm of MB Dye Using PAA-Chi NFs.*

Adsorption Isotherm				
Model	**Curve Equation**	**Parameters**		
Langmuir	y = 0.0128x + 0.62	R^2 = 0.9789	K_L= 0.021 (L/mg)	Q_m= 78.125
Freundlich	y = 0.4022x + 0.9009	R^2 = 0.8599	K_f= 1.187	n= 2.486

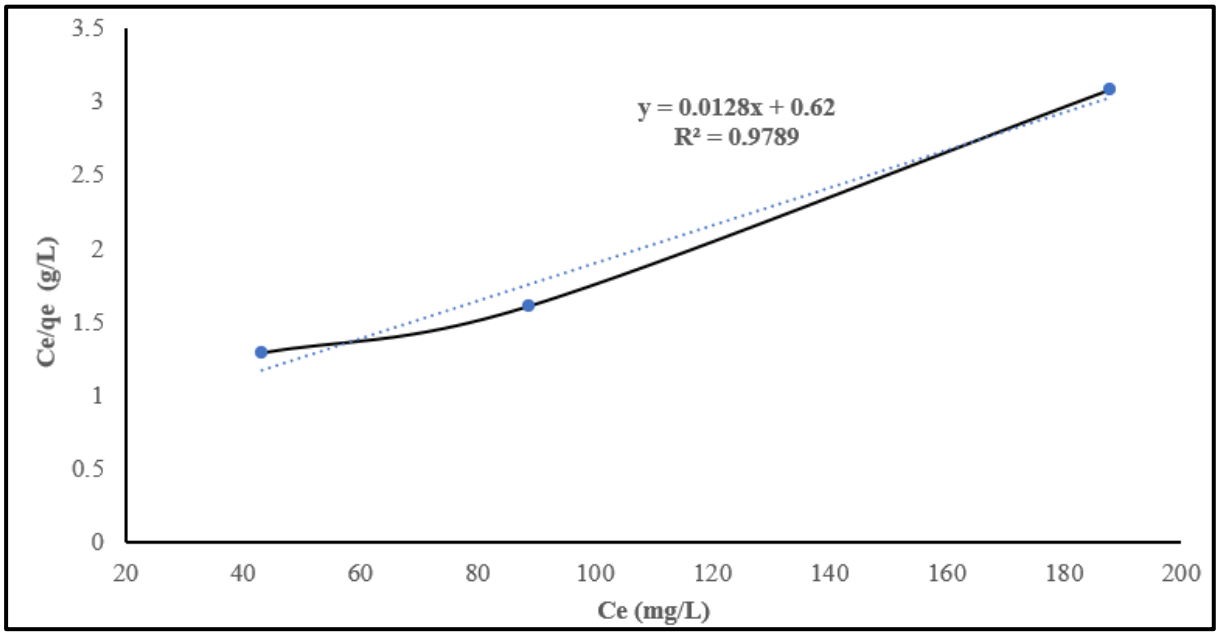

Figure 3-19 *The Adsorption Isotherms (Langmuir model)*

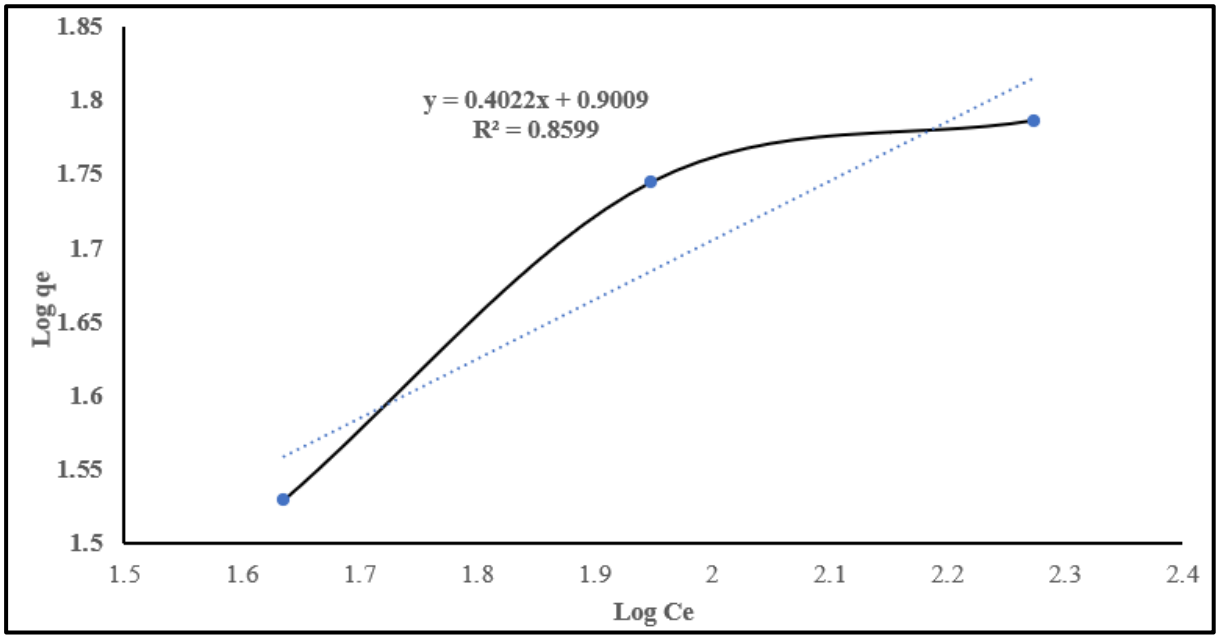

Figure 3-20 *The Adsorption Isotherms (Freundlich model)*

The Freundlich isotherm model, while still showing a good fit, had a lower R^2 value of 0.8599. The Freundlich constant (K_F) was found to be 1.187, and the adsorption intensity (n) was 2.486. The lower R^2 value compared to the Langmuir model suggests that the Freundlich model, which considers a heterogeneous surface where the adsorption energy is unevenly distributed, may not be as suitable for describing the adsorption process of PAA-Chi NFs.

The better fit of the Langmuir model implies that the adsorption sites on the PAA-Chi NFs surface are likely energetically equivalent and that the adsorption is limited to a monolayer. The relatively high Q_m value of 78.125 mg/g indicates that the PAA-Chi nanofibers have a considerable adsorption capacity, making them a promising material for various applications in adsorption processes.

Conclusion

&

Recomendations

Conclusion

This study details the synthesis and characterization of electrospun polyacrylic acid-chitosan (PAA-Chi) nanofibers, which exhibit a synergistic effect for the effective removal of MB dye from aqueous solutions. The combination of anionic PAA, rich in carboxyl binding sites and cationic chitosan, which provides amino groups and enhances structural stability, creating a highly porous adsorbent with a large surface-area-to-volume ratio. The primary removal mechanism is electrostatic attraction, which is critically dependent on pH; in neutral to alkaline solutions, the PAA's carboxyl groups deprotonate, creating a negative surface charge that strongly attracts the cationic MB dye, whereas acidic conditions reduce efficiency due to protonation and electrostatic repulsion. Kinetic studies reveal a rapid initial uptake, well-described by the pseudosecond-order model, suggesting chemisorption is the rate-limiting step, while equilibrium results frequently conform to the Langmuir isotherm, indicating uniform monolayer adsorption. The adsorption process is also influenced by initial dye concentration, temperature, and ionic strength. Critically for practical applications, these nanofibers exhibit excellent reusability, as the adsorbed dye can be effectively desorbed using an acidic solution to reverse the surface charge, allowing the material to be regenerated for multiple cycles while maintaining high removal efficiency. In conclusion, this study demonstrates a comprehensive approach to synthesize, characterize, and assess PAA–Chi electrospun nanofibers as efficient adsorbents for the uptake of MB from water-based solutions. The integration of chitosan into the PAA matrix enhances the adsorption performance of the nanofibers, supporting their potential use in wastewater treatment. The results contribute to the development of biocompatible, sustainable materials for addressing water pollution. This work advances the field of eco-friendly remediation technologies by offering a viable strategy for dye-contaminated water purification.

Recomendations

1- Repeat key adsorption experiments using real textile/manufacturing effluents to assess matrix effects (turbidity, salts, surfactants, natural organic matter). Report percent removal and capacity differences between synthetic and real matrices.

2- Study of electrical conductivity for polyacrylic acid, chitosan, and PAA-Chi (70:30) Nanofibers

3- Suggest extension to other classes of pollutants such as (cationic pharmaceuticals, heavy-metal–dye complexes) or modifying the nanofibers via (quaternization or grafting) to target anionic contaminants.

4- Examine the reusability and stability of the nanofibers for potential applications in wastewater treatment.

5- It is recommended to incorporate a third polymer that is solvent-compatible with PAA–Chi or using reactive fillers to improve electrospinning properties and enhance adsorption performance. Depending on the objective of the study, the following options are suggested: (1) Using of PVA to improve spinnability and mechanical strength; (2) Adding of sodium alginate to increase negatively charged sites and thereby enhance methylene blue adsorption; or (3) the incorporation of polyaniline (as a coating or nanosuspension) to promote π–π interactions and improve adsorption capacity.

References

1. Mekuye, B. and B. Abera, *Nanomaterials: An overview of synthesis, classification, characterization, and applications.* Nano select, 2023. **4**(8): p. 486-501.
2. Baig, N., I. Kammakakam, and W. Falath, *Nanomaterials: A review of synthesis methods, properties, recent progress, and challenges.* Materials advances, 2021. **2**(6): p. 1821-1871.
3. Ali, M.T. and S.S. Najim, *Synthesis and Characterization of Novel Ternary Nanocomposites BiC80/GO (x mg) for Water Treatment.* 2025.
4. Harish, V., D. Tewari, M. Gaur, A.B. Yadav, S. Swaroop, M. Bechelany, and A. Barhoum, *Review on nanoparticles and nanostructured materials: Bioimaging, biosensing, drug delivery, tissue engineering, antimicrobial, and agro-food applications.* Nanomaterials, 2022. **12**(3): p. 457.
5. Shah, S.S., M.N. Shaikh, M.Y. Khan, M.A. Alfasane, M.M. Rahman, and M.A. Aziz, *Present status and future prospects of jute in nanotechnology: A review.* The Chemical Record, 2021. **21**(7): p. 1631-1665.
6. Sudha, P.N., K. Sangeetha, K. Vijayalakshmi, and A. Barhoum, *Nanomaterials history, classification, unique properties, production and market*, in *Emerging applications of nanoparticles and architecture nanostructures*. 2018, Elsevier. p. 341-384.
7. Saleh, T.A., *Nanomaterials: Classification, properties, and environmental toxicities.* Environmental Technology & Innovation, 2020. **20**: p. 101067.
8. Pokropivny, V. and V. Skorokhod, *Classification of nanostructures by dimensionality and concept of surface forms engineering in nanomaterial science.* Materials science and engineering: C, 2007. **27**(5-8): p. 990-993.
9. Asghari, F., Z. Jahanshiri, M. Imani, M. Shams-Ghahfarokhi, and M. Razzaghi-Abyaneh, *Antifungal nanomaterials: synthesis, properties, and applications*, in *Nanobiomaterials in antimicrobial therapy*. 2016, Elsevier. p. 343-383.

10. Shiau, B.-W., C.-H. Lin, Y.-Y. Liao, Y.-R. Lee, S.-H. Liu, W.-C. Ding, and J.-R. Lee, *The characteristics and mechanisms of Au nanoparticles processed by functional centrifugal procedures.* Journal of Physics and Chemistry of Solids, 2018. **116**: p. 161-167.
11. Yang, Y., W. Li, D.-G. Yu, G. Wang, G.R. Williams, and Z. Zhang, *Tunable drug release from nanofibers coated with blank cellulose acetate layers fabricated using tri-axial electrospinning.* Carbohydrate polymers, 2019. **203**: p. 228-237.
12. Gonciarz, W., E. Balcerczak, M. Brzeziński, A. Jeleń, A.J. Pietrzyk-Brzezińska, V.H.B. Narayanan, and M. Chmiela, *Chitosan-based formulations for therapeutic applications. A recent overview.* Journal of Biomedical Science, 2025. **32**(1): p. 62.
13. Huesca-Urióstegui, K., E.J. García-Valderrama, J.A. Gutierrez-Uribe, M. Antunes-Ricardo, and D. Guajardo-Flores, *Nanofiber systems as herbal bioactive compounds carriers: current applications in healthcare.* Pharmaceutics, 2022. **14**(1): p. 191.
14. Goyal, R., L.K. Macri, H.M. Kaplan, and J. Kohn, *Nanoparticles and nanofibers for topical drug delivery.* Journal of Controlled Release, 2016. **240**: p. 77-92.
15. Keshvardoostchokami, M., S.S. Majidi, P. Huo, R. Ramachandran, M. Chen, and B. Liu, *Electrospun nanofibers of natural and synthetic polymers as artificial extracellular matrix for tissue engineering.* Nanomaterials, 2020. **11**(1): p. 21.
16. Zhang, W., S. Ronca, and E. Mele, *Electrospun nanofibres containing antimicrobial plant extracts.* Nanomaterials, 2017. **7**(2): p. 42.
17. Williams, G.R., B.T. Raimi-Abraham, and C. Luo, *Nanofibres in drug delivery*. 2018: UCL press.

18. Min, K., S. Kim, and S. Kim, *Silk protein nanofibers for highly efficient, eco-friendly, optically translucent, and multifunctional air filters.* Scientific reports, 2018. **8**(1): p. 9598.
19. Martí-Muñoz, J. and O. Castaño, *Bioactive fibers for bone regeneration*, in *Electrofluidodynamic Technologies (EFDTs) for Biomaterials and Medical Devices*. 2018, Elsevier. p. 205-220.
20. Rodríguez-Tobías, H., G. Morales, and D. Grande, *Comprehensive review on electrospinning techniques as versatile approaches toward antimicrobial biopolymeric composite fibers.* Materials Science and Engineering: C, 2019. **101**: p. 306-322.
21. Chahal, S., A. Kumar, and F.S.J. Hussian, *Development of biomimetic electrospun polymeric biomaterials for bone tissue engineering. A review.* Journal of biomaterials science, polymer edition, 2019. **30**(14): p. 1308-1355.
22. Jalvandi, J., M. White, Y. Gao, Y.B. Truong, R. Padhye, and I.L. Kyratzis, *Polyvinyl alcohol composite nanofibres containing conjugated levofloxacin-chitosan for controlled drug release.* Materials Science and Engineering: C, 2017. **73**: p. 440-446.
23. Keirouz, A., G. Fortunato, M. Zhang, A. Callanan, and N. Radacsi, *Nozzle-free electrospinning of Polyvinylpyrrolidone/Poly (glycerol sebacate) fibrous scaffolds for skin tissue engineering applications.* Medical engineering & physics, 2019. **71**: p. 56-67.
24. Gugulothu, D., A. Barhoum, R. Nerella, R. Ajmer, and M. Bechelany, *Fabrication of nanofibers: electrospinning and non-electrospinning techniques.* Handbook of nanofibers, 2019: p. 45-77.
25. Zhao, K., S.-X. Kang, Y.-Y. Yang, and D.-G. Yu, *Electrospun functional nanofiber membrane for antibiotic removal in water.* Polymers, 2021. **13**(2): p. 226.

26. Quoc Pham, L., M.V. Uspenskaya, R.O. Olekhnovich, and R.A. Olvera Bernal, *A review on electrospun pvc nanofibers: Fabrication, properties, and application.* Fibers, 2021. **9**(2): p. 12.
27. SalehHudin, H.S., E.N. Mohamad, W.N.L. Mahadi, and A. Muhammad Afifi, *Multiple-jet electrospinning methods for nanofiber processing: A review.* Materials and Manufacturing Processes, 2018. **33**(5): p. 479-498.
28. Rizvi, S.A. and A.M. Saleh, *Applications of nanoparticle systems in drug delivery technology.* Saudi pharmaceutical journal, 2018. **26**(1): p. 64-70.
29. Fatehi, P. and M. Abbasi, *Medicinal plants used in wound dressings made of electrospun nanofibers.* Journal of tissue engineering and regenerative medicine, 2020. **14**(11): p. 1527-1548.
30. Aman Mohammadi, M., S.M. Hosseini, and M. Yousefi, *Application of electrospinning technique in development of intelligent food packaging: A short review of recent trends.* Food Science & Nutrition, 2020. **8**(9): p. 4656-4665.
31. Huan, S., G. Liu, G. Han, W. Cheng, Z. Fu, Q. Wu, and Q. Wang, *Effect of experimental parameters on morphological, mechanical and hydrophobic properties of electrospun polystyrene fibers.* Materials, 2015. **8**(5): p. 2718-2734.
32. Li, R., J. Dou, Q. Jiang, J. Li, Z. Xie, J. Liang, and X. Ren, *Preparation and antimicrobial activity of β-cyclodextrin derivative copolymers/cellulose acetate nanofibers.* Chemical Engineering Journal, 2014. **248**: p. 264-272.
33. Ahmadian, A., A. Shafiee, N. Aliahmad, and M. Agarwal, *Overview of nano-fiber mats fabrication via electrospinning and morphology analysis.* Textiles, 2021. **1**(2): p. 206-226.
34. Avvari, V.D., P. Sreekanth, R. Shanmugam, S. Salunkhe, R. Cep, E.A. Nasr, and D. Kimmer, *Exploring electrospun Nafion nanofibers: Bibliographic*

insights, emerging possibilities, and diverse applications. AIP Advances, 2024. **14**(7).

35. Cheng, J., Y. Jun, J. Qin, and S.-H. Lee, *Electrospinning versus microfluidic spinning of functional fibers for biomedical applications.* Biomaterials, 2017. **114**: p. 121-143.
36. Higashi, S., T. Hirai, M. Matsubara, H. Yoshida, and A. Beniya, *Dynamic viscosity recovery of electrospinning solution for stabilizing elongated ultrafine polymer nanofiber by TEMPO-CNF.* Scientific Reports, 2020. **10**(1): p. 13427.
37. Yang, G.-Z., H.-P. Li, J.-H. Yang, J. Wan, and D.-G. Yu, *Influence of working temperature on the formation of electrospun polymer nanofibers.* Nanoscale research letters, 2017. **12**(1): p. 55.
38. AK S, S.P. and K. Chatterjee, *Fabrication of poly (Caprolactone) nanofibers by electrospinning.* J Polym Biopolym Phys Chem, 2014. **2**(4): p. 62-66.
39. Van-Pham, D.-T., T. Thi Bich Quyen, P. Van Toan, C.-N. Nguyen, M.H. Ho, and D. Van Hong Thien, *Temperature effects on electrospun chitosan nanofibers.* Green Processing and Synthesis, 2020. **9**(1): p. 488-495.
40. Mpukuta, O., K. Dincer, and İ. Özaytekin, *Effect of dynamic viscosity on nanofiber diameters and electrical conductivity of polyacrylonitrile nanofibers doped nano-cu particles.* International Journal of Innovative Engineering Applications, 2020. **4**(1): p. 1-8.
41. Xue, J., T. Wu, Y. Dai, and Y. Xia, *Electrospinning and electrospun nanofibers: Methods, materials, and applications.* Chemical reviews, 2019. **119**(8): p. 5298-5415.
42. Mirjalili, M. and S. Zohoori, *Review for application of electrospinning and electrospun nanofibers technology in textile industry.* Journal of Nanostructure in Chemistry, 2016. **6**: p. 207-213.

43. Mercante, L.A., V.P. Scagion, F.L. Migliorini, L.H. Mattoso, and D.S. Correa, *Electrospinning-based (bio) sensors for food and agricultural applications: A review.* TrAC Trends in Analytical Chemistry, 2017. **91**: p. 91-103.
44. Thenmozhi, S., N. Dharmaraj, K. Kadirvelu, and H.Y. Kim, *Electrospun nanofibers: New generation materials for advanced applications.* Materials Science and Engineering: B, 2017. **217**: p. 36-48.
45. Abutaleb, A., D. Lolla, A. Aljuhani, H.U. Shin, J.W. Rajala, and G.G. Chase, *Effects of surfactants on the morphology and properties of electrospun polyetherimide fibers.* Fibers, 2017. **5**(3): p. 33.
46. Young, R.J. and P.A. Lovell, *Introduction to polymers*. 2011: CRC press.
47. Pandey, N., S. Shukla, and N. Singh, *Water purification by polymer nanocomposites: an overview.* Nanocomposites, 2017. **3**(2): p. 47-66.
48. Jayaraman, K., M. Kotaki, Y. Zhang, X. Mo, and S. Ramakrishna, *Recent advances in polymer nanofibers.* Journal of Nanoscience and Nanotechnology, 2004. **4**(1-2): p. 52-65.
49. Bhat, G. and V. Kandagor, *Synthetic polymer fibers and their processing requirements*, in *Advances in filament yarn spinning of textiles and polymers*. 2014, Elsevier. p. 3-30.
50. Bhardwaj, N. and S.C. Kundu, *Electrospinning: A fascinating fiber fabrication technique.* Biotechnology advances, 2010. **28**(3): p. 325-347.
51. Garcia-Orue, I., G. Gainza, F.B. Gutierrez, J.J. Aguirre, C. Evora, J.L. Pedraz, R.M. Hernandez, A. Delgado, and M. Igartua, *Novel nanofibrous dressings containing rhEGF and Aloe vera for wound healing applications.* International journal of pharmaceutics, 2017. **523**(2): p. 556-566.
52. Miguel, S.P., D.R. Figueira, D. Simões, M.P. Ribeiro, P. Coutinho, P. Ferreira, and I.J. Correia, *Electrospun polymeric nanofibres as wound dressings: A review.* Colloids and surfaces B: Biointerfaces, 2018. **169**: p. 60-71.

53. Li, Y., J. Zhu, H. Cheng, G. Li, H. Cho, M. Jiang, Q. Gao, and X. Zhang, *Developments of advanced electrospinning techniques: A critical review.* Advanced Materials Technologies, 2021. **6**(11): p. 2100410.
54. Alavarse, A.C., F.W. de Oliveira Silva, J.T. Colque, V.M. da Silva, T. Prieto, E.C. Venancio, and J.-J. Bonvent, *Tetracycline hydrochloride-loaded electrospun nanofibers mats based on PVA and chitosan for wound dressing.* Materials Science and Engineering: C, 2017. **77**: p. 271-281.
55. Kołbuk, D., M. Heljak, E. Choińska, and O. Urbanek, *Novel 3D hybrid nanofiber scaffolds for bone regeneration.* Polymers, 2020. **12**(3): p. 544.
56. Yousefi, I., M. Pakravan, H. Rahimi, A. Bahador, Z. Farshadzadeh, and I. Haririan, *An investigation of electrospun Henna leaves extract-loaded chitosan based nanofibrous mats for skin tissue engineering.* Materials Science and Engineering: C, 2017. **75**: p. 433-444.
57. Zhang, L., S. Tang, F. He, Y. Liu, W. Mao, and Y. Guan, *Highly efficient and selective capture of heavy metals by poly (acrylic acid) grafted chitosan and biochar composite for wastewater treatment.* Chemical Engineering Journal, 2019. **378**: p. 122215.
58. Ribeiro, A.S., S.M. Costa, D.P. Ferreira, R.C. Calhelha, L. Barros, D. Stojković, M. Soković, I.C. Ferreira, and R. Fangueiro, *Chitosan/nanocellulose electrospun fibers with enhanced antibacterial and antifungal activity for wound dressing applications.* Reactive and Functional Polymers, 2021. **159**: p. 104808.
59. Rinaudo, M., *Chitin and chitosan: Properties and applications.* Progress in polymer science, 2006. **31**(7): p. 603-632.
60. Ahmadijokani, F., H. Molavi, A. Bahi, S. Wuttke, M. Kamkar, O.J. Rojas, F. Ko, and M. Arjmand, *Electrospun nanofibers of chitosan/polyvinyl alcohol/UiO-66/nanodiamond: Versatile adsorbents for wastewater remediation and organic dye removal.* Chemical Engineering Journal, 2023. **457**: p. 141176.

61. Rad, Z.P., J. Mokhtari, and M. Abbasi, *Calendula officinalis extract/PCL/Zein/Gum arabic nanofibrous bio-composite scaffolds via suspension, two-nozzle and multilayer electrospinning for skin tissue engineering.* International journal of biological macromolecules, 2019. **135**: p. 530-543.
62. Kowsalya, E., K. MosaChristas, P. Balashanmugam, A. Tamil Selvi, and I. Jaquline Chinna Rani, *Biocompatible silver nanoparticles/poly (vinyl alcohol) electrospun nanofibers for potential antimicrobial food packaging applications.* Food Packaging and Shelf Life, 2019. **21**: p. 100379.
63. Shahverdi, F., A. Barati, and M. Bayat, *Effective Methylene Blue Removal from Aqueous Solutions using PVA/Chitosan Electrospun Nanofiber Modified with CeAlO3 Nanoparticles.* Journal of Water and Environmental Nanotechnology, 2022. **7**(1): p. 55-68.
64. Shrestha, B.K., H.M. Mousa, A.P. Tiwari, S.W. Ko, C.H. Park, and C.S. Kim, *Development of polyamide-6, 6/chitosan electrospun hybrid nanofibrous scaffolds for tissue engineering application.* Carbohydrate polymers, 2016. **148**: p. 107-114.
65. Kim, J.Y., J.I. Kim, C.H. Park, and C.S. Kim, *Design of a modified electrospinning for the in-situ fabrication of 3D cotton-like collagen fiber bundle mimetic scaffold.* Materials Letters, 2019. **236**: p. 521-525.
66. Saleh, S., A. Salama, O.M. Awad, R. De Santis, V. Guarino, and E. Tolba, *Polyamide Electrospun Nanofibers Functionalized with Silica and Titanium Dioxide Nanoparticles for Efficient Dye Removal.* Journal of Composites Science, 2024. **8**(2): p. 59.
67. Xinzhe, Z., C. Jing, W. Lu, W. Fujun, and W. Wenbin, *Collagen-PEO composite nanofibers by electrospinning.* Chem Fibers Int, 2015. **65**(1): p. 50-51.

68. Law, J.X., L.L. Liau, A. Saim, Y. Yang, and R. Idrus, *Electrospun collagen nanofibers and their applications in skin tissue engineering.* Tissue engineering and regenerative medicine, 2017. **14**: p. 699-718.
69. da Silva, B.A., R. de Sousa Cunha, A. Valério, A.D.N. Junior, D. Hotza, and S.Y.G. González, *Electrospinning of cellulose using ionic liquids: An overview on processing and applications.* European Polymer Journal, 2021. **147**: p. 110283.
70. de Melo Brites, M., A.A. Cerón, S.M. Costa, R.C. Oliveira, H.G. Ferraz, L.H. Catalani, and S.A. Costa, *Bromelain immobilization in cellulose triacetate nanofiber membranes from sugarcane bagasse by electrospinning technique.* Enzyme and Microbial Technology, 2020. **132**: p. 109384.
71. Souriyan-Reyhani pour, H., R. Khajavi, M.E. Yazdanshenas, P. Zahedi, and M. Mirjalili, *Cellulose acetate/poly (vinyl alcohol) hybrid fibrous mat containing tetracycline hydrochloride and phenytoin sodium: Morphology, drug release, antibacterial, and cell culture studies.* Journal of Bioactive and Compatible Polymers, 2018. **33**(6): p. 597-611.
72. Elmaghraby, N., A. Omer, E. Kenawy, M. Gaber, M. Hassaan, S. Ragab, I. Hossain, and A. El Nemr, *Electrospun cellulose acetate/activated carbon composite modified by EDTA (rC/AC-EDTA) for efficient methylene blue dye removal, Sci. Rep. 13 (1)(2023) 9919*.
73. Sun, Z., T. Feng, Z. Zhou, and H. Wu, *Removal of methylene blue in water by electrospun PAN/β-CD nanofibre membrane.* e-Polymers, 2021. **21**(1): p. 398-410.
74. Rahmani, F., H. Ziyadi, M. Baghali, H. Luo, and S. Ramakrishna, *Electrospun PVP/PVA nanofiber mat as a novel potential transdermal drug-delivery system for buprenorphine: a solution needed for pain management.* Applied Sciences, 2021. **11**(6): p. 2779.

75. Mollahosseini, H., H. Fashandi, A. Khoddami, M. Zarrebini, and H. Nikukar, *Recycling of waste silk fibers towards silk fibroin fibers with different structures through wet spinning technique.* Journal of Cleaner Production, 2019. **236**: p. 117653.
76. Zulfi, A., D.A. Hapidin, C. Saputra, W.S. Mustika, M.M. Munir, and K. Khairurrijal, *The synthesis of fiber membranes from High-Impact Polystyrene (HIPS) Waste using needleless electrospinning as air filtration media.* Materials Today: Proceedings, 2019. **13**: p. 154-159.
77. Séon-Lutz, M., A.-C. Couffin, S. Vignoud, G. Schlatter, and A. Hébraud, *Electrospinning in water and in situ crosslinking of hyaluronic acid/cyclodextrin nanofibers: Towards wound dressing with controlled drug release.* Carbohydrate polymers, 2019. **207**: p. 276-287.
78. Bahrami, S., A. Solouk, H. Mirzadeh, and A.M. Seifalian, *Electroconductive polyurethane/graphene nanocomposite for biomedical applications.* Composites Part B: Engineering, 2019. **168**: p. 421-431.
79. Lou, T., X. Yan, and X. Wang, *Chitosan coated polyacrylonitrile nanofibrous mat for dye adsorption.* International journal of biological macromolecules, 2019. **135**: p. 919-925.
80. Pathirana, M.A., N.S. Dissanayake, N.D. Wanasekara, B. Mahltig, and G.K. Nandasiri, *Chitosan-graphene oxide dip-coated polyacrylonitrile-ethylenediamine electrospun nanofiber membrane for removal of the dye stuffs methylene blue and congo red.* Nanomaterials, 2023. **13**(3): p. 498.
81. Cui, S., X. Sun, K. Li, D. Gou, Y. Zhou, J. Hu, and Y. Liu, *Polylactide nanofibers delivering doxycycline for chronic wound treatment.* Materials Science and Engineering: C, 2019. **104**: p. 109745.
82. Godakanda, V.U., H. Li, L. Alquezar, L. Zhao, L.-M. Zhu, R. de Silva, K.N. de Silva, and G.R. Williams, *Tunable drug release from blend poly (vinyl pyrrolidone)-ethyl cellulose nanofibers.* International journal of pharmaceutics, 2019. **562**: p. 172-179.

83. Kianfar, P., A. Vitale, S. Dalle Vacche, and R. Bongiovanni, *Photo-crosslinking of chitosan/poly (ethylene oxide) electrospun nanofibers.* Carbohydrate polymers, 2019. **217**: p. 144-151.
84. Sadeghi, M., Z. Moghimifar, P.S. Kumar, H. Javadian, and M. Farsadrooh, *Fabrication of poly (acrylonitrile-co-methyl methacrylate) nanofibers containing boron via electrospinning method: a study on size distribution, thermal, crystalline, and mechanical strength properties.* Sustainability, 2021. **13**(8): p. 4342.
85. Nady, N., M.H. Abdel Rehim, and A.A. Badawy, *Dye removal membrane from electrospun nanofibers of blended polybutylenesuccinate and sulphonated expanded polystyrene waste.* Scientific Reports, 2023. **13**(1): p. 15455.
86. Li, Z., Y. Liu, J. Yan, K. Wang, B. Xie, Y. Hu, W. Kang, and B. Cheng, *Electrospun polyvinylidene fluoride/fluorinated acrylate copolymer tree-like nanofiber membrane with high flux and salt rejection ratio for direct contact membrane distillation.* Desalination, 2019. **466**: p. 68-76.
87. Rostami, M.S. and M.M. Khodaei, *Recent advances in chitosan-based nanocomposites for adsorption and removal of heavy metal ions.* International Journal of Biological Macromolecules, 2024. **270**: p. 132386.
88. Tsauria, Q.D., P.L. Gareso, and D. Tahir, *Systematic review of chitosan-based adsorbents for heavy metal and dye remediation.* Integrated Environmental Assessment and Management, 2025: p. vjaf037.
89. Kaczorowska, M.A. and D. Bożejewicz, *The application of chitosan-based adsorbents for the removal of hazardous pollutants from aqueous solutions—a review.* Sustainability, 2024. **16**(7): p. 2615.
90. Nasar, A. *Chitosan-based adsorbents for wastewater treatment*. 2018. Materials Research Forum LLC.
91. Chandrasekaran, M., K.D. Kim, and S.C. Chun, *Antibacterial activity of chitosan nanoparticles: a review.* Processes, 2020. **8**(9): p. 1173.

92. Teixeira-Santos, R., M. Lima, L.C. Gomes, and F.J. Mergulhão, *Antimicrobial coatings based on chitosan to prevent implant-associated infections: A systematic review.* Iscience, 2021. **24**(12).
93. Garg, U., S. Chauhan, U. Nagaich, and N. Jain, *Current advances in chitosan nanoparticles based drug delivery and targeting.* Advanced pharmaceutical bulletin, 2019. **9**(2): p. 195.
94. Antaby, E., K. Klinkhammer, and L. Sabantina, *Electrospinning of chitosan for antibacterial applications—current trends.* Applied Sciences, 2021. **11**(24): p. 11937.
95. Ibrahim, M.A., M.H. Alhalafi, E.-A.M. Emam, H. Ibrahim, and R.M. Mosaad, *A review of chitosan and chitosan nanofiber: Preparation, characterization, and its potential applications.* Polymers, 2023. **15**(13): p. 2820.
96. Kyzas, G.Z. and D.N. Bikiaris, *Recent modifications of chitosan for adsorption applications: a critical and systematic review.* Marine drugs, 2015. **13**(1): p. 312-337.
97. Omer, A.M., R. Dey, A.S. Eltaweil, E.M. Abd El-Monaem, and Z.M. Ziora, *Insights into recent advances of chitosan-based adsorbents for sustainable removal of heavy metals and anions.* Arabian Journal of Chemistry, 2022. **15**(2): p. 103543.
98. Upadhyay, U., I. Sreedhar, S.A. Singh, C.M. Patel, and K. Anitha, *Recent advances in heavy metal removal by chitosan based adsorbents.* Carbohydrate Polymers, 2021. **251**: p. 117000.
99. da Silva Bruckmann, F., J.O. Gonçalves, L.F.O. Silva, M.L.S. Oliveira, G.L. Dotto, and C.R.B. Rhoden, *Chitosan-based adsorbents for wastewater treatment: A comprehensive review.* International Journal of Biological Macromolecules, 2025: p. 143173.

100. Bhatt, P., S. Joshi, G.M.U. Bayram, P. Khati, and H. Simsek, *Developments and application of chitosan-based adsorbents for wastewater treatments.* Environmental Research, 2023. **226**: p. 115530.
101. da Silva Alves, D.C., B. Healy, L.A.d.A. Pinto, T.R.S.A. Cadaval Jr, and C.B. Breslin, *Recent developments in chitosan-based adsorbents for the removal of pollutants from aqueous environments.* Molecules, 2021. **26**(3): p. 594.
102. Meretoudi, A.D., I. Kalampogias, I. Koumentakou, I.K. Kalavrouziotis, A.K. Tolkou, and G.Z. Kyzas, *Chitosan/Montmorillonite/Graphene Oxide Composites for the Adsorption of Dyes from Single-Component Solutions, Binary Mixtures, and Real Textile Wastewaters: On Understanding the Adsorption Interactions.* Langmuir, 2025.
103. Kausar, A., *Poly (acrylic acid) nanocomposites: Design of advanced materials.* Journal of Plastic Film & Sheeting, 2021. **37**(4): p. 409-428.
104. Ma, L., Y. Zhang, X. Wang, R. Tang, X. Zheng, Y. Dong, G. Kong, Z. Hou, and L. Wei, *Poly (acrylic acid-co-N-methylol acrylamide-co-butyl acrylate) copolymer grafted carboxymethyl cellulose binder for silicon anode in lithium ion batteries.* Journal of Applied Electrochemistry, 2021. **51**: p. 131-141.
105. Zuo, Y., W. Yang, K. Zhang, Y. Chen, X. Yin, and Y. Liu, *Experimental and theoretical studies of carboxylic polymers with low molecular weight as inhibitors for calcium carbonate scale.* Crystals, 2020. **10**(5): p. 406.
106. Spagnol, C., F.H. Rodrigues, A.G. Pereira, A.R. Fajardo, A.F. Rubira, and E.C. Muniz, *Superabsorbent hydrogel composite made of cellulose nanofibrils and chitosan-graft-poly (acrylic acid).* Carbohydrate Polymers, 2012. **87**(3): p. 2038-2045.
107. Arkaban, H., M. Barani, M.R. Akbarizadeh, N. Pal Singh Chauhan, S. Jadoun, M. Dehghani Soltani, and P. Zarrintaj, *Polyacrylic acid*

nanoplatforms: antimicrobial, tissue engineering, and cancer theranostic applications. Polymers, 2022. **14**(6): p. 1259.

108. Sandu, T., A.-L. Chiriac, A. Zaharia, T.-V. Iordache, and A. Sarbu, *New Trends in Preparation and Use of Hydrogels for Water Treatment.* Gels, 2025. **11**(4): p. 238.
109. Laraib, U., S. Sargazi, A. Rahdar, M. Khatami, and S. Pandey, *Nanotechnology-based approaches for effective detection of tumor markers: A comprehensive state-of-the-art review.* International journal of biological macromolecules, 2022. **195**: p. 356-383.
110. Sylvester, M.A., F. Amini, and C.K. Tan, *Electrospun nanofibers in wound healing.* Materials Today: Proceedings, 2020. **29**: p. 1-6.
111. Hu, X., S. Liu, G. Zhou, Y. Huang, Z. Xie, and X. Jing, *Electrospinning of polymeric nanofibers for drug delivery applications.* Journal of controlled release, 2014. **185**: p. 12-21.
112. Alghoraibi, I. and S. Alomari, *Different methods for nanofiber design and fabrication*, in *Handbook of nanofibers*. 2018, Springer. p. 1-46.
113. Sista, D., *New perspective of nano fibers: synthesis and applications*, in *Nanofibers-Synthesis, Properties and Applications*. 2021, Intechopen.
114. Gizaw, M., A. Faglie, M. Pieper, S. Poudel, and S.-F. Chou, *The role of electrospun fiber scaffolds in stem cell therapy for skin tissue regeneration.* Med one, 2019. **4**: p. e190002.
115. Partheniadis, I., I. Nikolakakis, I. Laidmäe, and J. Heinämäki, *A mini-review: Needleless electrospinning of nanofibers for pharmaceutical and biomedical applications.* Processes, 2020. **8**(6): p. 673.
116. Heidari, Y., E. Noroozian, and S. Maghsoudi, *Electrospun nanofibers of cellulose acetate/metal organic framework-third generation PAMAM dendrimer for the removal of methylene blue from aqueous media.* Scientific Reports, 2023. **13**(1): p. 4924.

117. Rianjanu, A., K.D.P. Marpaung, E.K.A. Melati, R. Aflaha, Y.G. Wibowo, I.P. Mahendra, N. Yulianto, J. Widakdo, K. Triyana, and H.S. Wasisto, *Integrated adsorption and photocatalytic removal of methylene blue dye from aqueous solution by hierarchical Nb2O5@ PAN/PVDF/ANO composite nanofibers.* Nano Materials Science, 2024. **6**(1): p. 96-105.
118. Li, L., W. Guo, S. Zhang, R. Guo, and L. Zhang, *Electrospun nanofiber membrane: an efficient and environmentally friendly material for the removal of metals and dyes.* Molecules, 2023. **28**(8): p. 3288.
119. Fang, S., C. Hua, J. Yang, F. Liu, L. Wang, D. Wu, and L. Ren, *Combined pollution of soil by heavy metals, microplastics, and pesticides: Mechanisms and anthropogenic drivers.* Journal of Hazardous Materials, 2025. **485**: p. 136812.
120. Fereidoun, H., M.S. Nourddin, N.A. Rreza, A. Mohsen, R. Ahmad, and H. Pouria, *The effect of long-term exposure to particulate pollution on the lung function of Teheranian and Zanjanian students.* Pakistan Journal of physiology, 2007. **3**(2).
121. Dehmani, Y., B.B. Mohammed, R. Oukhrib, A. Dehbi, T. Lamhasni, Y. Brahmi, A. El-Kordy, D.S. Franco, J. Georgin, and E.C. Lima, *Adsorption of various inorganic and organic pollutants by natural and synthetic zeolites: A critical review.* Arabian Journal of Chemistry, 2024. **17**(1): p. 105474.
122. Dubey, S.P., K. Gopal, and J.-L. Bersillon, *Utility of adsorbents in the purification of drinking water: a review of characterization, efficiency and safety evaluation of various adsorbents.* J. Environ. Biol, 2009. **30**(3): p. 327-332.
123. Wang, S. and Y. Peng, *Natural zeolites as effective adsorbents in water and wastewater treatment.* Chemical engineering journal, 2010. **156**(1): p. 11-24.

124. Adeyemo, A.A., I.O. Adeoye, and O.S. Bello, *Metal organic frameworks as adsorbents for dye adsorption: overview, prospects and future challenges.* Toxicological & Environmental Chemistry, 2012. **94**(10): p. 1846-1863.
125. Gupta, S.S. and K.G. Bhattacharyya, *Adsorption of heavy metals on kaolinite and montmorillonite: a review.* Physical Chemistry Chemical Physics, 2012. **14**(19): p. 6698-6723.
126. Ngah, W.W., L. Teong, and M.M. Hanafiah, *Adsorption of dyes and heavy metal ions by chitosan composites: A review.* Carbohydrate polymers, 2011. **83**(4): p. 1446-1456.
127. Manisalidis, I., E. Stavropoulou, A. Stavropoulos, and E. Bezirtzoglou, *Environmental and health impacts of air pollution: a review.* Frontiers in public health, 2020. **8**: p. 14.
128. Liu, C., R. Chen, F. Sera, A.M. Vicedo-Cabrera, Y. Guo, S. Tong, E. Lavigne, P.M. Correa, N.V. Ortega, and S. Achilleos, *Interactive effects of ambient fine particulate matter and ozone on daily mortality in 372 cities: two stage time series analysis.* bmj, 2023. **383**.
129. Setu, S. and V. Strezov, *Impacts of non-ferrous metal mining on soil heavy metal pollution and risk assessment.* Science of The Total Environment, 2025. **969**: p. 178962.
130. Adepoju, A.O., A. Femi-Adepoju, A. Jalloh, and S. Faeflen, *Soil pollution and management practices*, in *Environmental pollution and public health*. 2024, Elsevier. p. 187-236.
131. Chowdhary, P., R.N. Bharagava, S. Mishra, and N. Khan, *Role of industries in water scarcity and its adverse effects on environment and human health.* Environmental concerns and sustainable development: Volume 1: Air, water and energy resources, 2020: p. 235-256.

132. Lin, L., H. Yang, and X. Xu, *Effects of water pollution on human health and disease heterogeneity: a review.* Frontiers in environmental science, 2022. **10**: p. 880246.
133. Kato, S. and Y. Kansha, *Comprehensive review of industrial wastewater treatment techniques.* Environmental Science and Pollution Research, 2024. **31**(39): p. 51064-51097.
134. Fernandes, J., P.J. Ramísio, and H. Puga, *A comprehensive review on various phases of wastewater technologies: Trends and future perspectives.* Eng, 2024. **5**(4): p. 2633-2661.
135. Islam, M.S., M.K. Ahmed, M. Raknuzzaman, M. Habibullah-Al-Mamun, and M.K. Islam, *Heavy metal pollution in surface water and sediment: a preliminary assessment of an urban river in a developing country.* Ecological indicators, 2015. **48**: p. 282-291.
136. Srivastav, A.L. and M. Ranjan, *Inorganic water pollutants*, in *Inorganic pollutants in water*. 2020, Elsevier. p. 1-15.
137. Ali, I. and H.Y. Aboul-Enein, *Chiral pollutants: distribution, toxicity and analysis by chromatography and capillary electrophoresis*. 2005: John Wiley & Sons.
138. Ali, I., M. Asim, and T.A. Khan, *Low cost adsorbents for the removal of organic pollutants from wastewater.* Journal of environmental management, 2012. **113**: p. 170-183.
139. Shanker, U., M. Rani, and V. Jassal, *Degradation of hazardous organic dyes in water by nanomaterials.* Environmental chemistry letters, 2017. **15**: p. 623-642.
140. Adeyemo, A.A., I.O. Adeoye, and O.S. Bello, *Adsorption of dyes using different types of clay: a review.* Applied Water Science, 2017. **7**: p. 543-568.

141. Blackburn, R.S., *Natural polysaccharides and their interactions with dye molecules: applications in effluent treatment.* Environmental science & technology, 2004. **38**(18): p. 4905-4909.
142. Chequer, F.M.D., G.A.R. de Oliveira, E.R.A. Ferraz, J.C. Cardoso, M.V.B. Zanoni, and D.P. de Oliveira, *Textile dyes: dyeing process and environmental impact*, in *Eco-friendly textile dyeing and finishing*. 2013, IntechOpen.
143. Zhang, Y., H. Ou, H. Liu, Y. Ke, W. Zhang, G. Liao, and D. Wang, *Polyimide-based carbon nanofibers: A versatile adsorbent for highly efficient removals of chlorophenols, dyes and antibiotics.* Colloids and surfaces A: Physicochemical and engineering aspects, 2018. **537**: p. 92-101.
144. Bal, G. and A. Thakur, *Distinct approaches of removal of dyes from wastewater: A review.* Materials Today: Proceedings, 2022. **50**: p. 1575-1579.
145. Pargai, D., *Chemistry of Natural Dye for Functional Applications.* Dye Chemistry-Exploring Colour From Nature to Lab: Exploring Colour From Nature to Lab, 2024: p. 3.
146. Benaissa, A., *Etude de la faisabilité d'élimination de certains colorants textiles par certains matériaux déchets d'origine naturelle.* Université Abou Bakr Balkaid, Tlemcen-Algérie, 2012.
147. LAURENT, A.D., V. WATHELET, M. BOUHY, D. JACQUEMIN, and E. PERPÈTE, *Simulation de la perception des couleurs de colorants organiques.* 2010.
148. Temesgen, F., N. Gabbiye, and O. Sahu, *Biosorption of reactive red dye (RRD) on activated surface of banana and orange peels: economical alternative for textile effluent.* Surfaces and interfaces, 2018. **12**: p. 151-159.

149. Oladoye, P.O., T.O. Ajiboye, E.O. Omotola, and O.J. Oyewola, *Methylene blue dye: Toxicity and potential elimination technology from wastewater.* Results in Engineering, 2022. **16**: p. 100678.
150. Khodaie, M., N. Ghasemi, B. Moradi, and M. Rahimi, *Removal of methylene blue from wastewater by adsorption onto ZnCl2 activated corn husk carbon equilibrium studies.* Journal of Chemistry, 2013. **2013**(1): p. 383985.
151. Dardouri, S. and J. Sghaier, *Adsorptive removal of methylene blue from aqueous solution using different agricultural wastes as adsorbents.* Korean Journal of Chemical Engineering, 2017. **34**(4): p. 1037-1043.
152. Al-Ghouti, M.A. and R.S. Al-Absi, *Mechanistic understanding of the adsorption and thermodynamic aspects of cationic methylene blue dye onto cellulosic olive stones biomass from wastewater.* Scientific Reports, 2020. **10**(1): p. 15928.
153. Altaher, H. and E. ElQada, *Investigation of the treatment of colored water using efficient locally available adsorbent.* International journal of energy and environment, 2011. **2**(6): p. 1113-1124.
154. Chakraborty, B., L. Ray, and S. Basu, *Biochemical degradation of Methylene Blue using a continuous reactor packed with solid waste by E. coli and Bacillus subtilis isolated from wetland soil.* Desalination and Water Treatment, 2016. **57**(30): p. 14077-14082.
155. Wijaya, R., G. Andersan, S. Permatasari Santoso, and W. Irawaty, *Green reduction of graphene oxide using kaffir lime peel extract (Citrus hystrix) and its application as adsorbent for methylene blue.* Scientific reports, 2020. **10**(1): p. 667.
156. Bayomie, O.S., H. Kandeel, T. Shoeib, H. Yang, N. Youssef, and M.M. El-Sayed, *Novel approach for effective removal of methylene blue dye from water using fava bean peel waste.* Scientific reports, 2020. **10**(1): p. 7824.

157. Sousa, H.R., L.S. Silva, P.A.A. Sousa, R.R.M. Sousa, M.G. Fonseca, J.A. Osajima, and E.C. Silva-Filho, *Evaluation of methylene blue removal by plasma activated palygorskites.* Journal of Materials Research and Technology, 2019. **8**(6): p. 5432-5442.
158. Salimi, A. and A. Roosta, *Experimental solubility and thermodynamic aspects of methylene blue in different solvents.* Thermochimica Acta, 2019. **675**: p. 134-139.
159. Nasrullah, A., H. Khan, A.S. Khan, Z. Man, N. Muhammad, M.I. Khan, and N.M. Abd El-Salam, *Potential biosorbent derived from Calligonum polygonoides for removal of methylene blue dye from aqueous solution.* The Scientific World Journal, 2015. **2015**(1): p. 562693.
160. Khan, I., K. Saeed, I. Zekker, B. Zhang, A.H. Hendi, A. Ahmad, S. Ahmad, N. Zada, H. Ahmad, and L.A. Shah, *Review on methylene blue: its properties, uses, toxicity and photodegradation.* Water, 2022. **14**(2): p. 242.
161. Isaev, N.K., E.E. Genrikhs, and E.V. Stelmashook, *Methylene blue and its potential in the treatment of traumatic brain injury, brain ischemia, and Alzheimer's disease.* Reviews in the Neurosciences, 2024. **35**(5): p. 585-595.
162. Hashmi, M.U., R. Ahmed, S. Mahmoud, K. Ahmed, N.M. Bushra, A. Ahmed, B. Elwadie, A. Madni, A.B. Saad, and N. Abdelrahman, *Exploring methylene blue and its derivatives in alzheimer's treatment: a comprehensive review of randomized control trials.* Cureus, 2023. **15**(10).
163. Taldaev, A., R. Terekhov, I. Nikitin, E. Melnik, V. Kuzina, M. Klochko, I. Reshetov, A. Shiryaev, V. Loschenov, and G. Ramenskaya, *Methylene blue in anticancer photodynamic therapy: systematic review of preclinical studies.* Frontiers in Pharmacology, 2023. **14**: p. 1264961.
164. Modi, S., V.K. Yadav, A. Gacem, I.H. Ali, D. Dave, S.H. Khan, K.K. Yadav, S.-u. Rather, Y. Ahn, and C.T. Son, *Recent and emerging trends in*

remediation of methylene blue dye from wastewater by using zinc oxide nanoparticles. Water, 2022. **14**(11): p. 1749.

165. Bužga, M., E. Machytka, E. Dvořáčková, Z. Švagera, D. Stejskal, J. Máca, and J. Král, *Methylene blue: a controversial diagnostic acid and medication?* Toxicology Research, 2022. **11**(5): p. 711-717.
166. Rafatullah, M., O. Sulaiman, R. Hashim, and A. Ahmad, *Adsorption of methylene blue on low-cost adsorbents: a review.* Journal of hazardous materials, 2010. **177**(1-3): p. 70-80.
167. Madrakian, T., A. Afkhami, M. Ahmadi, and H. Bagheri, *Removal of some cationic dyes from aqueous solutions using magnetic-modified multi-walled carbon nanotubes.* Journal of hazardous materials, 2011. **196**: p. 109-114.
168. Sajab, M.S., C.H. Chia, S. Zakaria, and P.S. Khiew, *Cationic and anionic modifications of oil palm empty fruit bunch fibers for the removal of dyes from aqueous solutions.* Bioresource Technology, 2013. **128**: p. 571-577.
169. Ayad, M.M., W.A. Amer, S. Zaghlol, I.M. Minisy, P. Bober, and J. Stejskal, *Polypyrrole-coated cotton textile as adsorbent of methylene blue dye.* Chemical Papers, 2018. **72**: p. 1605-1618.
170. Minisy, I.M., B.A. Zasońska, E. Petrovský, P. Veverka, I. Šeděnková, J. Hromádková, and P. Bober, *Poly (p-phenylenediamine)/maghemite composite as highly effective adsorbent for anionic dye removal.* Reactive and Functional Polymers, 2020. **146**: p. 104436.
171. Saleh, H.M., S. Albukhaty, G.M. Sulaiman, and M.M. Abomughaid, *Design, preparation, and characterization of polycaprolactone–chitosan nanofibers via electrospinning techniques for efficient methylene blue removal from aqueous solutions.* Journal of Composites Science, 2024. **8**(2): p. 68.
172. Muteeb, G., K. Ansari, M. Eyvaz, M. Farhan, M. Aatif, D. Agrawal, M.E. Oirdi, and M.H. Dehghani, *Removal of methylene blue (MB) dye from water*

and wastewater using acid-activated chicken bone in a batch adsorption process. Scientific Reports, 2025. **15**(1): p. 23098.

173. Abdrabou, D., M. Ahmed, A. Hussein, and T. El-Sherbini, *Photocatalytic behavior for removal of methylene blue from aqueous solutions via nanocomposites based on Gd2O3/CdS and cellulose acetate nanofibers.* Environmental Science and Pollution Research, 2023. **30**(44): p. 99789-99808.
174. Chen, Y., Y. Cheng, X. Guan, Y. Liu, J. Nie, and C. Li, *A Rapid Fenton treatment of bio-treated dyeing and finishing wastewater at second-scale intervals: kinetics by stopped-flow technique and application in a full-scale plant.* Scientific Reports, 2019. **9**(1): p. 9689.
175. Rajaniemi, K., S. Tuomikoski, and U. Lassi, *Electrocoagulation sludge valorization—a review.* Resources, 2021. **10**(12): p. 127.
176. Teixeira, Y.N., F.J. de Paula Filho, V.P. Bacurau, J.M.C. Menezes, A.Z. Fan, and R.P.F. Melo, *Removal of Methylene Blue from a synthetic effluent by ionic flocculation.* Heliyon, 2022. **8**(10).
177. Al-Abduljabbar, A. and I. Farooq, *Electrospun polymer nanofibers: processing, properties, and applications.* Polymers, 2022. **15**(1): p. 65.
178. Khan, G., S.K. Yadav, R.R. Patel, N. Kumar, M. Bansal, and B. Mishra, *Tinidazole functionalized homogeneous electrospun chitosan/poly (ε-caprolactone) hybrid nanofiber membrane: Development, optimization and its clinical implications.* International journal of biological macromolecules, 2017. **103**: p. 1311-1326.
179. Boyd, G., A. Adamson, and L. Myers Jr, *The exchange adsorption of ions from aqueous solutions by organic zeolites. II. Kinetics1.* Journal of the American Chemical Society, 1947. **69**(11): p. 2836-2848.
180. Yuh-Shan, H., *Citation review of Lagergren kinetic rate equation on adsorption reactions.* Scientometrics, 2004. **59**(1): p. 171-177.

181. Shin, J.R., G.S. An, and S.-C. Choi, *Influence of carboxylic modification using polyacrylic acid on characteristics of Fe3O4 nanoparticles with cluster structure.* Processes, 2021. **9**(10): p. 1795.
182. Wang, Y., J. Wang, Z. Yuan, H. Han, T. Li, L. Li, and X. Guo, *Chitosan cross-linked poly (acrylic acid) hydrogels: Drug release control and mechanism.* Colloids and Surfaces B: Biointerfaces, 2017. **152**: p. 252-259.
183. Hu, Y., X. Jiang, Y. Ding, H. Ge, Y. Yuan, and C. Yang, *Synthesis and characterization of chitosan–poly (acrylic acid) nanoparticles.* Biomaterials, 2002. **23**(15): p. 3193-3201.
184. Pervez, M.N., W.S. Yeo, M.M.R. Mishu, M.E. Talukder, H. Roy, M.S. Islam, Y. Zhao, Y. Cai, G.K. Stylios, and V. Naddeo, *Electrospun nanofiber membrane diameter prediction using a combined response surface methodology and machine learning approach.* Scientific Reports, 2023. **13**(1): p. 9679.
185. Agarwal, P., S. Pradhan, and D.B. Tripathy, *Electrospun nanofibers for water remediation: Functionalization, structural innovations, and mechanistic insights.* Desalination, 2025: p. 119086.
186. Nayl, A.A., A.I. Abd-Elhamid, N.S. Awwad, M.A. Abdelgawad, J. Wu, X. Mo, S.M. Gomha, A.A. Aly, and S. Bräse, *Review of the recent advances in electrospun nanofibers applications in water purification.* Polymers, 2022. **14**(8): p. 1594.
187. Panalytical, M. *Zeta potential: An introduction in 30 minutes*. 2025 September 1, 2025].
188. El-hefian, E.A. and A.H. Yahaya, *Rheological study of chitosan and its blends: An overview.* Maejo Int. J. Sci. Technol, 2010. **4**(02): p. 210-220.
189. Duan, X., J. Xu, B. He, J. Li, and Y. Sun, *PREPARATION AND RHEOLOGICAL PROPERTIES OF CELLULOSE/CHITOSAN HOMOGENEOUS SOLUTION IN IONIC LIQUID.* BioResources, 2011. **6**(4).

190. Pakravan, M., M.-C. Heuzey, and A. Ajji, *A fundamental study of chitosan/PEO electrospinning.* Polymer, 2011. **52**(21): p. 4813-4824.
191. Sakib, M.N., A.K. Mallik, and M.M. Rahman, *Update on chitosan-based electrospun nanofibers for wastewater treatment: A review.* Carbohydrate Polymer Technologies and Applications, 2021. **2**: p. 100064.
192. Vaz, M.G., A.G. Pereira, A.R. Fajardo, A.C. Azevedo, and F.H. Rodrigues, *Methylene blue adsorption on chitosan-g-poly (acrylic acid)/rice husk ash superabsorbent composite: kinetics, equilibrium, and thermodynamics.* Water, Air, & Soil Pollution, 2017. **228**(1): p. 14.
193. Wang, J. and S. Zhuang, *Removal of various pollutants from water and wastewater by modified chitosan adsorbents.* Critical Reviews in Environmental Science and Technology, 2017. **47**(23): p. 2331-2386.
194. Ahmed, M.J., *Application of agricultural based activated carbons by microwave and conventional activations for basic dye adsorption.* Journal of Environmental Chemical Engineering, 2016. **4**(1): p. 89-99.
195. Liu, Y. and Y.-J. Liu, *Biosorption isotherms, kinetics and thermodynamics.* Separation and purification technology, 2008. **61**(3): p. 229-242.
196. Abasalta, M., A. Asefnejad, M.T. Khorasani, and A.R. Saadatabadi, *Fabrication of carboxymethyl chitosan/poly (ε-caprolactone)/doxorubicin/nickel ferrite core-shell fibers for controlled release of doxorubicin against breast cancer.* Carbohydrate polymers, 2021. **257**: p. 117631.
197. Fadaie, M., E. Mirzaei, B. Geramizadeh, and Z. Asvar, *Incorporation of nanofibrillated chitosan into electrospun PCL nanofibers makes scaffolds with enhanced mechanical and biological properties.* Carbohydrate polymers, 2018. **199**: p. 628-640.
198. Aramesh, N., A.R. Bagheri, and M. Bilal, *Chitosan-based hybrid materials for adsorptive removal of dyes and underlying interaction mechanisms.*

International Journal of Biological Macromolecules, 2021. **183**: p. 399-422.

199. Zhang, Y., F. Wang, and Y. Wang, *Recent developments of electrospun nanofibrous materials as novel adsorbents for water treatment.* Materials Today Communications, 2021. **27**: p. 102272.

200. Zhang, R.-Y., E. Zaslavski, G. Vasilyev, M. Boas, and E. Zussman, *Tunable pH-responsive chitosan-poly (acrylic acid) electrospun fibers.* Biomacromolecules, 2018. **19**(2): p. 588-595.

الخلاصة :

التلوث الصناعي والزراعي والكوارث الطبيعية ونقص إمدادات المياه ومنشآت الصرف الصحي تُعد من أبرز الأسباب الرئيسة لتلوث المياه .ومن أكثر الصناعات مسؤولية عن هذا التلوث: الصناعات النووية، وصناعات الحديد والصلب، والصناعات الغذائية، والنسيجية، وصناعة اللب والورق، والمصانع الكحولية، والمدابغ، و البلاستيك. إذ تؤدي العديد من العمليات الصناعية إلى إطلاق كميات كبيرة من المذيبات السامة، والمركبات العضوية المتطايرة، والمواد الكيميائية الخطرة العضوية وغير العضوية. وتُعد هذه النفايات سببًا مباشرًا في تفاقم مشكلة تلوث المياه عند تصريفها إلى المسطحات المائية دون معالجة كافية.

تركّز هذه الدراسة بصورة رئيسة على الأصباغ، التي تمثل أحد أكثر هذه الملوثات شيوعًا. ويُعد الميثيلين الأزرق (MB) نموذجًا شائعًا للأصباغ الكاتيونية، يتميز بثباته في البيئة، فضلاً عن خصائصه السامة والمسرطنة والمطفّرة. ويُستخدم الميثيلين الأزرق على نطاق واسع في الصناعات النسيجية وصناعة الملابس في عمليات الصباغة، وكذلك في تلوين الورق والجلود. وبسبب هذه الاستخدامات الصناعية المتعددة، تنطلق كميات كبيرة من المخلفات الصناعية المحتوية على الميثيلين الأزرق إلى كلٍّ من المياه السطحية والجوفية. وقد ثبت أن الجرعات العالية لدى الإنسان (بمقدار 5 ملغم/كغم) تؤدي إلى تثبيط إنزيم أوكسيداز أحادي الأمين، مما ينتج عنه سمية قاتلة مرتبطة بارتفاع مستويات السيروتونين، إضافة إلى إحداث آثار بيئية خطيرة على الكائنات المائية داخل النظام البيئي. وعليه، هناك حاجة ملحّة للتخلّص من هذا الصباغ في مياه الصرف.

تُعنى هذه الدراسة بتصنيع وتوصيف ألياف نانوية من حمض البولي أكريليك–الكيتوسان (PAA-Chi) باستخدام تقنية الغزل الكهربائي، وذلك بهدف تطوير مادة فعّالة تُسهم في إزالة صبغة الميثيلين الأزرق (MB)من المحاليل المائية. ويُعد دمج الكيتوسان مع هيكل حمض البولي أكريليك خطوة استراتيجية لتعزيز قدرة الامتزاز لدى هذه الألياف النانوية، وجعلها أكثر فاعلية ليس فقط تجاه الميثيلين الأزرق، بل أيضًا تجاه ملوثات عضوية أخرى.

وقد أُجريت أبحاث مكثفة حول الخصائص التركيبية والبنيوية والريولوجية للألياف النانوية المُحضَّرة. وتمت دراسة عملية الامتزاز من خلال اختبارات حركية واتزانية، وأظهرت النتائج أن التركيز الابتدائي للأصباغ ودرجة حموضة الوسط يُؤثران بوضوح على الامتزاز. ومن المتوقع أن تُسهم هذه النتائج في توضيح خصائص الامتزاز للألياف ومدى فعاليتها في معالجة مياه الصرف.

تناول القسم الأول تحضير ألياف نانوية مؤلفة من مزيج حمض البولي أكريليك والشيتوزان (PAA-Chi) بنسبة (70:30) باستخدام تقنية الغزل الكهربائي، في حين لم يُرصد تشكّل لأي ألياف نانوية عند استخدام

النسبتين (50:50) و(85:15). وتُعد هذه التقنية أسلوباً شائعاً لإنتاج ألياف بوليمرية تتراوح أقطارها بين المقياسين الميكرومتري والنانومتري؛ مما يوفر مواداً تمتاز بمساحة سطح خارجية واسعة وبنية ذات مسامية عالية. وقد استلزمت العملية اتباع إجراءات منهجية محددة لضمان إنتاج ألياف نانوية متجانسة تتمتع بخصائص قيّمة تؤهلها للاستخدام في التطبيقات المنشودة.

يتناول القسم الثاني التوصيف الشامل للألياف النانوية المُحَضَّرة؛ حيث أظهر الفحص باستخدام المجهر الإلكتروني الماسح ذي الانبعاث المجالي (FESEM) بنية مورفولوجية متجانسة بمتوسط قطر يبلغ 276.15 نانومتر. كما أثبت قياس جهد زيتا (Zeta potential) أن سطح الألياف يحمل شحنة سالبة. وقد أكد طيف الأشعة تحت الحمراء بتحويل فورييه (FTIR) نجاح دمج المجموعات الوظيفية المميزة في كل من حمض البولي أكريليك والشيتوزان، حيث تساهم هذه المجموعات في تعزيز قدرة الصبغة على الارتباط بالعينة بفضل الروابط الهيدروجينية والتفاعلات الأيونية. علاوة على ذلك، قدمت تحليلات الريولوجيا واللزوجة معلومات قيّمة حول خصائص محلول التغذية، والتي يمكن الاستناد إليها لإنتاج ألياف مستقرة ومتجانسة.

في القسم الثالث، خُصص البحث لاستخدام ألياف PAA-Chi كمواد مازه جديدة لمعالجة المياه، مع التركيز على إزالة الملوث العضوي المتمثل في الميثيلين الأزرق. وقد بيّنت اختبارات الامتزاز في النظم الدفعية كفاءة عالية في الإزالة، إذ تجاوزت السعة الامتزازية العظمى (q_o) 60 ملغم/غم عند تركيز ابتدائي للصبغة بلغ 200 ملغم/لتر، مقارنة بـ 55 و31 ملغم/غم عند تركيز ابتدائي قدره 100 و50 ملغم/لتر على التوالي. أُجريت هذه التجارب في ظروف مثالية باستخدام كتلة مقدارها 10 ملغم من الألياف النانويةPAA-Chi ، بدرجة حرارة 25°م، ودرجة حموضة 6، وزمن تماس بلغ 720 دقيقة. وتشير هذه البيانات إلى أن الألياف النانوية من PAA-Chi تُعد خيارًا واعدًا لمعالجة مياه الصرف الصناعي، لما تتميز به من مورفولوجيا مستقرة، وخصائص سطحية فعّالة، وقدرة عالية على امتزاز الملوثات الكاتيونية.

جمهورية العراق
وزارة التعليم العالي والبحث العلمي
جامعة ميسان
كلية العلوم
قسم الكيمياء

تخليق وتوصيف ألياف نانوية بوليمرية منسوجة كهربائياً لامتزاز صبغة المثيلين الازرق من المحاليل المائية

رسالة مقدَّمة إلى
كلية العلوم / جامعة ميسان وهي جزء من متطلبات
نيل درجة الماجستير في العلوم ـ الكيمياء

الطالـــــب
مرتضى شهاب احمد

بكالوريوس علوم كيمياء / جامعة ميسان (2015)

بإشراف

الأستاذ المساعد

هند مهدي صالح

2025م **1446هـ**